DESIGN, SYNTHESIS, AND CALIBRATION OF PEROXYL-RADICAL CLOCKS

FOR THE DETERMINATION OF k_{inh}'s OF ANTIOXIDANTS AND k_p's OF

HYDROCARBONS

By

William P. Roschek, Jr.

Dissertation

Submitted to the Faculty of the

Graduate School of Vanderbilt University

in partial fulfillment of the requirements

for the degree of

DOCTOR OF PHILOSOPHY

In

Chemistry

May, 2006

Nashville, Tennessee

Approved:

Professor Ned A. Porter

Professor Carmelo J. Rizzo

Professor Piotr Kaszynski

Professor David E. Cliffel

ACKNOWLEDGEMENTS

Other members of the Porter group and members of the Vanderbilt University Chemistry Department have helped in many ways that are too extensive to list here, but too all of you, thank you for your patience, understanding, and help in so many ways.

I would like to express my extreme thanks and love to my fiancée Erica, and my daughter Avery. Without you two in my life, I would not be complete.

TABLE OF CONTENTS

LIST OF TABLES

LIST OF FIGURES

CHAPTER I

INTRODUCTION TO LIPID PEROXIDATION, PHENOLIC ANTIOXIDANTS,
FREE-RADICAL CLOCKS, AND THE ALLYLPEROXYL RADICAL
REARRANGEMENT

Lipid Peroxidation

Swiss chemist de Saussure conducted the first studies of lipid oxidation around 1800. Using a crude mercury manometer, de Saussure observed that a layer of walnut oil exposed to air could absorb nearly 150 times its own volume during a one year period.[1] Although there was a clear implication that oxygen was involved in a reaction with some constituent of the oil, it was not until the early 1900s, when pure hydrocarbons were isolated from lard and vegetable oils, that the picture became somewhat clear. In the 1920s, it was shown that linoleic acid was oxidized more rapidly than oleic acid,[2] and linolenic acid was oxidized more rapidly than linoleic acid.[3] Systematic studies of the mechanism of oxidation followed Stephens' successful isolation of a cyclohexene derived peroxide.[4]

In 1939, Creigee showed that hydroperoxides are the primary products of hydrocarbon oxidation.[5] Ten years later, Bolland firmly established that the primary oxidation products of linoleic acid (the most common polyunsaturated fatty acid found in animals) are conjugated hydroperoxides substituted at the 9- and 13-positions of the linoleate chain.[6] Later kinetic and thermodynamic studies provided a detailed and unified mechanism for hydrocarbon autoxidation.

The liquid phase autoxidation of organic compounds at temperatures less than $100^{\circ}C$ can be represented by the general equation:

$$R\text{-}H + O_2 \rightarrow ROOH \quad\quad\quad (1)$$

Where R-H is a hydrocarbon or aldehyde and ROOH is the corresponding hydroperoxide or peracid.[7] In cases in which the oxidizable material is a vinyl monomer, a copolymer of oxygen and the vinyl monomer is obtained. The reaction has the characteristics of a free radical chain reaction because the rate of the reaction is strongly catalyzed by light and accelerated by compounds which decompose to form free radicals.[8]

Over the past three decades, interest in lipid peroxidation has intensified. Reasons for this increase of interest include, but are not limited to, the following:

1. It was discovered that the reactive oxygen species (ROS) derived from superoxide radical lead to lipid peroxidation[9,10] and that superoxide dismutase exists in order to scavenge superoxide radicals.[11, 12] Because of this, superoxide radicals are viewed as an important cause of oxygen toxicity and are known to lead to lipid peroxidation via ROS such as hydroxyl radicals.

2. It was observed that products analogous to those expected from lipid peroxidation are formed enzymatically. The fatty acid hydroperoxides derived from arachidonic acid by lipoxygenase enzymes are an example of such products.[13] These fatty acid hydroperoxides serve as key intermediates in the biosynthesis of the leukotriene and lipoxin compounds that show immune response activity.[14]

3. Important enzymatic products with peroxide functionality are the prostaglandin endoperoxides. Arachidonic acid is the precursor to these endoperoxide compounds that also serve as key intermediates to the prostaglandin and thromboxane families.[15]

4. The involvement of lipid peroxidation in neoplastic transformation has also been suggested. Superoxide dismutase, for example, inhibits neoplastic transformations induced by X-rays or bleomycin in conjunction with phorbol myristyl acetate, and it has been speculated that events such as membrane lipid peroxidation are involved in these events.[16]

5. Lipid peroxidation has been related to initiation of the oxidative metabolism of polynuclear aromatic hydrocarbons. Some of the metabolites of these compounds are extremely mutagenic and may be the ultimate carcinogenic form of the parent hydrocarbon.[17]

6. It has been proposed that lipid peroxidation contributes to chemical debris that accumulates with age. Lipofuscin may be some of that chemical debris and a significant effort has been directed towards developing an understanding of the nature of the age pigment and how it forms.[18-20]

The most convenient and widely used technique for the kinetic studies of the oxidation of hydrocarbons is the measurement of oxygen absorption as a function of time by oxygen saturated liquid solution of the hydrocarbon, neat, or in an inert solvent (e.g. benzene). Because the absorption of oxygen is generally

a slow process, a compound that decomposes at a known rate and efficiency to form free radicals is usually added to these experiments. These compounds are called radical initiators, and are added to the oxidations in an amount so that, over the course of the oxidation, the rate of radical generation is many orders of magnitude greater than the rate of radical formation from the decomposition of the product hydroperoxides. Initiators that are commonly used for these purposes are 2,2'-azobis(isobutyrylnitrile) (AIBN), 2,2'-azobis(2-amidinopropane) dihydrochloride (AAPH) and 2,2'-azobis(2,4-dimethylvaleronitrile) (AMVN) seen in Figure I-1.
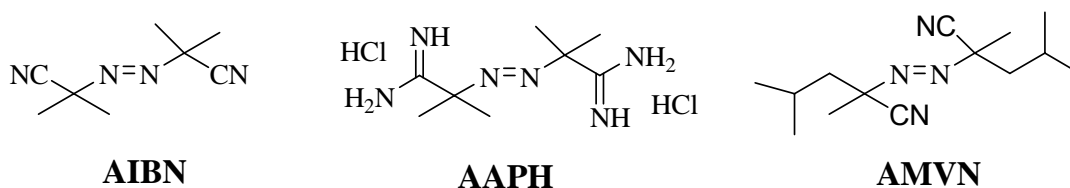
Figure I-1: Radical initiators commonly used in autoxidation experiments.

In hydrocarbon autoxidation, the observed initial rates of oxygen absorption are found to be (1) independent of oxygen, as long as the partial pressure of oxygen above the solution exceeds 100 torr, (2) one half order with respect to the concentration of the initiator, and (3) first order with respect to the concentration of the hydrocarbon. The classical mechanism for autoxidation (seen below) involves two propagation steps. A fast step (equation 4) in which oxygen adds to the intermediate alkyl radical, and a slower step (equation 5) involving hydrogen atom transfer.

Initiation:

$$R\text{-}N\text{=}N\text{-}R \rightarrow 2\,R^\bullet + N_2 \qquad (2)$$

$$R^\bullet + R_1\text{-}H \rightarrow R\text{-}H + R_1^{\,\bullet} \qquad (3)$$

Propagation:

$$R_1^{\,\bullet} + O_2 \rightarrow R_1OO^\bullet \qquad (4)$$

$$R_1OO^\bullet + R_1\text{-}H \rightarrow R_1OOH + R_1^{\,\bullet} \qquad (5)$$

Termination:

$$R_1OO^\bullet + R_1OO^\bullet \rightarrow \text{non-radical products} \qquad (6)$$
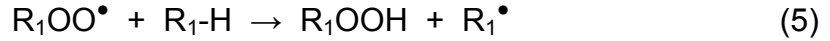
Where R-N=N-R is the initiator and $R_1^{\,\bullet}$ and $R_1OO^\bullet$ represent the chain-propagating carbon-centered radical and peroxyl radical respectively. At normal oxygen pressures, the rate constant for equation 4 is at or near the diffusion-controlled rate (between 10^8 and 10^9 $M^{-1}s^{-1}$) and the possible bimolecular termination carbon-centered radicals are not important. Under these conditions, equation 5 is the rate-limiting reaction and can be expressed by the following kinetic equation:

$$dO_2/dt = k_5[R_1OO^\bullet][R_1\text{-}H] \qquad (7)$$

Under steady state kinetics, the rate of formation of radicals from the decomposition of initiator (equation 2) is equal to the rate of disappearance of these radicals from the system via equation 8:

$$2k_2[R\text{-}N\text{=}N\text{-}R] = 2k_4[R_1OO^\bullet] \qquad (8)$$

Solving for $[R_1OO^\bullet]$ and substituting into equation 7 gives:

$$dO_2/dt = (k_5/(2k_4)^{1/2})(2k_2[R\text{-}N\text{=}N\text{-}R])^{1/2}[R_1\text{-}H] \qquad (9)$$

Which is in agreement with experiment.[21-23]

Provided that the value of $2k_2$, the rate constant for decomposition of the azo initiator, also written as k_d, is known, the ratio of the rate constants for propagation and termination, $k_5/(2k_4)^{1/2}$, can be determined from autoxidation studies. Howard and Ingold pioneered the rotating sector method,[24] which uses a combination of photochemical initiation and non-steady state techniques to determine values for k_5.[25] Because this is the rate-limiting reaction, the rate constant for this reaction is typically referred to as the propagation rate constant, k_p. The magnitude of this rate constant is almost entirely dependent upon the strength of the weakest C-H bond of the hydrocarbon.

Howard and Ingold were also able to define a range of values for k_6 (also referred to as the termination rate constant, k_t) as a function of the structure of the hydrocarbon moiety of the peroxyl radical. Primary peroxyl radicals have values of k_t in the range of 10^8 $M^{-1}s^{-1}$, secondary peroxyl radicals are in the 10^6-10^7 $M^{-1}s^{-1}$ range, and tertiary peroxyl radicals terminate between 10^3-10^5 $M^{-1}s^{-1}$ at 303 K. This ordering is consistent with the mechanism of peroxyl radical termination first proposed by Russell in his study of the oxidation of ethylbenzene.[26] The mechanism involves the formation of an intermediate tetroxide, which in the case of primary and secondary peroxyl radicals, decomposes to yield molecular oxygen, an alcohol, and a carbonyl compound:

$$2\,ROO^\bullet \rightarrow ROOOOR \rightarrow ROH + O_2 + R{=}O \tag{10}$$
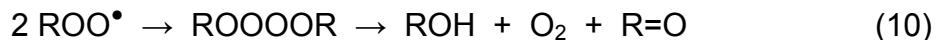
This reaction is slowed tremendously in the case of tertiary peroxyl radicals, and termination of the reaction is highly inefficient and complex in nature.[27]

Although hydrocarbon autoxidation has been studied for some time, and many of the mechanistic details have been well determined for two generations, the significance of lipid peroxidation in human health has only become evident over the last two decades. Over this time period, there has been an explosion of research in the area of radical-mediated damage to biomolecules in general, and attempts have been made to connect these events to the onset or development of various pathophysiological conditions. We now use the extent of lipid peroxidation as a marker of cellular oxidative stress.[28,29] Cellular oxidative stress is recognized to contribute to oxidative damage resulting from the metabolism of xenobiotic compounds, as well as from inflammatory processes, such as ischemia and reperfusion injury.[30,31]

Lipid peroxidation has the potential to affect humans on many levels. The peroxidation of membrane lipids can alter the structural dynamics of cell, organelle, and nuclear membranes, which affects cellular homeostasis and leads to apoptosis.[32] The peroxidation of low-density lipoproteins (LDL) lipids has been implicated in the oxidative modification of LDL and its uptake by macrophages, which are the initiating events of cardiovascular disease, such as atherosclerosis.[33] While the direct consequences of lipid peroxidation are of significance, the accumulation and fate of the secondary products of lipid peroxidation have the potential to be the most significant to human health.

Lipid hydroperoxides are the initial products of lipid peroxidation, but they are relatively short-lived species. They can either be reduced by glutathione peroxidases to unreactive lipid alcohols or they can undergo metal-catalyzed

decomposition reactions to give way to a variety of products that are generally more reactive than the parent lipid hydroperoxide. Most common among these are the electrophilic aldehydes acrolein (AC), malondialdehyde (MDA), and 4-hydroxynonenal (HNE).[34,35] Acrolein is known to cause DNA damage through cross-links.[36] Malondialdehyde is mutagenic in bacterial and mammalian cells and carcinogenic in rats.[37] 4-hydroxynonenal is weakly mutagenic but appears to be the major toxic product of lipid peroxidation.[34]

AC   **MDA**   **HNE**
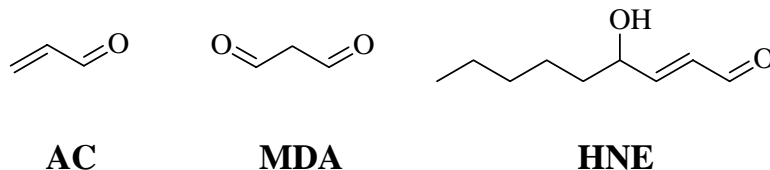
Figure I-2: Electrophilic aldehydes formed from lipid peroxidation.

To help understand the magnitude of oxidation products that can potentially form in our bodies, it is necessary to remember that most phospholipids in every membrane of every cell contain an unsaturated fatty acid residue esterified to the 2-position of the glycerol backbone. Many of these acids are polyunsaturated, and the presence of a methylene-interrupted diene such as in linoleic acid and arachidonic acid allows them to be easily oxidized. The high local concentration of these polyunsaturated fatty acids (PUFAs) in phospholipids makes the lipid bilayer a prime target for reaction with oxidizing agents and also provides the opportunity for these PUFAs to participate in lengthy free radical chain reactions. The susceptibility of the PUFAs in our membranes to oxidation

has prompted the evolution of an extensive framework of small molecule antioxidants (e.g. vitamins E and C) and enzymes (e.g. superoxide dismutase, catalase, and glutathione peroxidase) whose sole functions are to prevent radical chain oxidation of membrane lipids or to minimize damage caused by oxidation.

Phenolic Antioxidants

In 1922, Evans and Bishop found that when feeding rats a semi purified diet they would grow well, but when the female rats became pregnant, their pregnancies would not go to term.[38] Instead, their pups would either die in the womb and be resorbed, or they were born dead. When they supplemented the rats' diet with fresh lettuce, and in later studies wheat germ, healthy pups were born.[39]

Evans determined that the mysterious missing substance in the semi purified diet was present in the lipid extract of lettuce, and thus was a fat-soluble compound which prevented fetal resorption.[40] Evans also found that a deficiency of this component in the lipid extract caused damaging lesions in the testis and uterus of rats.[41,42] Dr. Barnett Sure at the University of Arkansas and Dr. H. A. Mattill at the University of Iowa, independently found that a missing factor in the diet made male rats sterile and atrophied their testis.[43] Evans proposed in 1925 that this mystery compound should be referred to as Vitamin E, as it was an essential element for life.[44]

Following these three influential studies, the next decade revealed several physiological consequences of Vitamin E deficiency beyond fetal resorption in

female rats and sterility in male rats. The most profound were muscle atrophy and adverse affects on the nervous system. Also described were chicken encephalomalacia, muscular dystrophy in guinea pigs and rabbits, and paralysis of baby rats suckling Vitamin E deficient mothers.[45-48]

In 1926, Evans and his group isolated an alcohol by distillation from plant oils. The properties of this alcohol were consistent with those of Vitamin E.[49] His group proposed the correct formula for α-tocopherol, the first isolated form of Vitamin E, now known as the most potent form. β- and γ-tocopherol were isolated by Evans in 1937.[50] Olcott and Emerson found the tocopherols to have the following relative activity as antioxidants: $\alpha > \beta > \gamma$.[51] Fernholtz determined the structure of α-tocopherol in 1938 (Figure I-3).[43]

	R_1	R_2
α	CH_3	CH_3
β	CH_3	H
γ	H	CH_3
δ	H	H
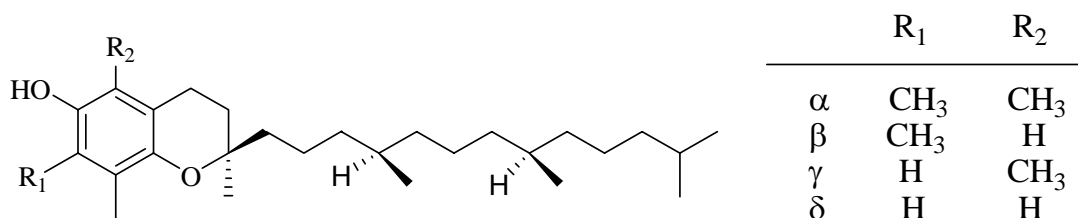
Figure I-3: The tocopherols.

Early structure activity studies of phenolic antioxidants revealed qualitative results similar to what investigators have more recently found experimentally. These early studies, done largely by Mattill and Olcott, revealed the basic requirements for a good antioxidant by measuring the induction period in rancidity tests with either lard or mixtures of lard and cod liver oil as the substrate fats.[52,53] Results were interpreted in terms of the ratio of the induction period with

10

inhibitor to that of the unprotected fat, known as the antioxidant index. Some general structure-activity relationships were derived from these antioxidant indices:

1.   An alcohol group directly attached to an aromatic ring (i.e., a phenolic moiety) is absolutely required. The monomethyl ether of hydroquinone was active, but the dimethylether was inactive.

2.   Substitution with electron-releasing groups at the ortho- and para-positions relative to the phenolic group increases the effectiveness of the phenol. Meta-substituents appeared to have no effect.

The mechanism of the inhibition lipid autoxidation by phenolic antioxidants did not become clear until the appropriate physical methods were available to study autoxidation. Much of this work, done by Ingold and co-workers in the 1960s, and then for Vitamin E in the 1980s, provided our current understanding of this topic.[54-62]

It is well established that phenolic compounds act as antioxidants by interrupting the free radical chain process.[63] This chain-breaking occurs by transfer of the phenolic hydrogen atom to a chain-carrying peroxyl radical, forming a hydroperoxide and phenoxyl radical:

$$ArOH + ROO^\bullet \rightarrow ArO^\bullet + ROOH \hspace{2cm} (11)$$

The phenoxyl radical is sufficiently stabilized so that it can no longer propagate the chain reaction by either of the two propagation steps: reaction with another substrate (R-H) to generate a carbon centered radical ($R^\bullet$) or reaction with

oxygen to yield an intermediate that reacts with R-H. The rate constant for equation 11 is commonly referred to as the inhibition rate constant, k_{inh}.

It has been shown for some time that, during lipid autoxidation, two oxidative chains are broken for every one molecule of antioxidant consumed.[64] The second chain is broken according to equation 12:

$$ArO^{\bullet} + ROO^{\bullet} \rightarrow \text{non-radical products} \qquad (12)$$

Although this is quite general, the first reaction is likely to be addition of the peroxyl radical at the C4 position of the phenol to generate the product in equation 13.

$$ROO^{\bullet} \;+\; \underset{R_4 \quad\quad R_6}{\overset{R_2}{\text{phenol}}}\!\!\text{-OH} \longrightarrow \underset{R_4 \quad\quad R_6}{\overset{R_2}{\text{ROO-cyclohexadienone}}}\!\!\text{=O} \qquad (13)$$
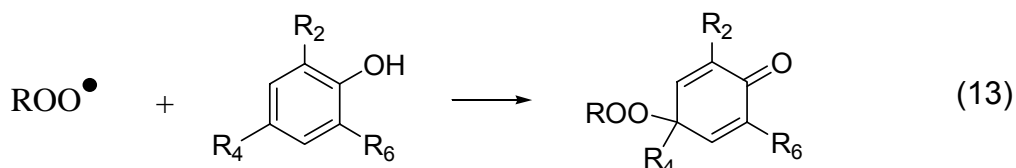
This final compound decomposes to form non-radical products.[64]

The intervention and sacrificial service of the phenolic compound as an antioxidant relies heavily on the relatively slow rate of chain propagation.[25] Typical second-order rate constants for the reactions of phenols with peroxyl radicals range from 10^3-10^6 M^{-1}s^{-1}.[54-62] There are two main reasons for the speed with which these reactions occur: 1) the relatively high (88-90 kcal mol^{-1}) O-H BDE in the hydroperoxide formed[65] and the relatively low (<88 kcal mol^{-1}) O-H BDE of the phenol;[66] and 2) the low triplet-repulsion in the transition state for hydrogen atom transfer reactions between two oxygen atoms.[67,68]

The competition between the phenol and the other chain-propagating reaction, the addition of oxygen to the carbon-centered radical (equation 14), is generally less important:

$$ArOH + R^\bullet \rightarrow ArO^\bullet + R\text{-}H \qquad (14)$$
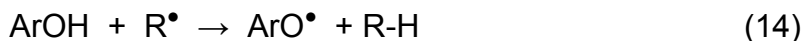
This is due to the diffusion-controlled reaction of molecular oxygen with most carbon-centered radicals to generate the chain-carrying peroxyl radical. In order for the antioxidant to compete effectively with oxygen addition the antioxidant must be present in a 10^4 to 10^5-fold higher concentration than oxygen because phenols react with primary alkyl radicals with second order rate constants in the range of 10^3 to 10^5 $M^{-1}s^{-1}$.[69] Because the solubility of O_2 in most non-polar organic solvents is 10^{-3} to 10^{-4} M, this is a condition rarely met, and only likely occurs in situations where the partial pressure of oxygen is very low.

Because the O-H BDEs of alkyl hydroperoxides are essentially constant around 88-90 kcal mol^{-1}, the O-H BDEs of phenols are more important in predicting the rate with which a phenol will react with a peroxyl radical. Good correlation between the O-H BDE and k_{inh} for phenols has been known since the early calorimetric work of Mahoney and DaRooge.[70] Since then, the O-H BDEs of a variety of substituted phenols have been measured in solution by various methods, including photoacoustic calorimetry,[66] electrochemistry,[71] and EPR using the radical equilibration technique.[72] These methods have served to validate one another, and it is now well accepted that the O-H BDE in phenol is 87-88 kcal mol^{-1}, and the O-H BDE in α-tocopherol is 77-78 kcal mol^{-1}. The

substituents on the phenolic ring of α-tocopherol produce a bond-weakening effect of 10 kcal mol^{-1} on the O-H bond compared to the unsubstituted phenol.

Because free radicals have been implicated in virtually every degenerative disorder from heart disease to Alzheimer's disease, there appears to be room for antioxidants to play a positive role, if not as therapeutic agents, then as preventative agents. The strong case for a destructive role of lipid peroxidation in human health has been made by looking at the accumulation of oxidized biomolecules, the harmful effects of these biomolecules *in vitro* and *in vivo* when subjected to oxidations, and the effect that antioxidants have on these processes. Because it has been shown *in vitro* that phenolic chain-breaking antioxidants such as α-tocopherol inhibit the oxidation of many lipids under various conditions, it stands to reason that they may do so *in vivo* as well.

The largest body of evidence for positive effects of α-tocopherol is derived from studies on its use as a preventative agent in the development of cardiovascular disease (CVD). CVD is the most common cause of death for both men and women in the United States each year. High levels of total plasma cholesterol (>200 mg/dl) and low-density lipoprotein (LDL, >130 mg/dl) have been identified as primary risk factors in the development of CVD. In contrast, low levels of high-density lipoprotein (HDL, <35 mg/dl) also correlate with an increase in CVD.[73,74]

Lipoproteins function as a vehicle for the body to transport insoluble, or slightly soluble, cholesterol and lipids through the bloodstream. The most commonly studied lipoprotein in the human body is LDL (Figure I-4), but there

are four other types of lipoproteins in human blood plasma which are classified by their density. Lipoproteins containing more lipids and less protein are of lower density, and those containing fewer lipids and more protein are of higher density. The classes of lipoproteins from lowest to highest density are: chylomicrons (CM), very-low density lipoproteins (VLDL), low density lipoproteins (LDL), intermediate density lipoproteins (IDL), and high density lipoproteins (HDL).

PROTEIN (~22%)
Apo B-100 1 molecule/LDL (550 kDa)

POLAR COAT LIPIDS
PC   ~700 molecules/LDL
        (~400 LH groups/LDL)
Cholesterol ~600 molecules/LDL

NEUTRAL CORE LIPIDS
Cholesteryl esters
        Ch18:2 ~720 LH groups/LDL
        Ch20:4 ~180 LH groups/LDL
Triacylglycerols (~10%)
        TG (18:2) ~150 LH groups/LDL

LIPOPHILIC ANTIOXIDANTS
α-TOH ~6-12molecules/LDL
γ-TOH ~0.5 molecules/LDL
ubiquinol-10 ~0.8 molecules/LDL

Phospholipid (~22%)

Cholesterol (~8%)

Cholesteryl ester (~38%)

LH group

Figure I-4: A schematic representation of the structure and function of an LDL particle.[75]

Each lipoprotein has a different role in cholesterol transport and metabolism. Cholesterol is synthesized in the liver and is delivered to tissues throughout the body as fatty acid esters by LDL. HDL collects excess or modified cholesterol and lipids from tissues to be removed from circulation. Therefore, LDL, commonly referred to as "bad" cholesterol, and HDL, considered the "good" cholesterol have attracted the most attention from the health science community for their potential involvement in CVD.

It is generally thought that the oxidation of fatty acids within the LDL particle is the first essential step in the oxidative modification of LDL. The oxidatively-modified LDL has different biological properties than the unmodified LDL, resulting in interactions with scavenger receptors on the surface of macrophages and smooth muscle cells. These interactions induce the formation of "foam" cells overloaded with lipids, a major factor in arterial narrowing. Given the implication of fatty acid oxidation in this mechanism, much work has gone into better understanding the role of the small molecule antioxidants in the LDL particle (α- and γ-tocopherol, ubiquinol-10, and carotenoids) in preventing LDL oxidation.[76-84]

Free-Radical Clocks

Griller and Ingold stated in 1980 that there is no general method for measuring the absolute rate constants of radical-molecule reactions.[85] One of the most common examples for measuring these rate constants is the rotating sector method. However, this method is restricted to radical chain processes

16

that can be initiated photochemically and are terminated by radical-radical reactions. The chain must be relatively long, and therefore the radical propagation steps must be quite rapid. Although this technique has proved valuable in kinetic studies of autoxidation and radical polymerization, there are many radical-molecule reactions that would be difficult or impossible to make into the rate-controlling propagation step of a chain reaction. Some of these types of reactions are amenable to study by flash photolysis, pulse radiolysis or other special techniques, but many are not.[86]

The 5-hexenyl radical cyclization (Figure I-5) is one of the better known radical clocks used to determine the rate constant k_H, for abstraction of a hydrogen atom from a substrate A-H by a primary carbon-centered radical (equation 15).

$$R^\bullet + A\text{-}H \rightarrow R\text{-}H + A^\bullet \tag{15}$$
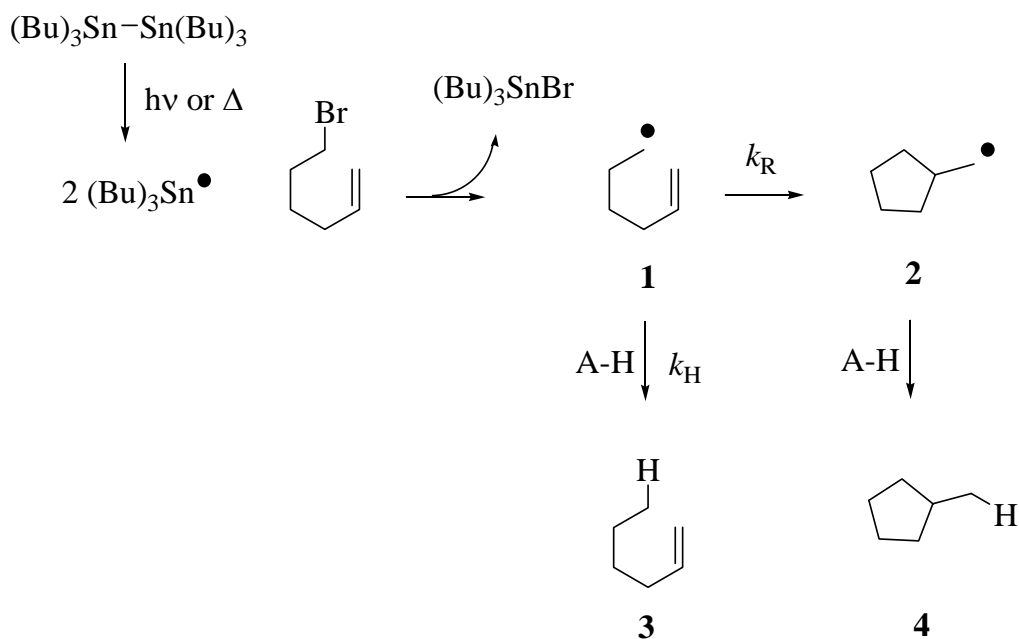
Figure I-5: The 5-exo-trig cyclization of the 5-hexen-1-yl radical as a radical clock.

17

A simple kinetic analysis of the competition of Figure I-5 reveals that the product ratio [**3**]/[**4**] is directly proportional to the unknown rate constant k_H, with the proportionality constant being the rate constant for the radical cyclization (k_R) over the concentration of A-H (equation 19).

$$d[\mathbf{3}]/dt = k_H[\text{A-H}][\mathbf{1}] \tag{16}$$

$$d[\mathbf{4}]/dt = k_R[\mathbf{1}] \tag{17}$$

$$[\mathbf{3}]/[\mathbf{4}] = (k_H[\text{A-H}])/k_R \tag{18}$$

$$k_H = (k_R/[\text{A-H}])([\mathbf{3}]/[\mathbf{4}]) \tag{19}$$

This is an incredibly powerful approach and has been used to study various radical-molecule reactions.[87,88]

Due to the large volume of literature documenting kinetics of carbon-skeleton rearrangements (including cyclizations) of alkyl radicals, the radical clock method is ideally suited for hydrogen atom abstractions by alkyl radicals. Because of this, dozens of clocks have been calibrated in order to determine rate constants for equation 15 anywhere from 0.1 to 10^{13} $M^{-1}s^{-1}$. This methodology has been used to study the kinetics of phenolic and 5-pyrimidinolic radical scavengers (ArOH).[89,90]

The reduction of alkyl radicals by phenolic compounds in equation 14 is an important chain-breaking reaction in radical polymerization, and as such, understanding the kinetics of the reaction is very important in the design of better polymerization inhibitors and/or monomer stabilizers. A lot can be considered anecdotal about the usefulness of a phenol as an antioxidant from the kinetics in equation 14, because it is generally unimportant in the context of autoxidation

18

because alkyl radicals undergo diffusion-controlled reactions with molecular oxygen to produce peroxyl radicals. Therefore, the more important chain-breaking reaction for radical trapping antioxidants is the reduction of peroxyl radicals, seen in equation 11.

Rate constants for equation 11, commonly referred to as inhibition rate constants, $k_{inh,}$ are typically determined by studying the antioxidant-inhibited autoxidation of an oxidizable substrate.[64] Styrene is the most commonly used substrate for these experiments and the consumption of oxygen is monitored in the presence, and absence, of an antioxidant. Unfortunately, these experiments are time-consuming and present some limitations. They require a rather extensive experimental setup because oxygen consumption is usually monitored by either a pressure transducer or EPR spectroscopy using a nitroxide spin probe.[91-93] For those antioxidants where no clear induction period exists, a series of autoxidations need to be performed with a wide range of antioxidant concentrations.[94] Given the relative ease with which conventional radical clock methods are carried out, and the lack of any requirement for specialized equipment, it would be very convenient to have a radical clock approach for the measurement of rate constants for equation 11.

The Allylperoxyl Radical Rearrangement

The principle chain-carrying radicals in the autoxidation of olefins are known as allylperoxyl radicals. These allylperoxyl radicals undergo [1, 3]-rearrangements in which the oxygen atoms migrate across the allylic backbone

(Figure I-6). The [1, 3]-allylperoxyl rearrangement is believed to be free radical in nature because this rearrangement can be initiated and inhibited with known radical initiators and inhibitors. Peroxyl radicals are known to propagate the free radical chain sequence by hydrogen atom transfer from a parent hydroperoxide to product peroxyl radicals. The mechanism of the allylperoxyl rearrangement has long been debated with several mechanisms proposed.
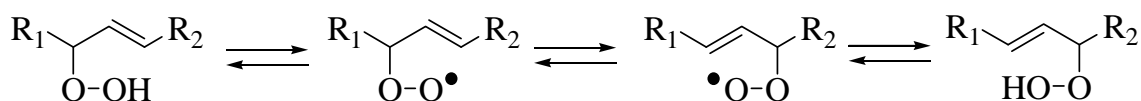
Figure I-6: The [1, 3]-allylperoxyl rearrangement.

The three most often suggested mechanisms for the [1, 3]-allylperoxyl rearrangement are shown in Figure I-7. In 1965, Brill made the first concrete proposal for the [1,3]-allylperoxyl rearrangement mechanism when he suggested a stepwise mechanism involving a 1,2-dioxolan-4-yl radical intermediate, **5**.[95] It has also been recognized that other viable possibilities include a concerted pathway (transition state **6**) or a stepwise mechanism involving fragmentation to a dioxygen-allyl radical pair, as shown in **7**.

The allylperoxyl rearrangement is frequently called the Schenck rearrangement because it was first described by Schenck and co-workers in 1958 when a novel rearrangement of a steroidal allylic hydroperoxide (**8**) occurred, leading to its regioisomer (**9**) (Figure I-8).[96] Fifteen years later, it was shown by Smith that a second, slower, rearrangement occurred leading to compound **10**.[97] In 1989, with the same steroidal system, Beckwith and Davies

performed the rearrangement under an atmosphere of $^{36}O_2$ and observed no ^{18}O incorporation into **9**, whereas **10** contained 73-83% ^{18}O.[98] It was suggested by these authors that the rearrangement of **8** to **9** involved a concerted mechanism, and the rearrangement of **9** to **10** proceeded via a dissociative mechanism
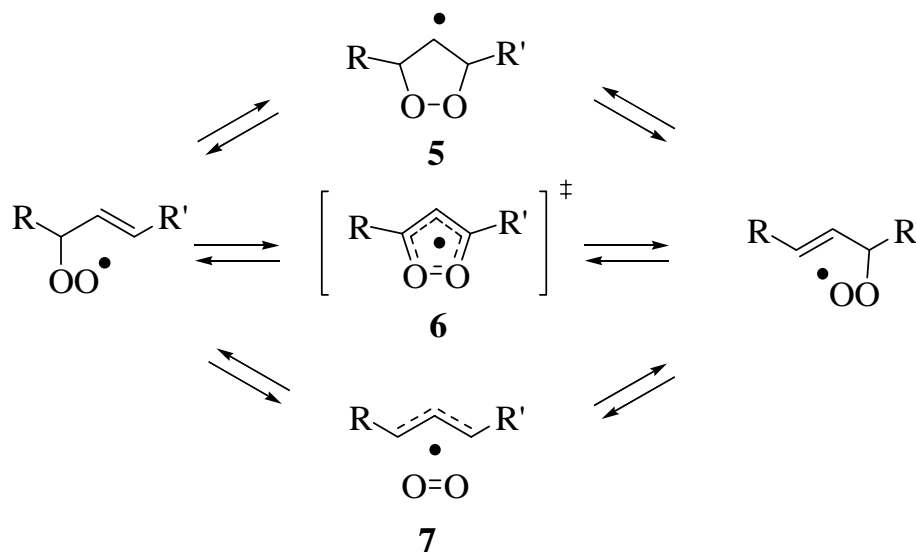
Figure I-7: Suggested mechanisms for the [1, 3]-allylperoxyl rearrangement.
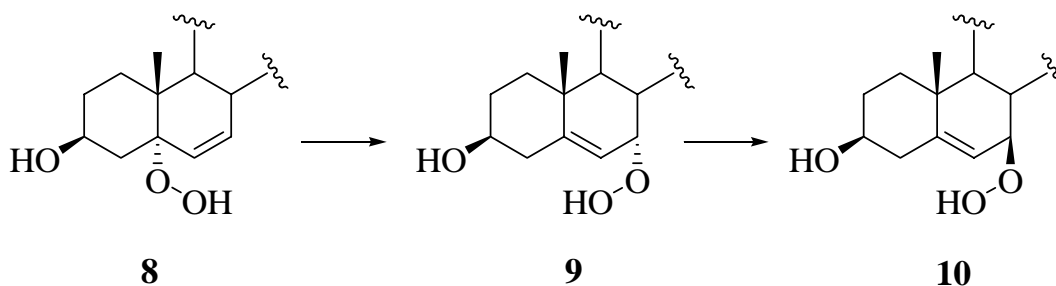
Figure I-8: The rearrangement of a steroidal allylic hydroperoxide.[99]

The initial work of Brill detailed the free radical rearrangements of (*E*)-2-hydroperoxy-2-methyl-3-pentene and its allylic isomer (*E*)-2-hydroperoxy-4-

methyl-3-pentene (Figure I-9). He observed that either the tertiary or the secondary isomer rearranges to an equilibrium mixture containing equal amounts of both hydroperoxides. Brill concluded that the rearrangement involved the five-membered cyclic dioxolanyl radical, **11**.[95,100]
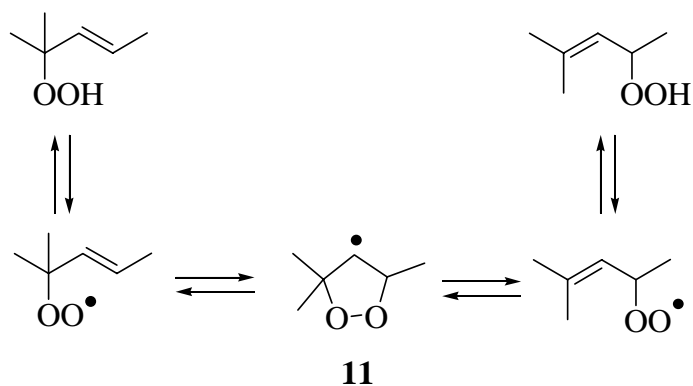
Figure I-9: Brill's mechanism of the [1, 3]-allylperoxyl rearrangement.

Subsequent work by Brill with the pinene derived hydroperoxides **12** and **13** disputed the possibility of a dioxolanyl radical intermediate when it was shown that the proposed intermediate **14** would not fragment to give the rearranged product **15**, nor be trapped by molecular oxygen to give **16** (Figure I-10).[101] The lack of evidence for products **15** or **16** strongly suggested that intermediate **14** was not involved in the [1, 3]-allylperoxyl rearrangement mechanism.

The final convincing evidence against the dioxolanyl radical intermediate was provided by Porter and Zuraw who independently synthesized a localized dioxolanyl radical and demonstrated that it could be trapped with molecular oxygen and did not suffer ring opening to peroxyl radicals (Figure I-11).[102] The

proposed intermediate **17** was synthesized from a mercuric bromide precursor and was successfully trapped with O_2 to give **18**. These studies suggested that in Brill's experiment (Figure I-9) oxygen entrapment should have occurred if the dioxolanyl radical was a discrete intermediate, and no such product was found.
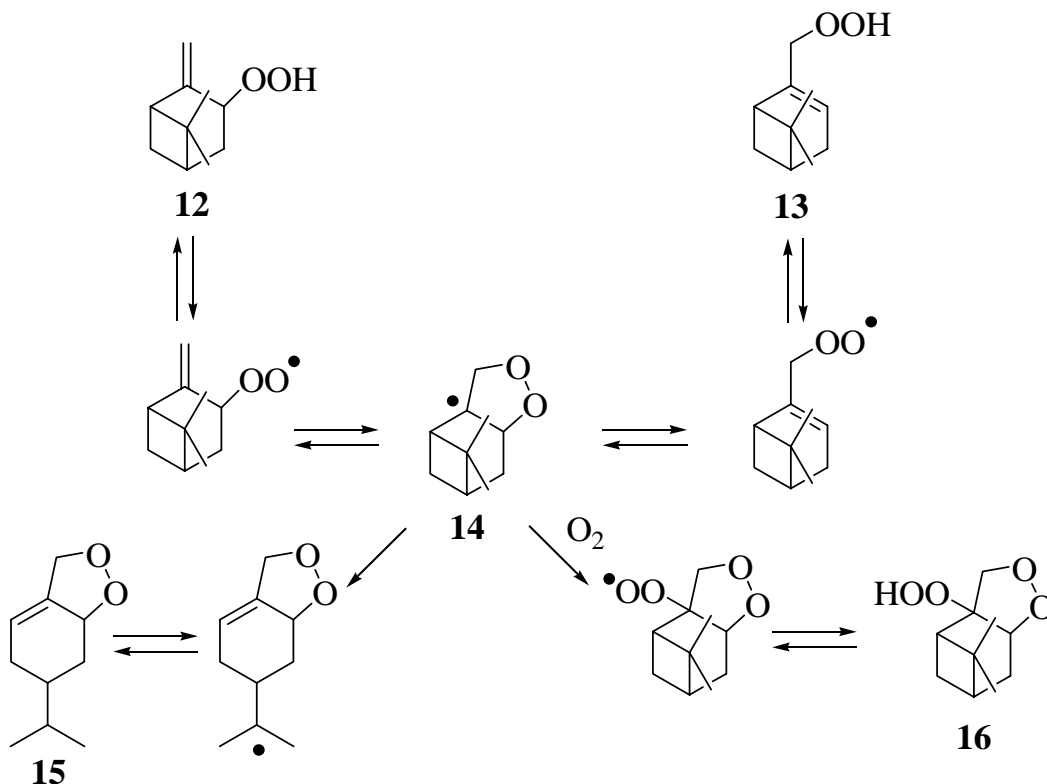
Figure I-10: The [1, 3]-allylperoxyl rearrangement of pinene derived hydroperoxides.
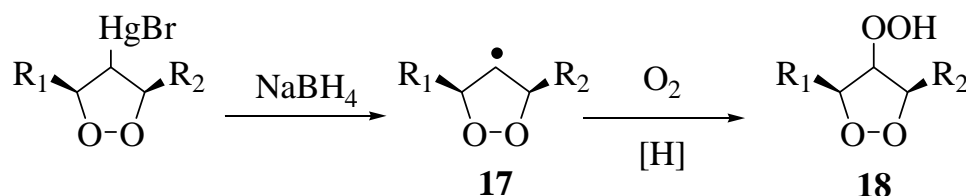
Figure I-11: Oxygen entrapment of a localized dioxolanyl radical.

Chan has shown that thermal rearrangement of ^{18}O labeled radical **19** derived from methyl linoleate, undergoes rearrangement under an $^{32}O_2$ atmosphere to give products corresponding to **20** and **21** in which atmospheric oxygen has been incorporated (Figure I-12).[103] This suggests a fragmentation mechanism to give a pentadienyl radical intermediate. However, a direct expansion to the allylperoxyl rearrangement cannot be assumed because of the fact that the dienyl radical has a much larger driving force for fragmentation; 11-14 kcal mol^{-1} more resonance stabilization energy than the allyl radical.[104]
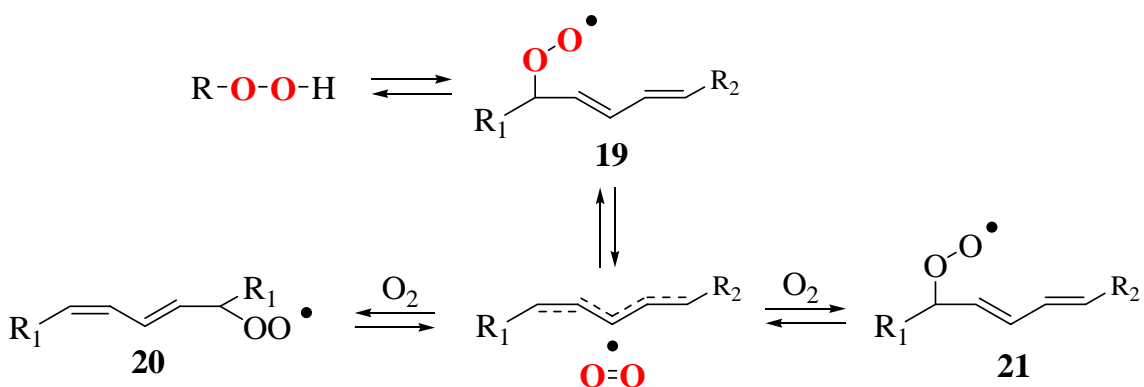
Figure I-12: Chan's thermal rearrangement of ^{18}O labeled methyl linoleate hydroperoxides.

The previously mentioned studies by Beckwith and Davies were paralleled by Porter and Wujek in order to distinguish between a concerted and a fragmentation pathway. Rearrangement of ^{18}O labeled (*E*)-9-hydroperoxyoctadec-10-enoic acid, **22**, under an atmosphere of $^{32}O_2$ led to no ^{16}O incorporation into the rearrangement product, **23** (Figure I-13A).[105] The authors showed that the rearrangement of **22** to **23** also proceeded with no

atmospheric oxygen incorporation. The results of these studies are in contrast to those obtained by Chan in the dienyl peroxyl rearrangements, but do not rule out the possibility of a caged radical pair species or a concerted rearrangement mechanism.

Further experiments by the Porter group with optically pure methyl oleate hydroperoxides (Figure I-13B) showed the peroxyl radical **24** at 40°C in hexane rearranged to **25** with essentially complete retention of stereochemical integrity, and *vice versa* for **24** to **25**.[106] Based on the observed stereochemistry and the labeling studies, the authors proposed an envelope-type transition state which collapses with ubiquitous retention of configuration.

A.

$$R_1 \diagup\diagdown R_2 \rightleftharpoons R_1 \diagup\diagdown R_2 \xrightarrow{O_2} R_1 \diagdown\diagup R_2 \rightleftharpoons R_1 \diagup\diagdown R_2$$

HO-O   •O-O   O-O•   O-OH

22   **23**

$$R_1 = C_7H_{15}, \; R_2 = (CH_2)_7CO_2H$$

B.

24   **25**
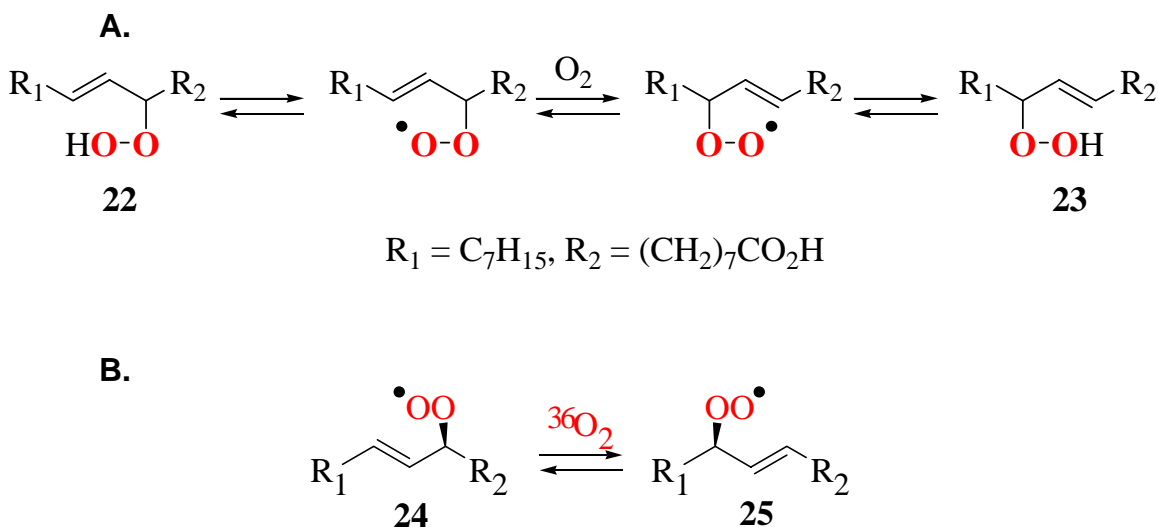
Figure I-13: Porter's studies of [1, 3]-allylperoxyl radical rearrangement in the oleate peroxyl system.

High level molecular orbital calculations by Boyd failed to find a concerted transition state as either minima or maxima on the energy surface of the

rearrangement. However, it was found that dioxolanyl radicals are minima on the energy surface, but the barrier to their formation and opening is prohibitively high. These calculations suggest that the lowest energy pathway is a fragmentation to give an allyl radical and oxygen within a solvent cage.[107] A more recent theoretical investigation by Olivella and Sole reinforces the findings of Boyd and shows that a loosely-bound radical-dioxygen caged pair is lower in energy than β-fragmentation to an allyl radical and molecular oxygen.[108] The transition state to this caged pair however, was calculated to be higher in energy than the free allyl radical and oxygen.

Another piece of evidence which has been obtained on the [1, 3]-allylperoxyl rearrangement was conducted by Porter and Mills who reinvestigated the rearrangements of optically pure *trans*-oleate peroxyl radicals in solvents of differing viscosity under a $^{36}O_2$ atmospheres.[109,110] Purposes of this study were to determine if there are observable cage effects in the rearrangement, as an allyl radical-dioxygen caged pair mechanism would suggest; and if so, how does solvent viscosity and temperature affect the stereo selectivity?

The generation of optically pure radical **26** in hydrocarbon solvents of varying degrees of viscosity, and under a $^{36}O_2$ atmosphere, gave rearranged products **27** and **28**. It was determined that products which did not contain ^{18}O (**27**) were formed with retention of stereochemistry and products which did contain ^{18}O (**28**) were formed with random stereochemistry, as Figure I-14 shows. It was also found that the ratio of products **27** and **28** was highly dependent on solvent viscosity. In less viscous solvents there was more **28**

formed with an identical decrease in the production of **27**. Lastly, the stereoselectivity of product **27** was found to be independent of solvent viscosity.[109,110]
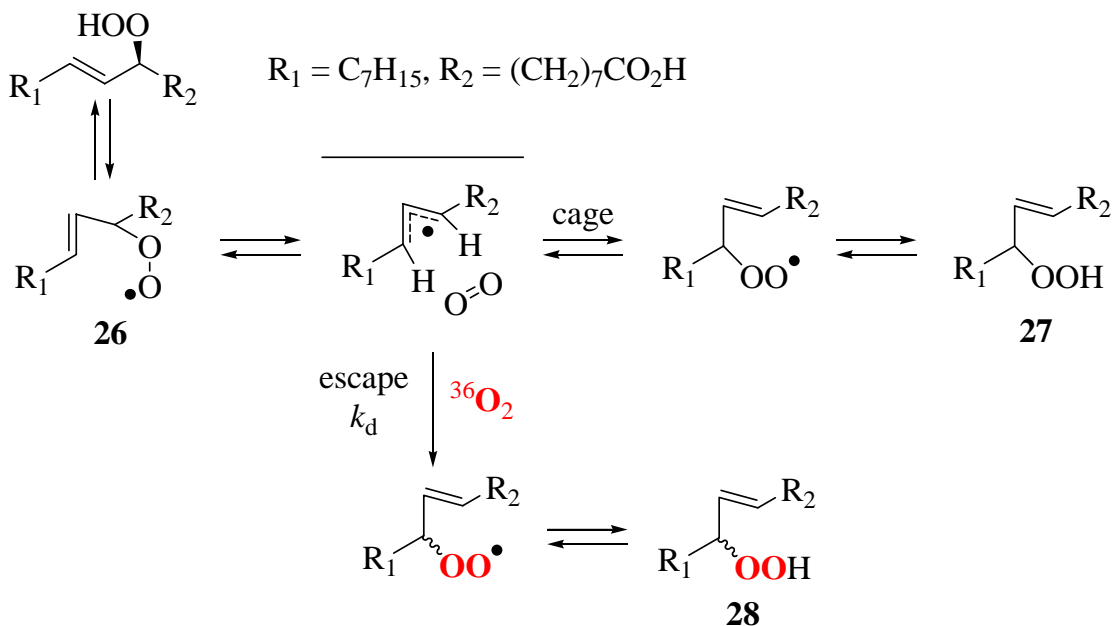
Figure I-14: Porter and Mills' investigation into the [1, 3]-allylperoxyl rearrangement using solvent with differing viscosity.

The simplest mechanism based on these rather complex yet well-designed experiments, coupled with theoretical calculations, involves an allyl radical-dioxygen caged pair that collapses with stereochemical memory at a rate faster than the diffusion controlled process, k_d. Allyl radicals which diffuse into solution incorporate labeled oxygen with racemization of stereochemistry, suggesting a planar allyl radical which escapes the initial solvent cage. These studies indicate that solvent viscosity affects the partitioning between escape and collapse as the pair collapsed product forms with a high degree of

stereoselectivity. Analogous stereochemical and solvent viscosity studies performed on *cis*-allyl hydroperoxides gave very similar results.[110]

The use of unsymmetrically labeled hydroperoxides have also been employed to study the [1, 3]-allylperoxyl rearrangement. Results of these studies show that a competition exists between a concerted [1, 3] transfer of oxygen, and an allyl-dioxygen pair (Figure I-15). Solvent studies with unsymmetrically labeled hydroperoxides indicated that solvent viscosity affects the partitioning between escape and cage collapse of the allyl-dioxygen caged pair. An increase in solvent viscosity results in a decrease in escape product and an increase in radical pair collapse.[111]
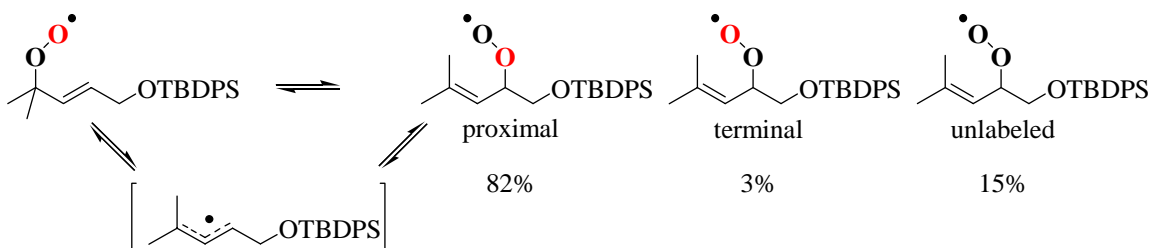
Figure I-15: The results of Lowe and Porter's ^{18}O unsymmetrically labeled allylperoxyl rearrangement experiments at 40°C with their proposed mechanism.[112]

Dissertation Aims

1. To determine and show the effect of olefin geometry on the oxidizability of biologically relevant polyunsaturated fatty acids

2. To introduce allylbenzene derived peroxyl radical clocks used to determine rate constants of hydrogen atom transfer processes in the 10^4 to 10^6 M^{-1}s^{-1} range.

3. To further discuss the allylperoxyl radical rearrangement. To give more insight into the mechanism of the rearrangement as well as introduce different techniques and substrates that can aid in its elucidation.

4. To introduce a peroxyl radical clock based upon methyl linoleate oxidation that can be used to determine rate constants for the propagation of hydrocarbons (R-H) in the range of 10^0 to 10^4 $M^{-1}s^{-1}$.

References

(1) Sausure, T. D. *Recherches Chimiques sur la vegetation*: Paris, 1804.

(2) Holm, G. E.; Greenbank, G. R.; Deysher, E. F. *Ind. Eng. Chem.* **1927**, *19*, 156.

(3) Kuhn, R.; Meyer, K. Z. *Physiol. Chem.* **1929**, *185*, 193.

(4) Stephens, N. H. *J. Am. Chem. Soc.* **1928**, *50*, 568.

(5) Creigee; al, e. *Chem. Ber.* **1939**, 1799.

(6) Bolland, J. L. *Quart. Reviews (London)* **1949**, *3*, 1.

(7) Mahoney, L. R. *Angew. Chem. Intl. Ed.* **1969**, *8*, 547-555.

(8) Walling, C. *Free Radicals in Solution*; Wiley: New York, 1957.

(9) Kellogg, E. W. I.; Fridovich, I. *J. Biol. Chem.* **1977**, *252*, 6721.

(10) Lynch, R. E.; Fridovich, I. *J. Biol. Chem.* **1978**, *253*, 1838.

(11) Fridovich, I. *Acc. Chem. Res.* **1972**, *5*, 321.

(12) Diguiseppi, J.; Fridovich, I. *CRC Crit. Rev. Toxicol.* **1984**, *12*, 315.

(13) Hamburg, M.; Samuelsson, B. *Proc. Natl. Acad. Sci. USA* **1974**, *70*, 899.

(14) Adams, J.; Fitzsimmons, B. J.; Girard, Y.; Leblanc, Y.; Evans, J. F. et al. *J. Am. Chem. Soc.* **1985**, *107*, 464.

(15)   Serhan, C. N.; Hamburg, M.; Samuelsson, B. *Proc. Natl. Acad. Sci. USA* **1984***, 81*, 5335.

(16)   *Free Radicals, Lipid Peroxidation, and Cancer*; Academic Press: London, 1982.

(17)   Dix, T. A.; Marnett, L. J. *Science* **1983***, 221*, 77.

(18)   Terman, A.; Brunk, U. T. *APMIS* **1998***, 106*, 265-276.

(19)   Szweda, P. A.; Camouse, M.; Lundberg, K. C.; Oberley, T. D.; Szweda, L. I. *Ageing Research Reviews* **2003***, 2*, 383-405.

(20)   Keller, J. N.; Dimayuga, E.; Chen, Q.; Thorpe, J.; Gee, J. et al. *International Journal of Biochemistry & Cell Biology* **2004***, 36*, 2376-2391.

(21)   Howard, J. A.; Ingold, K. U. *Can. J. Chem.* **1968***, 46*, 2601-2606.

(22)   Howard, J. A.; Ingold, K. U. *Can. J. Chem.* **1965***, 43*, 2729-2736.

(23)   Gardner, D. V.; Howard, J. A.; Ingold, K. U. *Can. J. Chem.* **1964***, 42*, 2847-2851.

(24)   Howard, J. A. *Adv. Free Rad. Chem.* **1972***, 4*, 49-173.

(25)   Howard, J. A.; Ingold, K. U. *Can. J. Chem.* **1967***, 45*, 793.

(26)   Russell, G. A. *J. Am. Chem. Soc.* **1957***, 79*, 3871.

(27)   Howard, J. A.; Ingold, K. U. *J. Am. Chem. Soc.* **1968***, 90*, 1056.

(28)   Awad, J. A.; Morrow, J. D.; Takahashi, K.; Roberts, L. J. *J. Biol. Chem.* **1993***, 268*, 4161-4169.

(29)   Morrow, J. D.; Roberts, L. J. *Biochem. Pharmacol.* **1996***, 51*, 1-9.

(30)   Ames, B. N. *Mutat. Res.* **1989**, 41-46.

(31)   Dargel, R. *Exp. Toxicol. Pathol.* **1992***, 44*, 169-181.

(32)   Sevanian, A.; Ursini, F. *Free Rad. Biol. Med.* **2000***, 29*, 306-311.

(33)   Chisolm, G.; Steinberg, D. *Free Rad. Biol. Med.* **2000***, 28*, 1815-1826.

(34)   Esterbauer, H.; Schaur, R. J.; Zollner, H. *Free Rad. Biol. Med.* **1991***, 11*, 81-128.

(35)   Schauenstein, E.; Esterbauer, H. *Submol. Biol. Cancer Ciba Fnd.* **1978***, 67*, 225-241.

(36)   Kurtz, A. J.; Lloyd, R. S. *J. Biol. Chem.* **2003***, 278*, 5970-5976.

(37)   Marnett, L. J. *Mutat. Res.* **1999***, 424*, 83-95.

(38)   Evans, H. M.; Bishop, K. S. *Science* **1922***, 56*, 650-651.

(39)   Emerson, G. A.; Evans, H. M. *Journal of Nutrition* **1937***, 14*, 169-178.

(40)   Evans, H. M.; Burr, G. O. *Proc. Natl. Acad. Sci.* **1925***, 11*, 334-341.

(41)   Evans, H. M. *Journal of Nutrition* **1928***, 1*, 1-2.

(42)   Evans, H. M.; Lepkovsky, S.; Murphy, E. A. *J. Biol. Chem.* **1934***, 106*, 445-450.

(43)   Papas, A. M. The Vitamin E Factor; Harper Collings: New York, 1999.

(44)   Raacke, I. D. *Nutrition* **1983***, 113*, 929-943.

(45)   Evans, H. M.; Burr, G. O. *J. Biol. Chem.* **1928***, 76*, 273-297.

(46)   Sure, B.; Kik, M. C.; Walker, D. J. *J. Biol. Chem.* **1929***, 83*, 401-408.

(47)   Adamstone, F. B. *J. Morph. Phys.* **1931***, 52*, 47-90.

(48)   Barnum, G. L. *J. Nutr.* **1935***, 9.*

(49)   Evans, H. M.; Emerson, O. H.; Emerson, G. A. *J. Biol. Chem.* **1936***, 112*, 319.

(50)   Emerson, O. H.; Emerson, G. A.; Mohammad, A.; Evans, H. M. *J. Biol. Chem.* **1937***, 122*, 99-107.

(51)   Olcott, H. S.; Emerson, O. H. *J. Am. Chem. Soc.* **1937***, 59*, 1008-1009.

(52)   Mattill, H. A. *J. Biol. Chem.* **1931***, 90*, 141.

(53)   Olcott, H. S. *J. Am. Chem. Soc.* **1934***, 56*, 2492-2493.

(54)   Howard, J. A.; Ingold, K. U. *Can. J. Chem.* **1962***, 40*, 1851-1864.

(55)   Howard, J. A.; Ingold, K. U. *Can. J. Chem.* **1963***, 41*, 2800-2806.

(56)   Howard, J. A.; Ingold, K. U. *Can. J. Chem.* **1963***, 41*, 1744-1751.

(57)   Howard, J. A.; Ingold, K. U. *Can. J. Chem.* **1964***, 42*, 1044-1056.

(58)   Brownlie, I. T.; Ingold, K. U. *Can. J. Chem.* **1966***, 44*, 861-868.

(59)   Brownlie, I. T.; Ingold, K. U. *Can. J. Chem.* **1967***, 45*, 2419-2425.

(60)   Burton, G. W.; Le Page, Y.; Gabe, E. J.; Ingold, K. U. *J. Am. Chem. Soc.*
        1980*, 102*, 7791-7792.

(61)   Burton, G. W.; Ingold, K. U. *J. Am. Chem. Soc.* **1981***, 103*, 6472-6477.

(62)   Burton, G. W.; Doba, T.; Gabe, E. J.; Hughes, L.; Lee, F. L. et al. *J. Am.
        Chem. Soc.* **1985***, 107*, 7053-7065.

(63)   Bolland, J. L.; Ten Haave, P. *Trans. Faraday Soc.* **1947***, 43*, 201.

(64)   Ingold, K. U. *Acc. Chem. Res.* **1969***, 2*, 1-9.

(65)   Luo, Y.-R. *Handbook of Bond Dissociation Energies in Organic
        Compounds*; CRC Press: Boca Raton, FL, 2003; 166-170.

(66)   Laarhoven, L. J. J.; Mulder, P.; Wayner, D. D. M. *Acc. Chem. Res.* **1999***,
        32*, 342-349.

(67)   Zavitsas, A. A.; Melikian, A. A. *J. Am. Chem. Soc.* **1975***, 97*, 2757-2763.

(68)   Zavitsas, A. A.; Chatgilialoglu, C. *J. Am. Chem. Soc.* **1995***, 117*, 10645-
        10654.

(69)   Franchi, P.; Lucharini, M.; Pedulli, G.-F.; Valgimigli, L.; Lunelli, B. *J. Am.
        Chem. Soc.* **1999***, 121*, 507-514.

(70)   Mahoney, L. R.; DaRooge, M. A. *J. Am. Chem. Soc.* **1976***, 97*, 4722-4731.

(71)   Bordwell, F. G.; Cheng, J.-P. *J. Am. Chem. Soc.* **1991***, 113*, 1736-1743.

(72)   Lucarini, M.; Pedulli, G.-F.; Cipollone, M. *J. Org. Chem.* **1995***, 59*, 5063-
        5070.

(73)   Steinberg, D. *Nutrition and Biotechnology in Heart Disease and Cancer*;
        Plenum Press: New York, 1995; pp 39-48.

(74)   Upton, J. M.; Kritharides, L.; Stocker, R. *Proj. Lipid Res.* **2003***, 42*, 405-
        422.

(75)   Pratt, D. A. Ph.D. Dissertation; Vanderbilt University: Nashville TN, 2003.

(76)   Tucker, J. M.; Townsend, D. M. *Biomedicine & Pharmacotherapy* **2005***,
        59*, 380-387.

(77)   Azzi, A. *Eur. J. Nutr.* **2004***, 43 (Suppl. 1),* I/18-I/25.

(78)   Ferroni, F.; Maccaglia, A.; Pietraforte, D.; Turco, L.; Minetti, M. *Journal of Agricultural and Food Chemistry* **2004***, 52*, 2866-2874.

(79)   Thomas, S. R.; Witting, P. K.; Stocker, R. *BioFactors* **1999***, 9*, 207-224.

(80)   Neuzil, J.; Witting, P. K.; Stocker, R. *Proc. Natl. Acad. Sci. USA* **199***, 94*, 7885-7890.

(81)   Thomas, S. R.; Neuzil, J.; Stocker, R. *Arteriosclerosis, Thrombosis, and Vascular Biology* **1996***, 16*, 687-696.

(82)   Kontush, A.; Huebnor, C.; Finckh, B.; Kohlschuetter, A.; Beisiegel, U. *Biochim. Biophys. Acta, Lipids and Lipid Metabolism* **1995***, 1258*, 117-187.

(83)   Grassman, J.; Hippeli, S.; Spitzenberger, R.; Elstner, E. F. *Phytomedicine* **2005***, 12*, 416-423.

(84)   Kritchevsky, S. B. *Journal of Nutrition* **1999***, 129*, 5-8.

(85)   David, G.; Ingold, K. U. *Acc. Chem. Res.* **1980***, 13*, 317-323.

(86)   Burnett, G. M.; Melville, H. W. *Techniques of Organic Chemistry*; Interscience: New York, 1963.

(87)   Newcomb, M. *Tetrahedron* **1993***, 49*, 1151-1176.

(88)   Newcomb, M.; Toy, P. H. *Acc. Chem. Res.* **2000***, 33*, 449-455.

(89)   Tallman, K. A.; Pratt, D. A.; Porter, N. A. *J. Am. Chem. Soc.* **2001***, 123*, 11827-11828.

(90)   Wijtmans, M.; Pratt, D. A.; Valgimigli, L.; DiLabio, G. A.; Pedulli, G.-F. et al. *Angew. Chem. Intl. Ed.* **2003***, 42*, 4370.

(91)   Cipollone, M.; Di Palma, C.; Pedulli, G.-F. *Appl. Magn. Res.* **1992***, 3*, 99.

(92)   Pedulli, G.-F.; Lucarini, M.; Pedrielli, P.; Sagrini, M.; Cipollone, M. *Res. Chem. Intermed.* **1996***, 22*, 1.

(93)   Lucarini, M.; Pedulli, G.-F.; Valgimigli, L. *J. Org. Chem.* **1998***, 63*, 4497-4499.

(94)   Darlay-Usmar, V. M.; Hersey, A.; Garland, L. G. *Biochem. Pharmacol.* **1989***, 38.*

(95)   Brill, W. F. *J. Am. Chem. Soc.* **1965***, 87*, 3286.

(96)   Schenck, G. D.; Neumuller, O. A.; Eisfeld, K. C. *Angew. Chem.* **1958**, 595.

(97)   Teng, J. I.; Kulig, M. J.; Smith, L. L.; Kan, G.; van Lier, J. E. *J. Org. Chem.* **1973***, 38*, 119.

(98)   Beckwith, A. L. J.; Davies, A. G.; Davison, I. G.; Macol, A.; Mruzek, M. H. *J. Chem. Soc. Perkin Trans. II* **1989**, 815-824.

(99)   Schenck, G. O.; Eisfeld, K. C. *Angew. Chem.* **1958***, 70*, 595.

(100)   Brill, W. F. *Adv. Chem. Ser.* **1968***, 75*, 93.

(101)   Brill, W. F. *J. Chem. Soc. Perkin Trans. II* **1984**, 621-627.

(102)   Porter, N. A.; Zuraw, P. *J. Chem. Soc. Chem. Commun.* **1985**, 1473.

(103)   Chan, H. W.; Levett, G.; Matthew, J. A. *Chem. Phys. Lipids* **1979***, 24*, 245.

(104)   Korth, H.-G.; Heinrich, T.; Sustmann, R. *J. Am. Chem. Soc.* **1981***, 103*, 4483.

(105)   Porter, N. A.; Wujek, S. J. *J. Org. Chem.* **1987***, 52*, 5085-5089.

(106)   Porter, N. A.; Kaplan, J. K.; Dussault, P. H. *J. Am. Chem. Soc.* **1990***, 112*, 1266-1267.

(107)   Boyd, S. L.; Boyd, R. J.; Shi, Z.; Barclay, R. C.; Porter, N. A. *J. Am. Chem. Soc.* **1993***, 115*, 687-693.

(108)   Olivella, S.; Sole, A. *J. Am. Chem. Soc.* **2003***, 125*, 10641-10650.

(109)   Porter, N. A.; Mills, K. A.; Caldwell, S. E.; Dubay, G. R. *J. Am. Chem. Soc.* **1994***, 116*, 6697-6705.

(110)   Mills, K. A.; Caldwell, S. E.; Dubay, G. R.; Porter, N. A. *J. Am. Chem. Soc.* **1992***, 114*, 9689-9691.

(111)   Lowe, J. R.; Porter, N. A. *J. Am. Chem. Soc.* **1997***, 119*, 11534.

(112)   Lowe, J. R. In *Chemistry*; Duke University: Durham, NC, 1998; pp 201.

CHAPTER II

THE EFFECT OF OLEFIN GEOMETRY ON THE NON-CONJUGATED DIENE
SYSTEM DURING POLYUNSATURATED FATTY ACID OXIDATIONS

Introduction

As discussed in chapter I, the autoxidation of polyunsaturated fatty acids
(PUFAs) and esters has been the focus of intense investigation due to its
potential importance in biology.[1-5] When PUFAs and their esters are exposed to
oxidative stress, the primary products are hydroperoxides.[6-8] This oxidation
process is a free radical chain reaction, which targets the non-conjugated diene
moiety of PUFAs, such as methyl linoleate (**1**). Oxidation is initiated by
abstraction of the bis-allylic hydrogen atom generating a pentadienyl radical (**2**).
Upon formation of the pentadienyl radical in methyl linoleate, O_2 adds to the 13,
11, or 9 positions (Figure II-1). A sufficient hydrogen atom donor will trap the
peroxyl radicals **3**-**5** generating hydroperoxides **6**-**8**.

Even though lipid peroxidation has been the focus of much research,
details of the chemical mechanisms involved in the process have been scarce
until recent years. Most biological studies of peroxidation have utilized
calorimetric assays such as the formation of conjugated dienes[9] or the reaction
of a lipid oxidation product with thiobarbituric acid to give a colored adduct[10,11] as
a measure of autoxidation. Titrimetric methods have also been used to measure
peroxide formation in the oxidations.[12] All of these assays give only a crude
indication of the autoxidation mechanism, and the nature of the chemical events

35

involved in the autoxidation of fatty acids and unsaturated phospholipids have remained a "black box" so to speak. With new analytical techniques, the nature of the chemical processes involved in the autoxidation of lipids could be revealed.
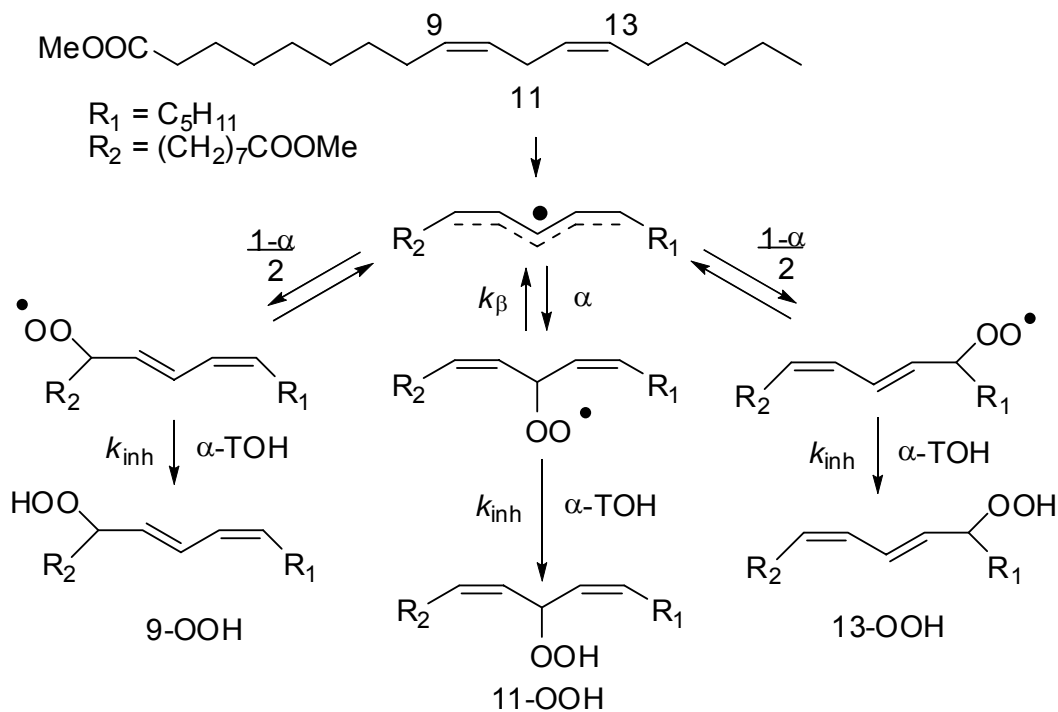
Figure II-1: General mechanism of the kinetically controlled linoleate oxidation.

Product mixtures obtained in polyunsaturated fatty acid random autoxidation are complex. However, the primary processes leading to products have been firmly established.[8, 13-16] Nevertheless, some kinetic and product studies are needed to address the important mechanistic questions in free-radical lipid oxidation.

The hydroperoxides formed during the course of the oxidation are highly dependent on the efficiency and concentration of the hydrogen atom donor. For

example, when methyl linoleate is oxidized in the presence of low concentrations of α-tocopherol (<10 mM); *trans*, *cis* conjugated hydroperoxides (**6**, **8**) are the major products formed. However, in the absence of any antioxidant, the thermodynamic products (the analogous *trans*, *trans* conjugated hydroperoxides) are the major products formed.[16] Under these conditions, β-fragmentation of the intermediate peroxyl radicals leads to products having the more stable *trans*, *trans* diene geometry.

Brash[13] and Porter[14] have independently shown that the bis-allylic hydroperoxide is the major product formed when oxidations of methyl linoleate are carried out in the presence of high concentrations of α-tocopherol (>0.05M).[14] The mechanism shown in Figure II-1 was used as a basis for the analysis of product distribution in these oxidations. Because the peroxyl radical leading to the hydroperoxide undergoes a very rapid β-fragmentation (10^6 s^{-1}), high concentrations of antioxidant are necessary in order to observe the bis-allylic product. It was also shown that this β-fragmentation serves as a useful radical clock for antioxidant hydrogen atom transfer to peroxyl radicals with bimolecular rate constants of ca. 10^6 M^{-1} s^{-1}.[14]

This chapter discusses more detailed studies on the formation of the bis-allylic peroxyl radical and the subsequent β-fragmentation in the oxidation of octadecadienoates and model diene systems. In addition to studies involving methyl linoleate previously reported, the effect of olefin geometry (*trans, cis* and *trans, trans*) on the formation and reactivity of other bis-allylic peroxyl radicals is discussed. Although little is known about their reactivity, there is evidence that

geometric isomers of methyl linoleate (i.e. *trans* fatty acids) can play a significant role in biological systems.[17-19]

Synthesis of Octadecadienoates and Model Dienes
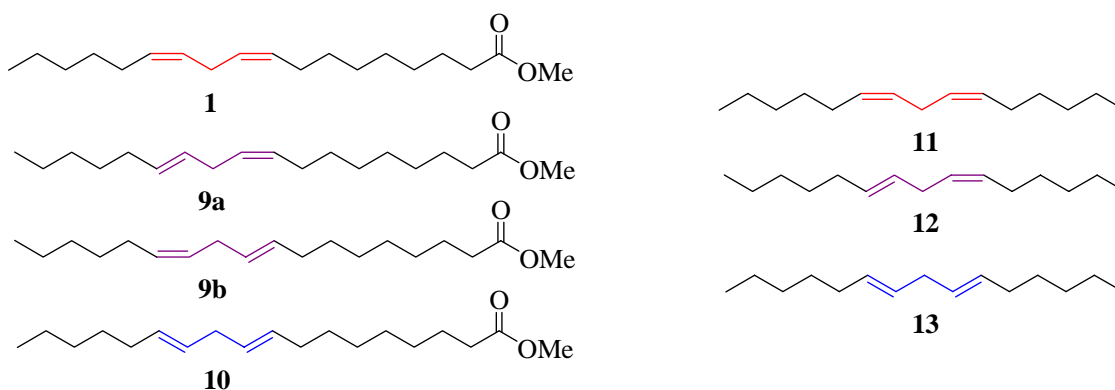
Methyl linoleate (**1**) and linoelaidate (**10**) are commercially available, and the *cis, trans* octadecadienoates (**9a**, **9b**) can be synthesized as reported by Porter and Wujek.[16] The model dienes are not commercially available. However, they can be synthesized in a straightforward manner, as seen in Figure II-2.
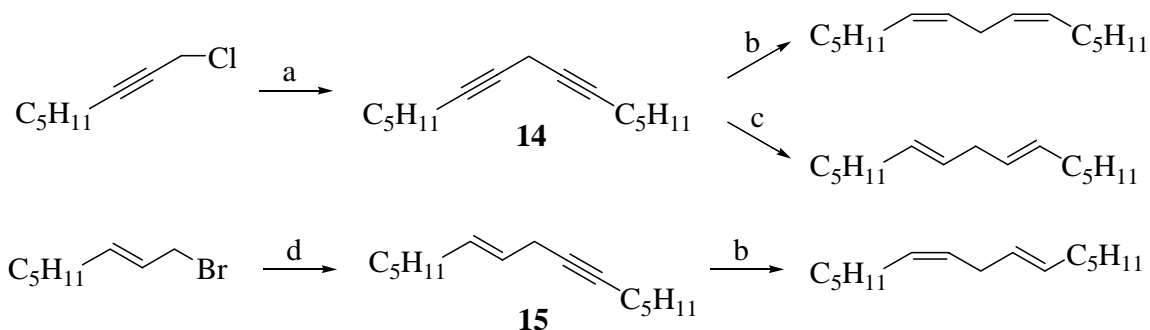
Figure II-2: Synthesis of model dienes. Reagents: a) 1-heptyne, CuI, NaI, K_2CO_3, DMF; b) Pd/BaSO$_4$, H_2, EtOAc; c) NH$_3$/ether, Li^0, (NH$_4$)$_2$SO$_4$; d) 1-heptyne, *n*-BuLi, DMPU, THF, -78°C.

The *cis, cis* (**11**) and *trans, trans* (**13**) dienes are synthesized from a common intermediate diyne (**14**). The diyne (**14**) was synthesized by a copper cross-coupling of 1-heptyne with 1-chloro-2-octyne.[20-22] Lindlar hydrogenation using the more reactive Pd/BaSO$_4$ catalyst gave **11**, and a buffered Birch reduction[23] of **14** yielded **13**. 1-heptynyl lithium was added to *trans*-1-bromo-2-octene[24] and followed by the Lindlar hydrogenation used above in order to synthesize the unsymmetrical diene **12**. The synthesis of **15** via copper coupling has been reported, [25] but it was found that this procedure resulted in a mixture of regioisomers. The desired regioisomer can be reached exclusively through the coupling of 1-heptynyl lithium with the allylic bromide in the presence of DMPU. The model dienes were purified by column chromatography on silver nitrate impregnated silica gel (SNIS) to ensure high isomeric purity.[26]

Oxidation of Octadecadienoates and Model Dienes

Oxidations of the model dienes and octadecadienoates (0.2 M) were carried out in benzene in the presence of varying concentrations of α-tocopherol (0.05-1.8 M) and were initiated by 2,2'-azobis(4-methoxy-2,4-dimethylvaleronitrile) (MeOAMVN). The reaction vials were incubated at 37 °C for 4 h. The relatively short reaction times allowed for low conversion of the substrate so that α-tocopherol was not consumed to a significant extent during any of the oxidations, ensuring pseudo-first order conditions. The octadecadienoate hydroperoxides were analyzed directly by normal phase HPLC. The diene hydroperoxides from **11**-**13** were reduced to the corresponding

alcohols **24**-**28** with PPh$_3$ and subsequently analyzed by GC. Only the kinetic products (Figure II-3) were observed under these conditions.
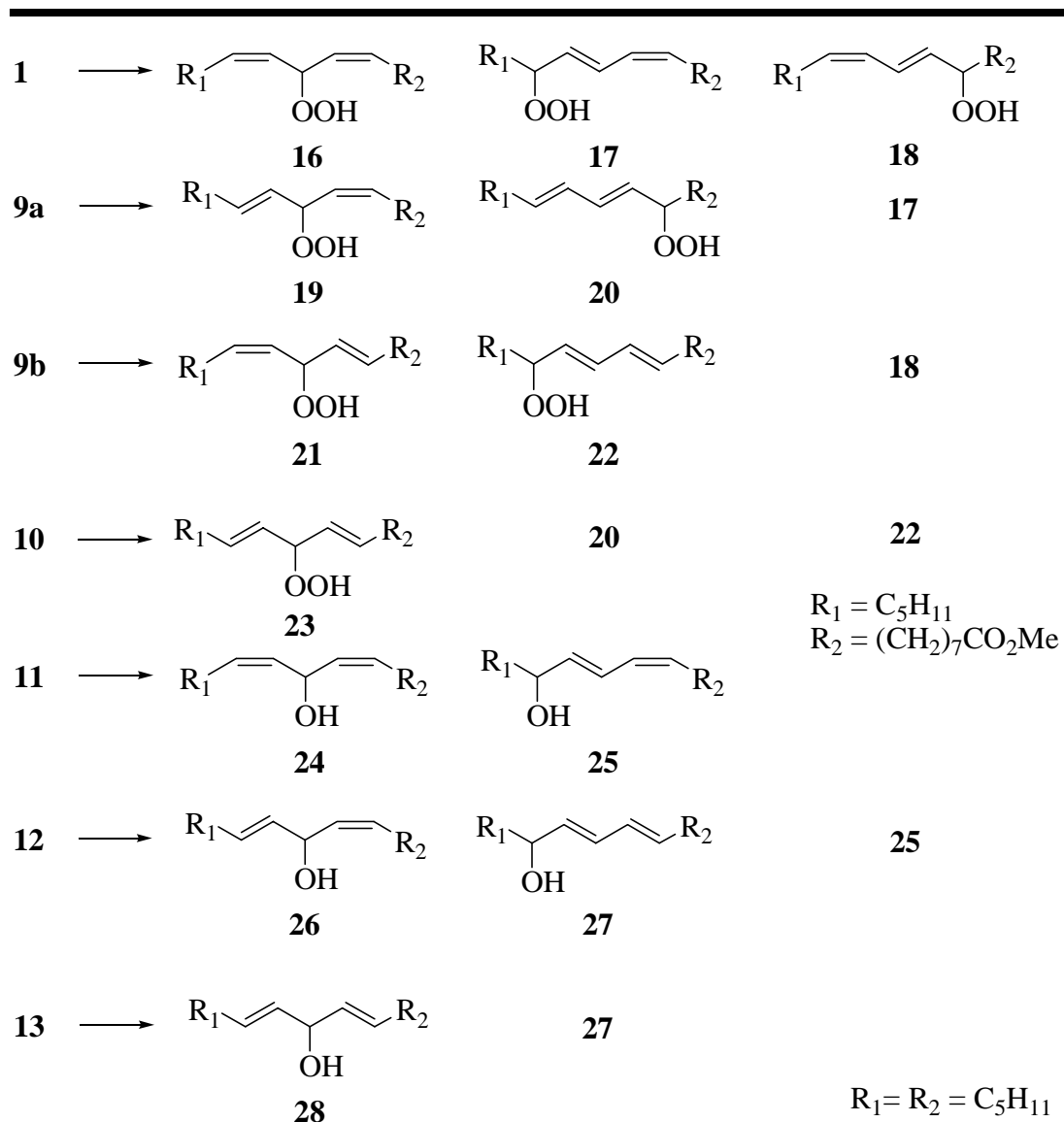
Figure II-3: Oxidation products of octadecadienoates (**1**, **9**-**10**) and dienes (**11**-**13**) in the presence of α-tocopherol.

The non-conjugated hydroperoxide formed in each oxidation contained the same olefin geometry as the parent substrate. The *cis, cis* and *trans, trans*

substrates generated only the *cis*, *trans* and *trans*, *trans* conjugated hydroperoxides, respectively. A mixture of the two conjugated hydroperoxides (**17** and **18**, **20** and **22**) was generated upon oxidation of the *cis*, *trans* substrates.

Methyl octadecadienoates (**1**, **9**-**10**) and the analogous model diene compounds (**11**-**13**) were used to study the effect of olefin geometry on the formation of the bis-allylic hydroperoxides. The generality of the proposed mechanism (Figure II-1) can be analyzed by following the oxidations of the model dienes and focusing on the reactivity of the non-conjugated diene moiety without possible interference from another functional group in the compound. The ester group present in the octadecadienoates should be too far removed from the reactive site of interest to have any significant effect on the oxidation of the octadecadienoates. This potential issue was addressed by using the model dienes in parallel oxidation experiments. The oxidation profiles of these model dienes are identical to the octadecadienoates, suggesting that the ester has no influence at the site of oxidation.

The plot of the ratio of bis-allylic to conjugated products *versus* the concentration of α-tocopherol is shown in Figure II-4. The profile for the product distribution is essentially the same for the octadecadienoates and dienes. This indicates that the ester functionality does not influence the site of oxidation. The oxidation profiles are nearly identical regardless of the substrate or the method of analysis, validating the analytical procedure.

The data clearly shows that for all compounds studied, the amount of bis-allylic hydroperoxide increases with increasing α-tocopherol concentration at the expense of the conjugated products until a maximum limit is reached. This observation is consistent with the proposed mechanism for linoleate shown in Figure II-1.[14]
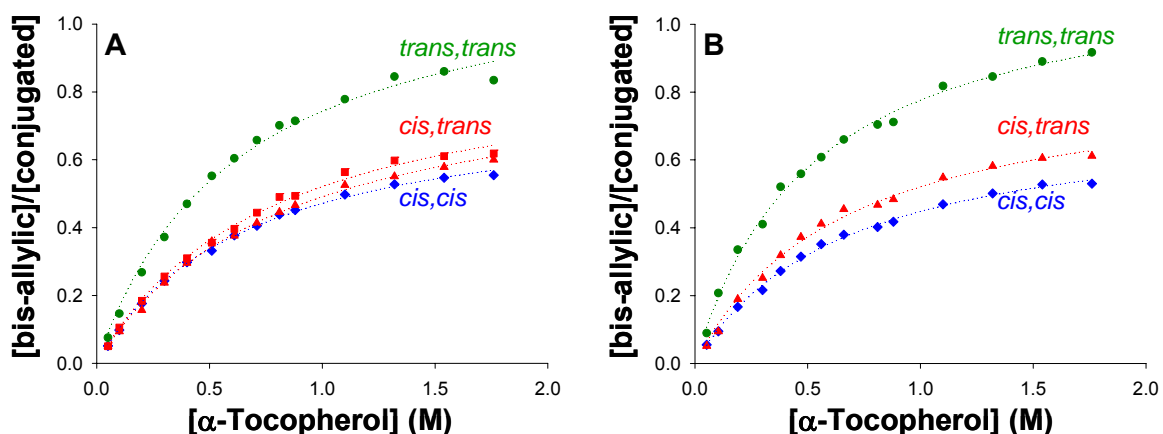
Figure II-4: Oxidation profile of octadecadienoates and dienes, ratio of bis-allylic/conjugated products versus [α-Tocopherol]: A: Octadecadienoates ♦ methyl linoleate, ■ 9-*cis*-13-*trans*-methyl linoleate, ▲ 9-*trans*-13-*cis*-methyl linoleate, ● methyl linoelaidate; B: Dienes ♦ 9, 13-*cis, cis*-pentadecadiene, ▲ 9-*trans*-13-*cis*-pentadecadiene, ● 9, 13-*trans, trans*-pentadecadiene. Conditions: [α-tocopherol] = 0.05-1.8 M, [MeOAMVN] = 0.01 M, [substrate] = 0.15 M, T = 37°C, t = 4 h.

In the proposed mechanism from Figure II-1, O_2 is partitioned among the three positions of the pentadienyl radical as follows: terminal = 1-α/2, bis-allylic = α, and terminal = 1-α/2. The peroxyl radicals subsequently abstract a hydrogen atom from α-tocopherol to generate the hydroperoxides. Under the oxidation conditions used in these studies, the conjugated peroxyl radicals do not undergo β-fragmentation to generate the thermodynamic *trans, trans* conjugated

hydroperoxides. Since the rate constant for this β-fragmentation is so slow (620 s^{-1}),[16] it cannot compete with trapping of the peroxyl radicals by α-tocopherol.

In contrast to the conjugated peroxyl radicals, the non-conjugated peroxyl radical undergoes a rapid β-fragmentation (k_β), regenerating the pentadienyl radical. Competing with this β-fragmentation is hydrogen atom transfer (k_{inh}) to the peroxyl radical by α-tocopherol with a rate constant of 3.5 x 10^6 M^{-1}s^{-1}.[27-29] β-fragmentation becomes negligible and a limit is reached as the concentration of α-tocopherol increases. At this limit, the product distribution reflects the O$_2$ partition to the three positions of the pentadienyl radical.

From Figure II-4 it can be seen that olefin geometry influences the partitioning of O$_2$ across the pentadienyl radical. The ratio of products arising from the oxidation of *trans*, *trans* compounds reaches a higher limit than the other compounds. This indicates that as the *trans* character of the pentadienyl radical increases, so does O$_2$ addition at the bis-allylic position. Analysis of the mechanism leads to a kinetic expression (equation 1), which describes the product ratio as a function of α, k_β, k_{inh}, and [α-tocopherol]. Non-linear least squares analysis of the oxidation data, using equation 1, allows the determination of values for α and k_β for the octadecadienoates and the model dienes (Table II-1). The data clearly shows that olefin geometry has an effect on the O$_2$ partitioning (α) and on β-fragmentation (k_β) of the bis-allylic peroxyl radical.

$$\frac{[\text{bis-allylic}]}{[\text{conjugated}]} = \left(\frac{\alpha}{1-\alpha}\right) \frac{k_{inh}\,[\alpha\text{-Toc}]}{k_{inh}\,[\alpha\text{-Toc}] + k_\beta} \tag{1}$$

There is also a rather small influence of olefin geometry on the tendency for β-fragmentation of non-conjugated peroxyl radicals. The BDEs for the 4-peroxyl radical derived from *cis, cis*; *cis, trans*; and *trans, trans*-2,5-heptadiene have been calculated to be 7.4, 7.9, and 8.4 kcal/mol, respectively.[30] Since the *trans, trans* peroxyl radical has a stronger C-OO$^\bullet$ bond than the analogous *cis, cis* substrate; k_β is expected to be slower for the *trans, trans* peroxyl radical. However, the *cis, trans* substrates do not follow this trend. These compounds have the highest observed k_β of the substrates studied.

Table II-1: Values for O_2 partitioning to the bis-allylic position (α) and the rate constant for subsequent β-fragmentation (k_β) of the bis-allylic peroxyl radical.

Substrate	α	k_β (x10^6 s^{-1})
methyl linoleate	0.44 (± 0.01)	2.32 (± 0.09)
9-*cis*-13-*trans*-methyl linoleate	0.48 (± 0.01)	2.74 (± 0.18)
9-*trans*-13-*cis*-methyl linoleate	0.47 (± 0.01)	2.84 (± 0.14)
methyl linoelaidate	0.55 (± 0.02)	2.18 (± 0.17)
9, 13-*cis, cis*-pentadecadiene	0.43 (± 0.01)	2.36 (± 0.10)
9-*trans*-13-*cis*-pentadecadiene	0.48 (± 0.01)	2.69 (± 0.11)
9, 13-*trans, trans*-pentadecadiene	0.55 (± 0.01)	2.02 (± 0.09)

The oxidation profile demonstrates the delicate balance between the prooxidant and antioxidant properties of α-tocopherol.[31-33] The extent of oxidation of the substrate increases as the concentration of α-tocopherol increases, up to a certain point. This tendency is indicative of the ability of the α-tocopheroxyl radical to mediate oxidation. However, when the concentration of

α-tocopherol is increased beyond this point, the extent of substrate oxidation is decreased, showing the ability of α-tocopherol to act as an antioxidant (Figure II-5). Peroxyl radicals are more effectively scavenged when higher concentrations of antioxidant are present, thereby interrupting the free radical chain propagation steps (equations 4 and 5, Chapter I).
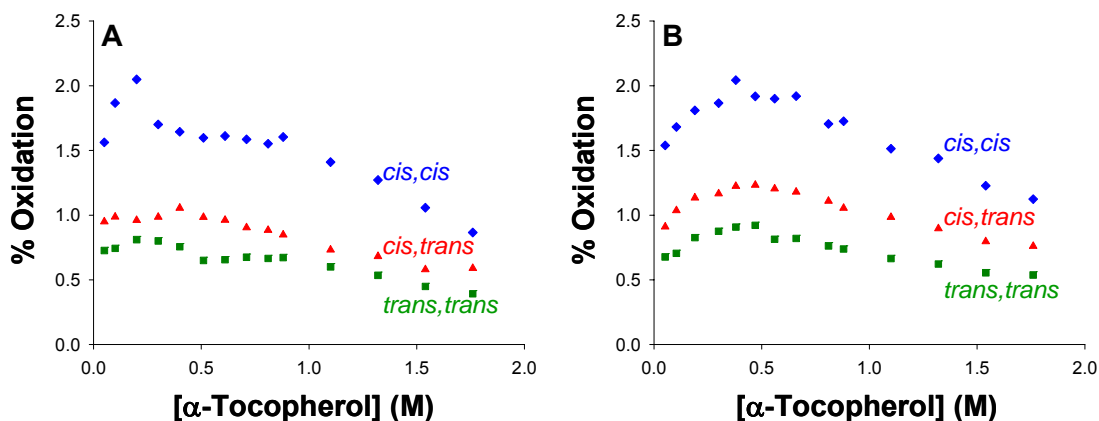
Figure II-5: % Oxidation of octadecadienoates and dienes in the presence of α-tocopherol. A: Octadecadienoates ♦ methyl linoleate, ▲ 9-*cis*-13-*trans*-methyl linoleate, ▪ methyl linoelaidate; B: Dienes ♦ 9, 13-*cis, cis*-pentadecadiene, ▲ 9-*trans*-13-*cis*-pentadecadiene, ▪ 9, 13-*trans, trans*-pentadecadiene. Conditions: [α-tocopherol] = 0.05-1.8 M, [MeOAMVN] = 0.01 M, [substrate] = 0.15 M, T = 37°C, t = 4 h.

It is also clear from the plot that olefin geometry influences the extent of oxidation. The *cis, cis* substrates (**1**, **11**) undergo nearly twice as much oxidation as the *trans, trans* substrates (**10**, **13**), with the *cis, trans* dienes (**9a**, **9b**, **12**), as expected, having oxidation levels falling between the *cis, cis* and *trans, trans* substrates. This trend is also consistent with the BDEs that have been calculated for these types of compounds. The bis-allylic C-H BDEs for *cis, cis*;

cis, trans; and *trans, trans*-2, 5-heptadiene have been calculated as 72.7, 73.1, and 73.5 kcal/mol, respectively.[30] Since the *trans, trans* diene has the strongest C-H bond; it is less prone to oxidation than the other compounds. This is also consistent with reports that *trans* fatty acids undergo less oxidation than their *cis* counterparts in LDL oxidations.[17]
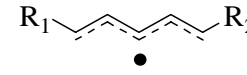
As the *trans* character of the pentadienyl radical increases, the addition of O_2 at the bis-allylic position (α) increases, consistent with ESR and theoretical predictions. ESR[34,35] and theoretical calculations[30] (Table II-2) indicate that the pentadienyl radical formed from the *trans, trans* diene precursor should have higher unpaired spin (38% from the ESR data) at the bis-allylic carbon compared to the unpaired spin of the pentadienyl radical formed from the *cis ,cis* diene (36%).   For this pair of reactants, unpaired electron spin density on the intermediate pentadienyl radical parallels trapping by O_2 at the bis-allylic position and a higher value for α (0.55) is observed for the *trans, trans* diene oxidations compared to the *cis, cis* precursor (0.43).   Similarly, ESR experiments suggest that the pentadienyl radical formed from the *trans, cis* precursors has 37% unpaired spin at the bis-allylic position and the values of α obtained (0.47) for these substrates (**9a**, **9b**, and **12**) are consistent with the fact that unpaired spin density is important in controlling the kinetic product distribution during oxidations of the octadecadienoates and the model dienes.

Although experiment and theory show the same trends, the experimentally determined values for α are somewhat higher than the spin density ratios that have been calculated for model compounds and for those that have been

46

observed by ESR experiments. The calculations were carried out using 2,5-heptadiene as the model for octadecadienoates and recently published experiments indicate that there is a significant substituent effect on the partitioning of oxygen to pentadienyl radicals.[36, 37]

Table II-2: Unpaired Spin as Determined by ESR and Theory on Isomeric Pentadienyl Radicals.

	$R_1 \diagup\!\!\!\diagdown\!\!\!\diagup R_2$	$R_1 \diagdown\!\!\!\diagup\!\!\!\diagdown R_2$	$R_1 \diagdown\!\!\!\diagup\!\!\!\diagdown R_2$
ESR[a]	0.32 : 0.36 : 0.32	0.30 : 0.37 : 0.33	0.31 : 0.38 : 0.31
Theory[b]	0.326 : 0.353 : 0.326	0.31 : 0.36 : 0.33	0.313 : 0.365 : 0.313
O_2 Trapping[c]	0.28 : 0.44 : 0.28	0.34 : 0.48 : 0.18	0.225 : 0.55 : 0.225

[a] R and R'= methyl[35]; [b] R and R'= methyl[30]; the values given here were the result of UB3LYP/6-311+G(2d,2p); [c] Average distribution from diene substrates having identical diene geometry: (**1** and **11**), (**9a, 9b** and **12**), and (**10** and **13**).[15]

In addition to probing the generality of the oxidation mechanism, the use of the octadecadienoates and model dienes offers the opportunity to use complimentary methods of product analysis to validate the methodology. The fatty acid ester hydroperoxides (**16**-**23**) were analyzed by HPLC, whereas the diene oxidation products (**24**-**28**) were analyzed by GC. These two methods allow the product distribution from each substrate to be verified. The oxidation products of the model dienes can be independently synthesized which offers another advantage to the confirmation and characterization of compounds **24**-**28**.

The product mixtures of the octadecadienoates (**1**, **9**-**10**) were analyzed by HPLC-MS utilizing silver coordination ion spray mass spectrometry (Ag-CIS-

MS)[38,39]   This method has proven to be very useful in identifying intact hydroperoxides, as well as distinguishing the regioisomers present in an oxidation mixture.[40,41]   Coordination of silver to the hydroperoxides provides a mild method of generating a positively charged species that is detectable by MS.

The silver ions present promote Hock fragmentation[42-45] of the hydroperoxides in the MS to generate two aldehydes (Figure II-6). The 13- and 9-hydroperoxides (**16**, **17**) fragment to generate aldehydes having a mass of 333 and 293, respectively. The 11-hydroperoxide (**18**) undergoes fragmentation on either side of the bis-allylic hydroperoxide, generating a mixture of two aldehydes (m/z 319 and 307).   The characteristic fragments that arise from each hydroperoxide are diagnostic and allow the assignment of each regioisomer present in the oxidation mixture.[46]   It should be noted that only the aldehyde fragment containing the ester functionality is detected by MS. In addition to the HPLC-MS analysis, the hydroperoxides were isolated and analyzed by ^{1}H NMR to confirm the double-bond geometry.

The products formed from oxidation of the model dienes **11**-**13** were identified and verified by independent synthesis of the diene alcohols (Figure II-7). The *cis*, *cis* bis-allylic alcohol (**24**) was synthesized by addition of 1-heptynyl lithium to ethyl formate, giving diynol **29**, followed by a Lindlar hydrogenation with the mild Pd/CaCO$_3$/Pb catalyst.[47]   Addition of 1-heptyne to *trans*-2-octenal yielded **30**. This intermediate was converted to the *cis*, *trans* (**26**) and *trans*, *trans* (**28**) alcohols by the same Lindlar hydrogenation and lithium aluminum hydride (LiAlH$_4$) reduction, respectively.
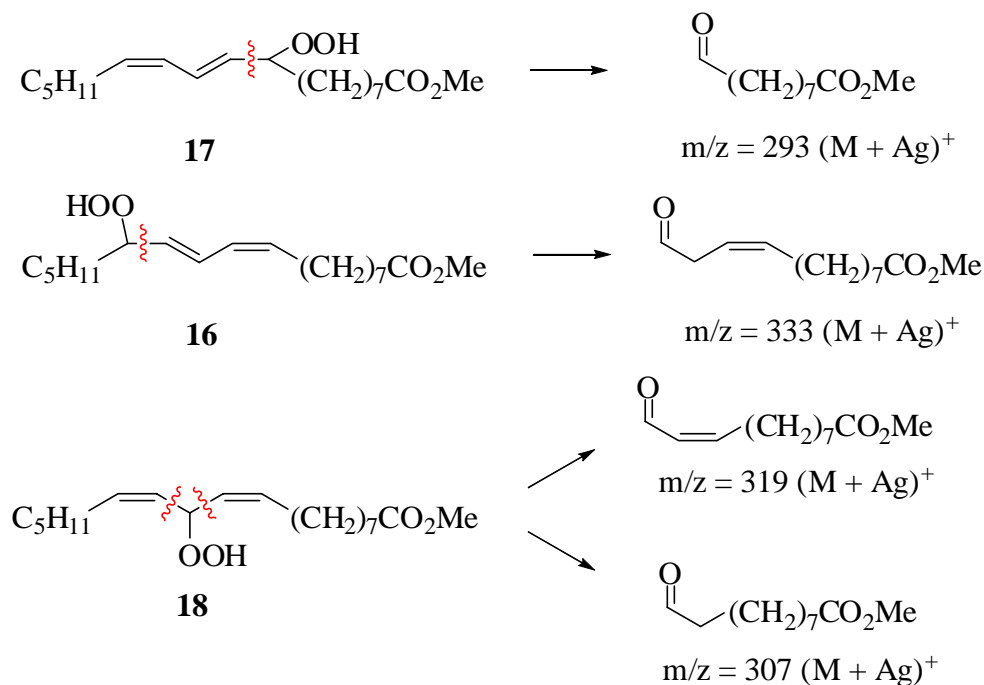
Figure II-6: Hock fragments of linoleate hydroperoxide silver adducts.

Synthesis of the *cis, trans* conjugated alcohol was achieved through a cascade of reactions.[48] First, *cis*-3-nonenol was converted to the selenide (**31**) by displacement of the mesylate. Oxidation of the selenide to the selenoxide with *m*-CPBA increases the acidity of the α-protons. Deprotonation of the selenoxide (not shown) followed by addition of hexanal generates the necessary intermediate, which undergoes a selenoxide elimination to yield the desired compound **25**. The *trans, trans* conjugated alcohol (**27**) was easily prepared in one step by addition of pentylmagnesium bromide to *trans,trans*-2, 4-decadienal.
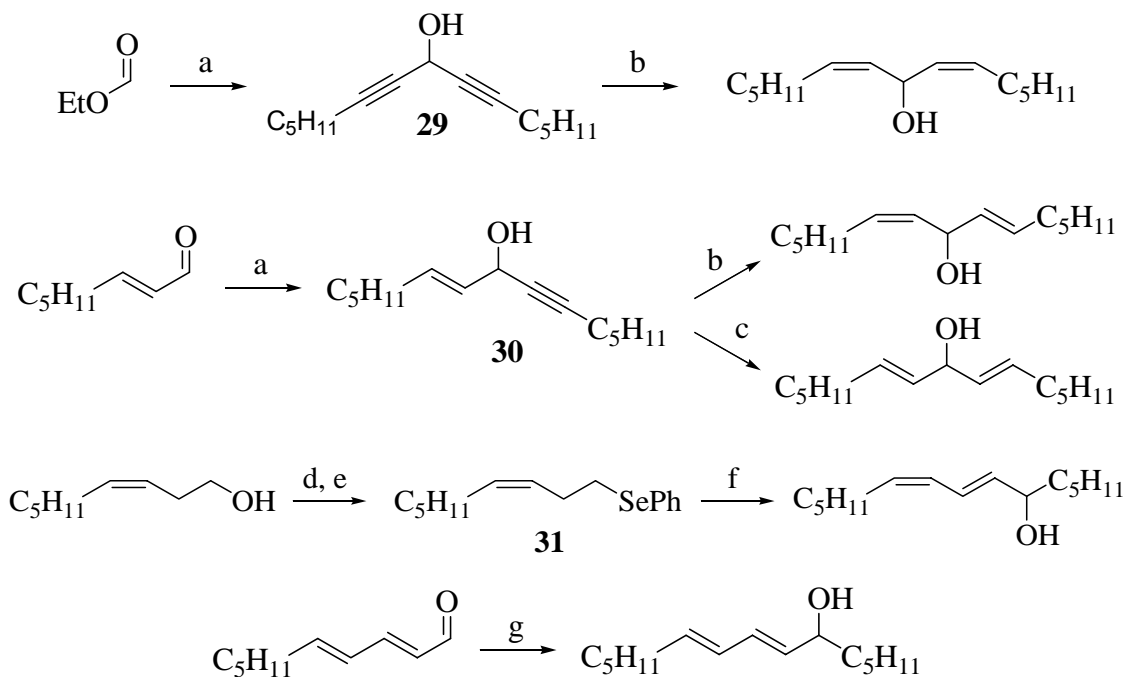
Figure II-7: Synthesis of diene alcohols. Reagents: a) 1-heptyne, *n*-BuLi, THF, -78°C; b) Pd/CaCO₃/PB, H₂, EtOAc; c) LiAlH₄, THF, reflux; d) MsCl, pyr; LDA, hexanal, -78°C, iPr₂NH, reflux; e) (PhSe)₂, LiAlH₄, THF; f) *m*-CPBA, THF, -78°C; g) H₁₁C₅MgBr, THF.

Terminal Trapping of the Pentadienyl Radical

The results for oxidation of the octadecadienoates with both alkenes having the same geometry (*cis, cis* or *trans, trans*) showed that O₂ trapping at the terminal positions of the pentadienyl radicals (C9 and C13) were identical (Figure II-8A and D). Due to the fact that the unpaired electron spin density is expected to be identical at the terminal pentadienyl positions for these substrates, this does not come as a surprise. Unpaired spin density for the radicals derived from *cis, trans* dienes is not equal at the pentadienyl terminal positions (Figure II-8B and C), as indicated by theoretical calculations and ESR spectroscopy.[30,34,35]
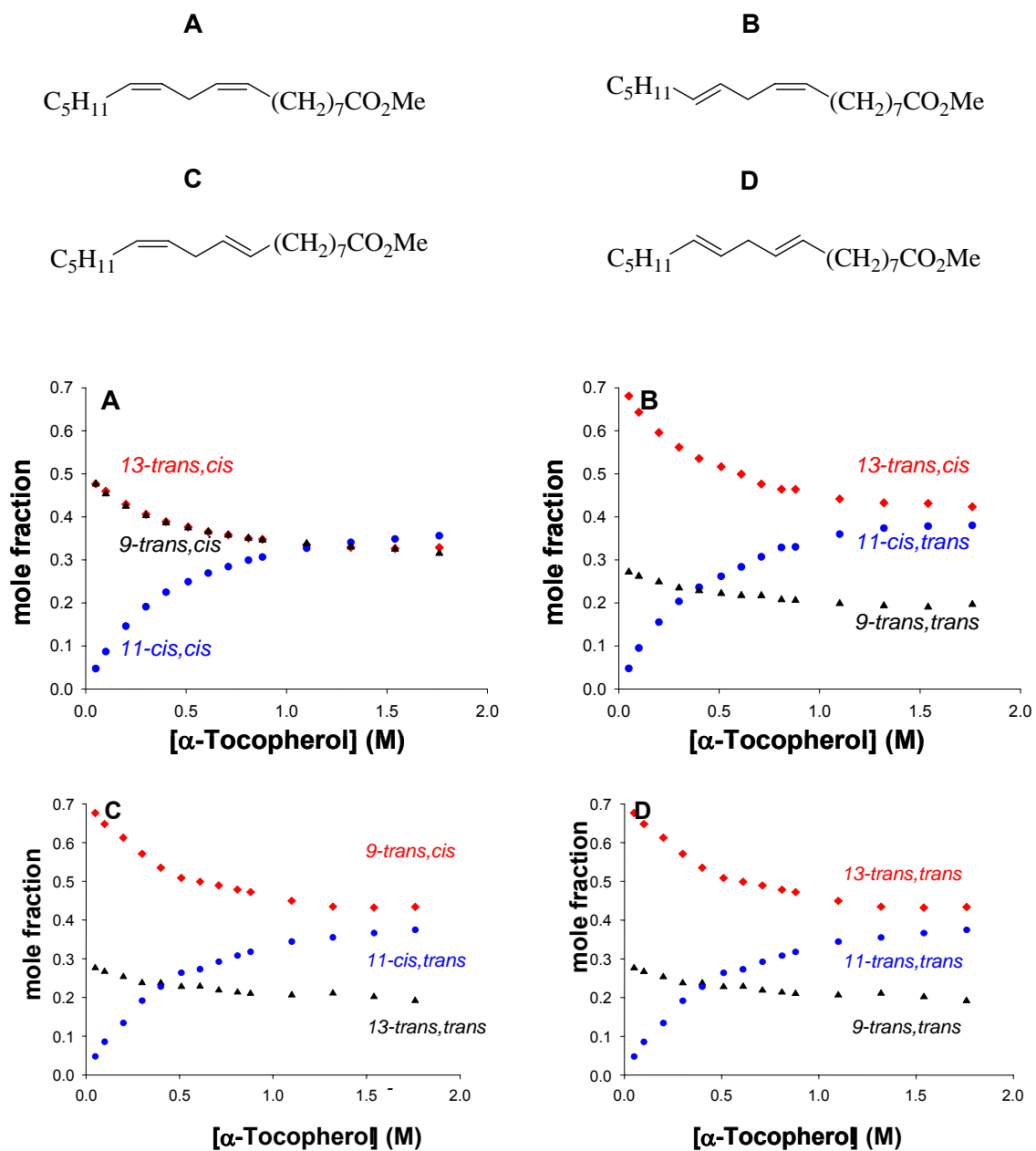
Figure II-8: Mole fractions of oxidation products. A: oxidation of methyl linoleate; ♦ 13-*cis, trans* conjugated, ▲ 9-*cis, trans* conjugated, ● 11-*cis, cis*. B: oxidation of 9-*cis*-13-*trans*-methyl linoleate; ♦ 13-*cis, trans* conjugated, ▲ 9-*trans, trans* conjugated, ● 11-*cis, trans*. C: oxidation of 9-*trans*-13-*cis*-methyl linoleate; ♦ 9-*trans, cis*, ▲ 13-*trans, trans*, ● 11-*trans, cis*; D: oxidation of methyl linoelaidate, ▲ 9-*trans,trans*, ♦ 13-*trans,trans*, ● 11-*trans,trans*. Conditions: [α-tocopherol] = 0.05-1.8 M, [MeOAMVN] = 0.01 M, [substrate] = 0.15 M, T = 37°C, t = 4 h.

A previously reported study of the oxidations of **9a** and **9b,** in the absence of phenolic antioxidants, showed that twice as much *trans, cis* conjugated diene product was formed as compared to the *trans, trans* product.[16]   Data for O_2 trapping[15] indicates that the *trans, cis* conjugated diene product is formed in preference to the *trans, trans* compound at the kinetic limit.   Theory and ESR experiments cannot account for the observed distribution of products based upon unpaired spin for these "unsymmetrical" systems.

The data from Figures II-8B and C were analyzed under the assumption that formation of each conjugated hydroperoxide is a separate pathway, leading to Equations 2 and 3. These equations are essentially the same as equation 1, but now it is <u>not</u> assumed that O_2 is partitioned equally at the terminal positions of the pentadienyl radical. The fraction of trapping at the bis-allylic position is still denoted as α, whereas trapping at the *transoid* and *cisoid* ends of the pentadienyl radical are denoted as β and γ, respectively (Table II-3). Instead of collectively referring to terminal trapping as 1-α, the two termini are treated separately (i.e. $\beta + \gamma = 1-\alpha$). Analysis of the data using these equations, in conjunction with Equation 1, gives the ratio of O_2 trapping at the three positions of the "unsymmetrical" pentadienyl radical.   The data presented in Table II-3 show the results of this analysis for **9a, 9b,** and **12**.

If spin density controls the site of initial addition of oxygen to delocalized radicals, the major conjugated product would be expected to be the *trans, trans* conjugated diene hydroperoxide. Table II-4, and the results seen in Figures II-8

and II-10 (for the model dienes) show that spin appears to be slightly greater at the *cisoid* end of the pentadienyl radical compared to the *transoid* position for these unsymmetrical radicals. Because of this discrepancy, the distribution of products formed from **9a**, **9b,** and **12** were analyzed as a function of antioxidant concentration by a more complex kinetic model (equations 2 and 3).

$$\textbf{Transoid:} \quad \frac{\text{[bis-allylic]}}{\text{[conjugated]}} = \left(\frac{\alpha}{\beta} \right) \frac{k_{inh} \, [\alpha\text{-Toc}]}{k_{inh} \, [\alpha\text{-Toc}] + k_\beta} \qquad (2)$$

$$\textbf{Cisoid:} \quad \frac{\text{[bis-allylic]}}{\text{[conjugated]}} = \left(\frac{\alpha}{\gamma} \right) \frac{k_{inh} \, [\alpha\text{-Toc}]}{k_{inh} \, [\alpha\text{-Toc}] + k_\beta} \qquad (3)$$

Table II-3: Kinetically controlled O_2 trapping of unsymmetrical pentadienyl radicals.

$$R_1 \diagup\!\!\!\diagdown\!\!\!\diagup\!\!\!\diagdown R_2$$

$$\beta \quad \alpha \quad \gamma$$
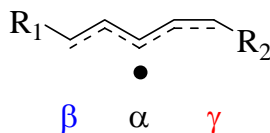
Substrate	β	α	γ
9-*cis*-13-*trans*-methyl linoleate	0.35	0.48	0.16
9-*trans*-13-*cis*-methyl linoleate	0.36	0.47	0.17
9-*trans*-13-*cis*-pentadecadiene	0.32	0.48	0.21

Figure II-9 shows the terminology used in classifying the sites of oxygen addition to an unsymmetrical pentadienyl radical. The cisoid end (the parent *cis*-double bond) of the pentadienyl radical is the position to which oxygen is added, leading to the *trans*, *trans*-conjugated product. Likewise, the transoid end (the

parent *trans*-double bond) is where oxygen adds giving the *trans, cis*-conjugated product.
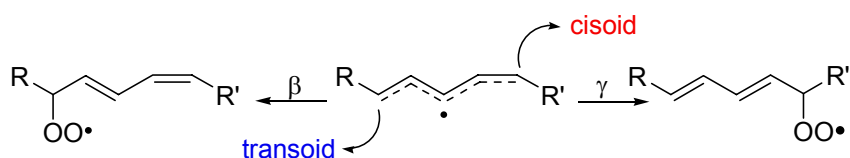
Figure II-9: Terminal Trapping of Pentadienyl Radical.

The best-fit parameters for the analysis shown in Figure II-8 for octadecadienoates **9a** and **9b** and in Figure II-10 for diene **12** indicate that oxygen addition at the *transoid* end of a pentadienyl radical, β, is almost twice the value of oxygen addition at the *cisoid* end of the radical, γ. This analysis is consistent with the earlier experimental results and confirms the conclusion that the unpaired spin density does not observably control the partitioning of oxygen in this geometrically unsymmetrical pentadienyl radical. The product analysis of the *cis, cis* (**1** and **11**), *trans, trans* (**10** and **13**), and *cis*, trans (**9a**, **9b**, and **12**) octadecadienoates and dienes are identical to those substrates having the same double bond geometry around the pentadiene core (Figures II-8 and II-10).
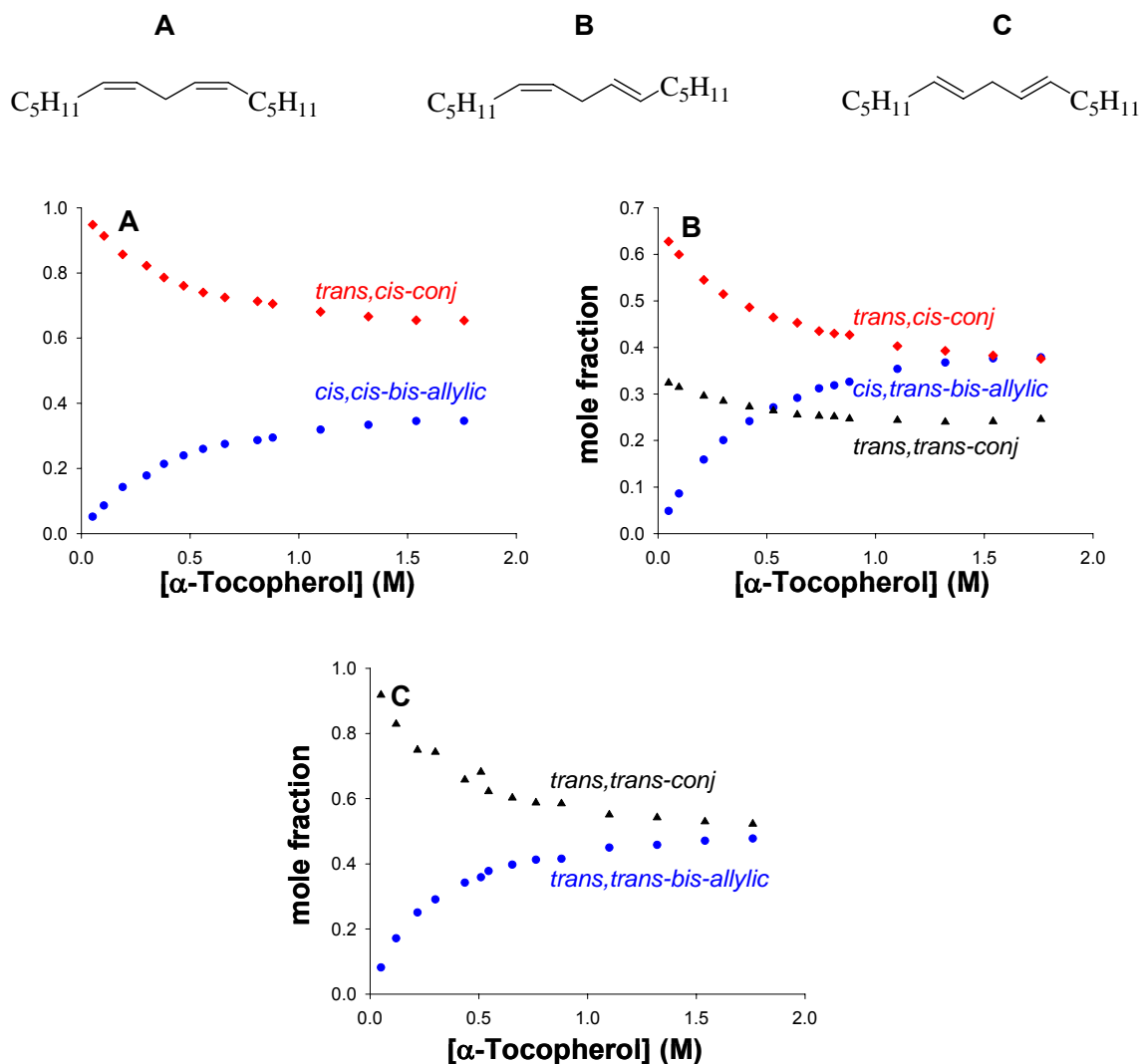
Figure II-10: Mole fractions of the model diene oxidation products. A: 9, 13-*cis, cis*-pentadecadiene; ♦ 13-*cis, trans* conjugated, ▲ 9-*cis, trans* conjugated, ● 11-*cis, cis*. B: 9-*trans*-13-*cis*-pentadecadiene; ♦ 13-*trans, cis* conjugated, ▲ 9-*trans, trans* conjugated, ● 11-*cis, trans* bis-allylic. C: 9, 13-*trans, trans*-pentadecadiene; ▲ 13-*trans, trans* conjugated, ● 11-*trans, cis* bis-allylic. Conditions: [α-tocopherol] = 0.05-1.8 M, [MeOAMVN] = 0.01 M, [substrate] = 0.15 M, T = 37°C, t = 4 h.

Dioxygen-Radical Complexes as Intermediates in Chain Oxidation

The results from the oxidations of the octadecadienoates and model dienes have been analyzed with the assumption that a simple β-fragmentation of

the bis-allylic peroxyl radical, back to the parent pentadienyl radical, is the sole and decisive process that will interconvert the non-conjugated and conjugated peroxyl radicals. However, there exists a large body of work on peroxyl radical rearrangements that should not be ignored when considering product distributions in autoxidations of unsaturated substrates.[49-55] The use of isotopically labeled hydroperoxides or molecular oxygen in studies of hydroperoxide rearrangements has led to the conclusion that the rearrangement of conjugated diene hydroperoxides proceeds via a β-fragmentation.[6,56] The rearrangement of simple allylic hydroperoxides, on the other hand, is more complex.

A recent computational study has led to the proposal of an allyl-triplet dioxygen complex **32**, as an intermediate in the rearrangement (Figure II-11).[57] Oxygen labeling and stereochemical studies of such rearrangements are consistent with this proposal.[58-65] Calculations suggest that oxygen and an allyl radical are held in this complex by dispersion forces and that the observed degree of stereoselectivity of the rearrangement is due to the formation of complex **32**, which prevents the allyl radical and triplet dioxygen complex from being released from the solvent cage, maintaining stereocontrol along the fragmentation-recombination processes.[57]
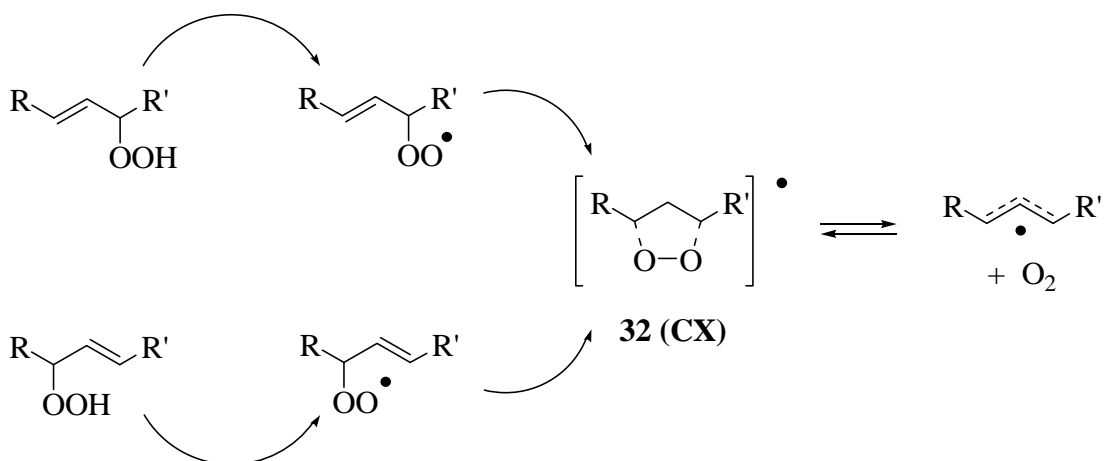
Figure II-11: The allylperoxyl rearrangement mechanism with an allyl-triplet dioxygen intermediate.

It is speculated that such radical-dioxygen triplet complexes may intervene in the chemistry of the bis-allylic peroxyl radicals that are intermediates in this study. The bis-allylic peroxyl radical derived from the oxidation of an unsymmetrical diene such as **12** from Figure II-3 could rearrange to the conjugated peroxyl radicals through two distinct isomeric radical-dioxygen complexes, **33** and **34** (Figure II-12).
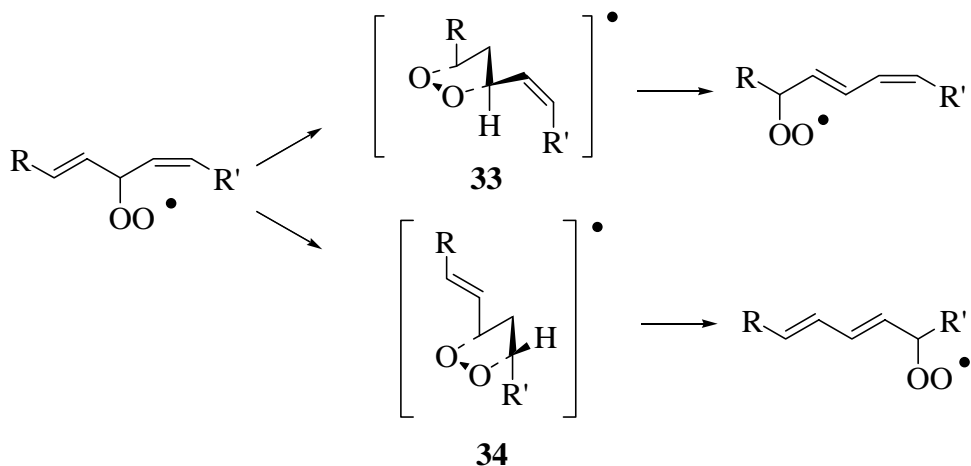
Figure II-12: Bis-allylic peroxyl rearrangements through isomeric radical-dioxygen intermediates.

The complex **33** derives from rearrangement across the *trans*-double bond, while **34** is formed from rearrangement across the *cis*-double bond. The calculated low-energy conformation of **32** is a typical five-membered ring envelope structure and based upon that structure, one anticipates that the formation of **33** would be favored over the formation of **34**.[59] Substitution in **33** is di-equatorial on the ring while **34** must have one axial substituent. Thus, product distribution in the oxidation may be biased due to the preferential formation of **33** over **34**, the consequence of which is the formation of the *trans, cis* hydroperoxide. Experiments exploring the allylperoxyl radical rearrangement will be discussed in greater detail in Chapter III.

Olefin Geometry Conclusions

The autoxidations of *cis*, *cis*; *cis*, *trans*; and *trans*, *trans* non-conjugated dienes and their corresponding octadecadienoates give rise to kinetically controlled hydroperoxides. Formation of the bis-allylic peroxyl radical and its subsequent β-fragmentation depends on the geometry of the alkene precursor and as a result the pentadienyl radical intermediate. Significant unpaired electron spin density is present at the central carbon of the pentadienyl radicals and the bis-allylic hydroperoxide product that arises from addition at this position is the major kinetic product for each of the systems studied, provided a sufficient hydrogen atom donor is present.

Unpaired spin density is not the only factor that determines the position of oxygen addition to a delocalized radical, however. We speculate that radical-triplet dioxygen complexes may be intermediates in the formation and rearrangement of delocalized radicals. Rearrangement of the bis-allylic peroxyl radicals to the conjugated peroxyl radicals occurs with rate constants between 2.2 and 2.8 x 10^6 s^{-1}. This rearrangement can be used as a peroxyl radical clock regardless of the mechanism by which this rearrangement occurs.[14]

Although the previous studies were carried out using methyl linoleate, any of the substrates discussed here could be used in clocking experiments depending on the preference for HPLC or GC analysis. This offers a very straightforward method for determining the rate constant of H-atom transfer to a peroxyl radical in the kinetic range of 10^5 to 10^6 M^{-1} s^{-1}.[14,66] Although the formation of bis-allylic hydroperoxides can only be observed at concentrations of α-tocopherol that are not normally encountered *in vivo*, the formation of these products may become important in confined systems, such as an enzyme active site,[67] or a lipid particle having excellent H-atom donors present.[29,66,68]

This work was completed with the help of Dr. Keri Tallman who conducted oxidation experiments on methyl linoleate, the *cis*, *trans* isomers of methyl linoleate, as well as the *cis, cis*- and *cis, trans*-pentadecadienes. Dr. Tallman also synthesized the oxidation products of the *cis*, *cis*- and *cis, trans*-pentadecadienes discussed in this chapter and described in detail below.

Experimental Methods

General methods

^{1}H and ^{13}C NMR spectra were collected on a 300 or 400 MHz NMR, using Bruker software. HPLC analyses were carried out with a Waters 600 liquid chromatograph interfaced to a Waters 996 PDA detector. Linoleate hydroperoxides were separated on a Beckman Ultrasphere silica column (0.46 x 25 cm) using 0.5% *iso*-propanol/hexanes at 1.0 mL/min and detected at 207 nm. HPLC-MS analyses were carried out as previously described[40] using a Beckman Ultrasphere narrow bore silica column (0.20 x 25 cm) with 0.5% iPrOH/hexanes (0.15 mL/min) and post-column addition of $AgBF_4$/iPrOH (0.3 mM, 0.075 mL/min) (Figure II-13). GC analyses were carried out with a Hewlett-Packard 6890 gas chromatograph equipped with a DB-5 (30 m x 0.32 mm x 0.25 mm) fused silica column from J&W Scientific. The diene alcohols were separated using a temperature program of 100-180 ºC @ 5 º/min, 180-280 ºC @ 20 º/min (10 min) (Figure II-14).
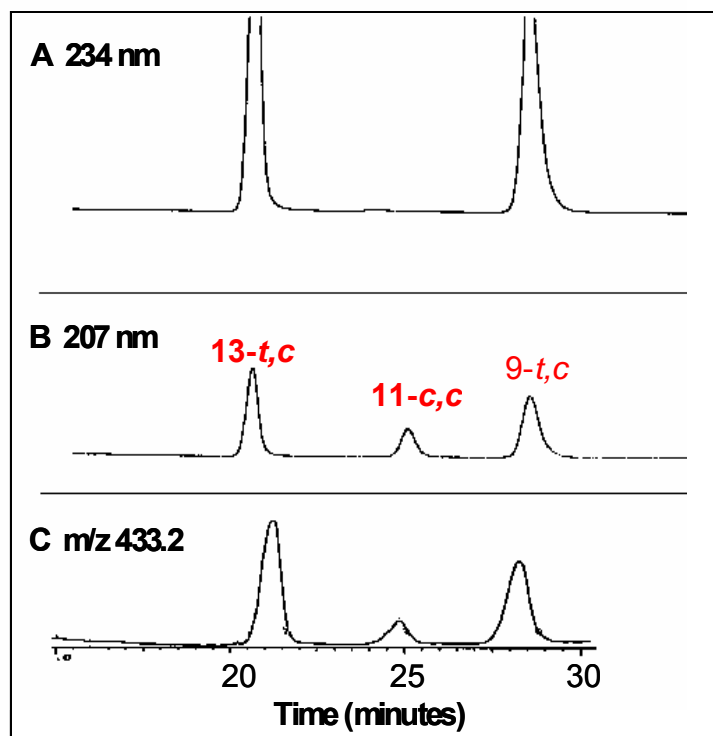
Figure II-13: Representative HPLC-MS chromatograms of a methyl linoleate oxidation mixture. A: HPLC-UV detection at 234 nm; B: HPLC-UV detection at 207 nm; C: HPLC-MS (Ag CIS), intact hydroperoxides detected at 433.2 (M+Ag). HPLC-MS analyses were carried out using a Beckman Ultrasphere narrow bore (0.20 x 25 cm) silica column with 0.5% iPrOH/hexanes (0.15 mL/min) and post-column addition of AgBF$_4$/iPrOH (0.3 mM, 0.075 mL/min) as described in reference 40.
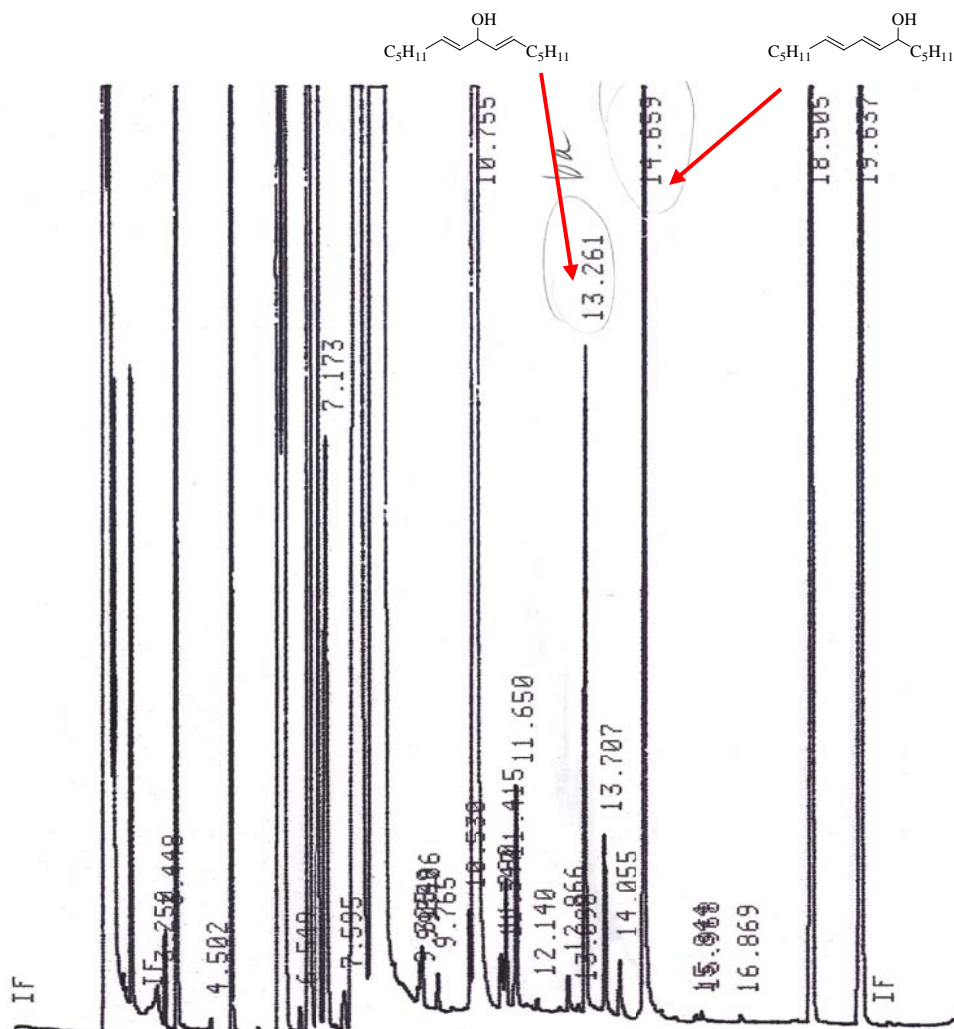
Figure II-14: Representative GC chromatogram of the oxidation of 6, 9-*trans, trans*-pentadecadiene at 20x magnification. The hydroperoxides formed in the oxidation were reduced to their corresponding diene alcohols with an excess of PPh₃ and GC analyses were carried out on a Hewlett-Packard 6890 gas chromatograph equipped with a DB-5 (30 m x 0.32 mm x 0.25 mm) fused silica column from J&W Scientific. The diene alcohols were separated using a temperature program of 100-180 °C @ 5 °/min, 180-280 °C @ 20 °/min (10 min). many of the peaks seen here are initiator derived, associated with α or present in the solvent, but do not interfere with the kinetic analysis.

All synthetic reactions were carried out in oven-dried glassware under an atmosphere of argon. All reagents were purchased from Aldrich unless otherwise specified. Methyl linoleate and linoelaidate were purchased from Nu-

Chek Prep and chromatographed on silica (10% EtOAc/hexanes) prior to use. The initiator, 2,2'-azobis(4-methoxy-2, 4-dimethylvaleronitrile) (MeOAMVN), was obtained from Wako and dried under high vacuum for 2 h. α-Tocopherol was purchased from Aldrich and purified by flash chromatography (10% EtOAc/hexanes on silica), protected from light and oxygen. It is crucial that the α-tocopherol be purified prior to use and dried overnight under high vacuum.

THF and CH_2Cl_2 were dried using a solvent purification system from SolvTech. Anhydrous DMF was used in the propargyl chloride copper coupling reactions. Pyridine, Et_3N, iPr_2NH, and DMPU were distilled from CaH_2. Benzene was passed through a column of alumina. NBS was recrystallized from H_2O and dried under high vacuum overnight. *m*-CPBA was purified by washing a benzene solution with phosphate buffer (pH 7.4).

The synthesis of the *cis, trans*-octadecadienoates (**9a** and **9b**) have been reported.[16,69] All other compounds were synthesized and freshly chromatographed on silica (**9a** and **9b** with 10% EtOAc/hexanes, the pentadecadienes with hexanes) prior to use to remove any oxidation products.

All dienes were purified on silver nitrate impregnated silica gel (SNIS).[26] SNIS TLC plates were made by elution of silica plates in aqueous $AgNO_3$ (10%). The plates were air-dried, then dried at 100 ºC for 1 h. The silica gel was made by making slurry of silica gel in 10% $AgNO_3$/MeOH and stirring for 10-15 minutes. CH_3CN was added to aid in dissolution of the $AgNO_3$. The solvent was removed *in vacuo* and the silica gel dried overnight under high vacuum. The TLC plates and silica gel were stored protected from light.
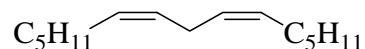
General Procedure for oxidations

Stock solutions of each octadecadienoate or diene (1.5-1.7 M), MeOAMVN (0.1 M), and α-tocopherol (1.0 M) were made up in benzene. For samples containing high concentrations, neat α-tocopherol (2.2 M) was used. Samples were made up in autosampler vials with a total reaction volume of 100 µL. It was important to add the solutions in the following order to avoid premature oxidation: α-tocopherol (0.05-1.8 M), octadecadienoate or diene (0.15-0.17 M), MeOAMVN (0.01 M) and diluted to 100 µL with benzene. The sealed samples were then incubated at 37 °C for 4 h.
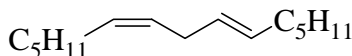
After 4 h, the oxidation was stopped by the addition of BHT (50 µL of 1.0 M solution in hexanes), followed by the addition of the internal standard (benzyl alcohol (5 mM) for octadecadienoates and tetradecane (5 mM) for dienes). The octadecadienoate samples were diluted to 1.0 mL with hexanes and analyzed by HPLC as their hydroperoxides. The diene samples were reduced with PPh_3 (50 µL of 1.0 M solution/hexanes) and analyzed by GC.

Synthetic procedures
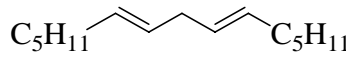
Synthesis of (Z, Z)-6, 9-pentadecadiene (11). C_5H_{11} —— C_5H_{11} Pd/BaSO$_4$ (0.26 g, 10% (wt)) and quinoline (0.90 mL, 40% (wt)) were added to a solution of 6, 9-pentadecadiyne (2.56 g, 0.013 mol) in EtOAc (130 mL) and charged with H_2. After 7 h, the reaction mixture was filtered through Celite. The organics were washed with 5% HCl (50 mL), saturated $NaHCO_3$ (50 mL), brine, and dried over $MgSO_4$. The product was purified by
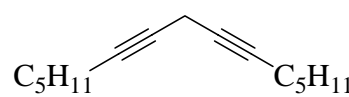
column chromatography (hexanes) and isolated as a colorless liquid (1.97 g, 75%). Product of higher purity (>95% by GC) was obtained after SNIS chromatography (9:1 to 4:1, hexanes: toluene). ^{1}H NMR (CDCl$_3$) δ 5.38 (m, 4H), δ 2.80 (t, 2H, J=6.1Hz), δ 2.08 (q, 4H, J=6.5Hz), δ 1.38 (m, 12H), δ 0.92 (t, 6H, J=6.6Hz); ^{13}C NMR (CDCl$_3$) δ 130.4, 128.2, 31.8, 29.6, 27.4, 25.9, 22.8, 14.3; HRMS (EI) calculated 208.2186, observed 208.2169.

Synthesis of (6E, 9Z)-6, 9-pentadecadiene (12). Pd/BaSO$_4$ (0.27 g, 10% (wt)) and quinoline (1.0 mL, 40% (wt)) were added to a solution of *cis*-6-pentadecadien-9-yne (2.64 g, 0.013 mol) in hexanes (65 mL) and the reaction mixture charged with H$_2$. After 3.5 h, the reaction mixture was filtered through Celite. The filtrate was washed with 5% HCl (50 mL), brine, and dried over MgSO$_4$. The product (2.37 g, 88%) was purified by column chromatography (hexanes) and isolated as a colorless liquid. SNIS chromatography (9:1 to 4:1, hexanes: toluene) yielded product with purity >95%, as determined by GC. ^{1}H NMR (CDCl$_3$) δ 5.43 (m, 4H), δ 2.75 (t, 2H, J=5.1Hz), δ 2.03 (m, 4H), δ 1.33 (m, 12H), δ 0.913 (t, 3H, J=7.1Hz), δ 0.908 (t, 3H, J=6.9Hz); ^{13}C NMR (CDCl$_3$) δ 131.0, 130.6, 128.5, 127.9, 32.8, 31.8, 31.7, 30.7, 29.6, 29.5, 27.3, 22.8, 14.3; HRMS (EI) calculated 208.2186, observed 208.2202.

Synthesis of (E, E)-6, 9-pentadecadiene (13).[23] NH_3 (200 mL) was condensed into a flask at –78 °C. A solution of 6, 9-pentadecadiyne (6.27 g, 0.031 mol) in ether (60 mL), *tert*-butanol (75 mL, 0.78 mol), and $(NH_4)_2SO_4$ (41.5 g, 0.31 mol), was added to the NH_3. Li° (2.17 g, 0.31 mol) was subsequently added in portions. The reaction mixture turned blue upon the addition of Li°, then slowly dissipated over time. After 30 min, NH_4Cl (33.4 g, 0.61 mol) was added, the reaction mixture warmed to room temperature, and the NH_3 allowed to evaporate. The reaction mixture was diluted with H_2O (200 mL) and extracted with hexanes (3 x 150 mL). The organics were washed with 5% HCl (100 mL), brine, and dried over $MgSO_4$. Column chromatography (hexanes) yielded the product as a colorless liquid (5.21 g, 82%). Higher purity (>95% by GC) product was obtained after SNIS chromatography (9:1 to 4:1, hexanes: toluene). ^{1}H NMR (CDCl$_3$) δ 5.42 (m, 4H), δ 2.69 (t, 2H, *J*=3.8Hz), δ 2.00 (q, 4H, *J*=6.8Hz), δ 1.32 (m, 12H), δ 0.90 (t, 6H, *J*=6.5Hz); ^{13}C NMR (CDCl$_3$) δ 131.3, 128.8, 35.9, 32.8, 31.7, 29.5, 22.8, 14.3; HRMS (EI) calculated 208.2186, observed 208.2202.

Synthesis of 6, 9-pentadecadiyne (14).[20-22] 1-Heptyne (7.2 mL, 0.055 mol) and 1-chloro-2-octyne (6.0 mL, 0.039 mol) were added to a suspension of K_2CO_3 (7.58 g, 0.055 mol), CuI (11.1 g, 0.058 mol), and NaI (8.83 g, 0.059 mol) in DMF (80 mL). Upon stirring, the reaction mixture turned green. The reaction was monitored by GC. After stirring overnight, the reaction mixture was diluted with ether (150 mL) and

filtered through Celite. The organics were washed with NH_4Cl (100 mL), then the aqueous layer was back-extracted with ether (150 mL). The organic layer was washed with brine and dried over $MgSO_4$. Column chromatography (hexanes to 19:1, hexanes: EtOAc) yielded the product (7.39 g, 93%) as a yellow liquid. ^1H NMR ($CDCl_3$) δ 3.06 (p, 2H, J=2.4Hz), δ 2.10 (tt, 4H, J_1=2.4Hz, J_2=7.0Hz), δ 1.44 (m, 8H), δ 1.28 (m, 8H), δ 0.85 (t, 6H, J=7.1Hz); ^{13}C NMR ($CDCl_3$) δ 80.4, 74.6, 31.2, 28.5, 22.4, 18.8, 14.1, 9.7; HRMS (EI) calculated 204.1873, observed 204.1913.
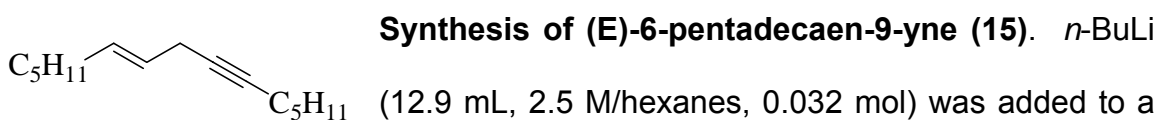
Synthesis of (E)-6-pentadecaen-9-yne (15). *n*-BuLi (12.9 mL, 2.5 M/hexanes, 0.032 mol) was added to a solution of 1-heptyne (4.5 mL, 0.034 mol) in THF (100 mL) at –78 °C. After 15 min, DMPU (8.3 mL, 0.069 mol) and a solution of *trans*-1-bromo-2-octene (4.35 g, 0.023 mol) in THF (5 mL) were added. The reaction was allowed to warm slowly to room temperature. After stirring overnight, the reaction mixture was poured into saturated NH_4Cl (100 mL) and extracted with hexanes (3 x 100 mL). The organics were washed with brine and dried over $MgSO_4$. Column chromatography (hexanes) yielded the product (3.76 g, 80%) as a colorless liquid. ^1H NMR ($CDCl_3$) δ 5.67 (m, 1H), δ 5.39 (m, 1H), δ 2.86 (dt, 2H, J_1=1.3Hz, J_2=3.7Hz), δ 2.17 (tt, 2H, J_1=2.4Hz, J_2=7.0Hz), δ 2.00 (q, 2H, J=6.8Hz), δ 1.50 (m, 2H), δ 1.31 (m, 10H), δ 0.90 (t, 3H, J=6.9Hz), δ 0.88 (t, 3H, J=6.9Hz); ^{13}C NMR ($CDCl_3$) δ 132.0, 124.9, 82.2, 77.7, 32.5, 31.6, 31.3, 29.3, 29.0, 22.8, 22.5, 22.2, 19.0, 14.3, 14.2; HRMS (EI) calculated 206.2029, observed 206.1987.
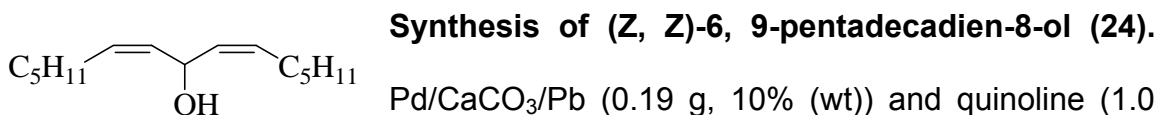
Synthesis of (Z, Z)-6, 9-pentadecadien-8-ol (24).
Pd/CaCO$_3$/Pb (0.19 g, 10% (wt)) and quinoline (1.0 mL, 8.46 mmol) were added to a solution of 6, 9-pntadecadiyn-8-ol (1.83 g, 8.34 mmol) in hexanes (40 mL) and charged with H$_2$. After 2 h, the reaction mixture was filtered through Celite. The filtrate was washed with 5% HCl (25 mL), saturated NaHCO$_3$ (25 mL), brine, and dried over MgSO$_4$. Column chromatography (5:1 to 4:1, hexanes:EtOAc) yielded the product (1.57 g, 84%) as a pale yellow liquid. ^{1}H NMR (CDCl$_3$) δ 5.45 (m, 4H), δ 5.24 (dt, 1H, J_1=1.9Hz, J_2=7.4Hz), δ 2.11 (m, 4H), δ 1.64 (br s, 1H), δ 1.42-1.25 (m, 12H), δ 0.88 (t, 6H, J=7.0Hz); ^{13}C NMR (CDCl$_3$) δ 132.1, 131.3, 63.9, 31.7, 29.5, 28.0, 22.7, 14.2; HRMS (ES$^+$) calculated (M+Na) 247.2032, observed 247.2040.
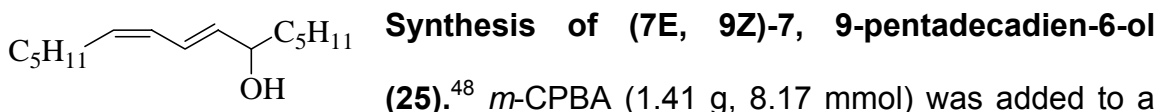
Synthesis of (7E, 9Z)-7, 9-pentadecadien-6-ol (25).[48] m-CPBA (1.41 g, 8.17 mmol) was added to a solution of 1-phenylseleno-3-nonene (2.04 g, 7.25 mmol) in THF (36 mL) at -78°C. After 30 min, LDA [prepared by the addition of n-BuLi (6.4 mL, 2.5 M/hexanes, 16.0 mmol) to a solution of iPr$_2$NH (2.3 mL, 16.4 mmol) in THF (3 mL)] was added and the reaction mixture stirred for 10 min. Hexanal (1.1 mL, 9.16 mmol) was subsequently added dropwise. After 1.5 h, iPr$_2$NH (1.3 mL, 9.28 mmol) and hexanes (30 mL) were added and the reaction mixture refluxed for 15 min. The reaction mixture was cooled to room temperature and diluted with hexanes (50 mL). The organics were washed with 10% K$_2$CO$_3$ (50 mL), 5% HCl (50 mL), saturated NaHCO$_3$ (50 mL), brine, and dried over MgSO$_4$. Column

chromatography (9:1, hexanes:EtOAc) yielded the product as a yellow liquid (1.13 g, 70%). ^{1}H NMR (CDCl$_3$) δ 6.48 (dd, 1H, J_1=11.0Hz, J_2=15.2Hz), δ 5.97 (t, 1H, J=11.0Hz), δ 5.65 (dd, 1H, J_1=6.9Hz, J_2=15.2Hz), δ 5.45 (dt, 1H, J_1=7.6Hz, J_2=10.7Hz), δ 4.12 (q, 1H, J=6.6Hz), δ 2.18 (q, 2H, J=7.1Hz), δ 1.66 (br s, 1H), δ 1.50 (m, 2H), δ 1.41-1.31 (m, 12H), δ 0.89 (t, 6H, J=6.7Hz); ^{13}C NMR (CDCl$_3$) δ 136.0, 133.2, 127.9, 126.0, 73.1, 37.5, 32.0, 31.7, 29.5, 27.9, 25.3, 22.8, 22.7, 14.2; HRMS (ES$^+$) calculated (M+Na) 247.2032, observed 247.2023.
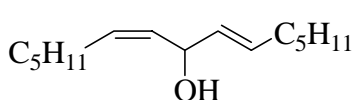
Synthesis of (6E, 9Z)-6, 9-pentadecadien-8-ol (26). Pd/CaCO$_3$/Pb (1.18 g, 20% (wt)) and quinoline (2.1 mL, 40% (wt)) were added to a solution of 6-pentadecadien-9-yn-8-ol (5.79 g, 0.026 mol) in EtOAc (260 mL) and charged with H$_2$. After 2 h, the reaction mixture was filtered through Celite. The filtrate was washed with 5% HCl (50 mL), saturated NaHCO$_3$ (50 mL), brine, and dried over MgSO$_4$. After column chromatography (9:1 to 4:1, hexanes:EtOAc), the product was isolated as a pale yellow liquid (4.82 g, 82%). ^{1}H NMR (CDCl$_3$) δ 5.69 (dt, 1H, J_1=6.6Hz, J_2=15.3Hz), δ 5.44 (m, 3H), δ 4.88 (t, 1H, J=7.0Hz), δ 2.08 (q, 2H, J=6.5Hz), δ 2.01 (q, 2H, J=7.0Hz), δ 1.75 (br s, 1H), δ 1.41-1.28 (m, 12H), δ 0.87 (t, 6H, J=6.4Hz); ^{13}C NMR (CDCl$_3$) δ 132.1, 131.7, 131.3, 69.0, 32.4, 31.65, 31.57, 29.4, 29.0, 27.8, 22.6, 14.2; HRMS (ES$^+$) calculated (M+Na) 247.2032, observed 247.2037.
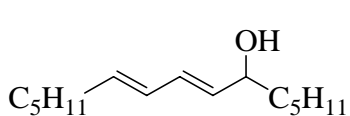
Synthesis of (7E, 9E)-7, 9-pentadecadien-6-ol (27).
Pentylmagnesium bromide (4.2 mL, 2.0 M/ether, 8.40 mmol) was added to a solution of *trans, trans*-2, 4-decadienal (1.0 mL, 5.63 mmol) in THF (28 mL) at −78 °C, then warmed to room temperature. After stirring overnight, the reaction mixture was poured into saturated NH_4Cl (50 mL) and extracted with hexanes (3 x 70 mL). The organics were washed with brine and dried over $MgSO_4$. Column chromatography (4:1, hexanes:EtOAc) yielded the product as a pale yellow liquid (1.21 g, 96%). ^1H NMR ($CDCl_3$) δ 6.13 (dd, 1H, J_1=10.4Hz, J_2=14.9Hz), δ 5.99 (dd, 1H, J_1=10.5Hz, J_2=14.9Hz), δ 5.65 (dt, 1H, J_1=6.9Hz, J_2=14.9Hz), δ 5.53 (dd, 1H, J_1=7.0Hz, J_2=15.0Hz), δ 4.05 (q, 1H, J=6.3Hz), δ 2.33 (s, 1H), δ 2.05 (q, 2H, J=6.8Hz), δ 1.48 (m, 2H), δ 1.41-1.27 (m, 12H), δ 0.87 (t, 6H, J=6.9Hz); ^{13}C NMR ($CDCl_3$) δ 135.3, 133.9, 130.9, 129.7, 72.8, 37.4, 32.7, 31.9, 31.5, 29.1, 25.3, 22.7, 22.6, 14.14, 14.12; HRMS (ES^+) calculated (M+Na) 247.2032, observed 247.2040.
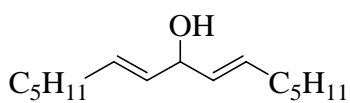
Synthesis of (E, E)-6, 9-pentadecadien-8-ol (28).
$LiAlH_4$ (0.28 g, 7.43 mmol) was added to a solution of 6-pentadecadien-9-yn-8-ol (0.54 g, 2.45 mmol) in THF (12 mL) and refluxed. The reaction was monitored by GC. After 30 min, the reaction mixture was cooled to room temperature and quenched with H_2O (2 mL) and NaOH (2 mL), then diluted with additional H_2O (25 mL). The aqueous layer was extracted with hexanes (3 x 40 mL). The organics were washed with brine and dried over

MgSO$_4$. The product (0.33 g, 60 %) was isolated as a pale yellow liquid after column chromatography (9:1, hexanes:EtOAc). ^{1}H NMR (CDCl$_3$) δ 5.64 (t, 2H, J_1=6.6Hz, J_2=15.4Hz), δ 5.48 (dd, 2H, J_1=1.0Hz, J_2=6.3Hz, J_3=15.4Hz), δ 4.50 (t, 1H, J=6.3Hz), δ 2.01 (q, 4H, J=6.6Hz), δ 1.88 (s, 1H), δ 1.39-1.24 (m, 12H), δ 0.87 (t, 6H, J=6.7Hz); ^{13}C NMR (CDCl$_3$) δ 132.2, 131.8, 73.8, 32.3, 31.5, 28.9, 22.7, 14.2; HRMS (ES$^+$) calculated (M+Na) 247.2032, observed 247.2045.
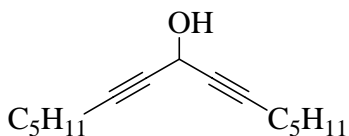
**Synthesis of 6, 9-pentadecadiyn-8-ol (29).**[47] *n*-BuLi (21.0 mL, 2.5 M/hexanes, 0.053 mol) was added to a solution of 1-heptyne (7.5 mL, 0.057 mol) in THF (100 mL) at −78 °C. After 10 min, ethyl formate (2.0 mL, 0.025 mol) was added and the reaction mixture allowed too warm slowly to room temperature. After 2 h, the reaction mixture was poured into saturated NH$_4$Cl (70 mL) and extracted with EtOAc (3 x 100 mL). The organic layer was washed with brine and dried over MgSO$_4$. The product (5.24 g, 96%) was isolated as a yellow liquid after column chromatography (5:1 to 4:1, hexanes:EtOAc). ^{1}H NMR (CDCl$_3$) δ 5.06 (dt, 1H, J_1=2.0Hz, J_2=6.9Hz), δ 2.58 (d, 1H, J=7.0Hz), δ 2.18 (dt, 4H, J_1=1.7Hz, J_2=7.1Hz), δ 1.48 (p, 4H, J=7.1Hz), δ 1.29 (m, 8H), δ 0.86 (t, 6H, J=7.0Hz); ^{13}C NMR (CDCl$_3$) δ 84.9, 78.2, 52.4, 31.1, 28.1, 22.2, 18.7, 14.0.
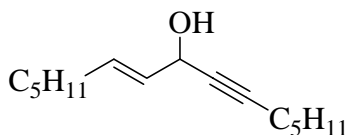
Synthesis of (E)-6-pentadecadien-9-yn-8-ol (30). *n-*BuLi (13.0 mL, 2.5 M/hexanes, 0.033 mol) was added to a solution of 1-heptyne (4.6 mL, 0.035 mol) in THF (100 mL) at –78 °C. After 15 min, *trans*-2-octenal (4.0 mL, 0.027 mol) was added. After 30 min, the reaction mixture was poured into saturated NH_4Cl (100 mL) and extracted with hexanes (3 x 130 mL). The organic layer was washed with brine and dried over $MgSO_4$. The product was purified by column chromatography (9:1 to 4:1, hexanes:EtOAc) and isolated as a pale yellow liquid (5.79 g, 97%). ^1H NMR (CDCl$_3$) δ 5.84 (dt, 1H, J_1=6.7Hz, J_2=15.2Hz), δ 5.55 (dd, 1H, J_1= 6.0Hz, J_2=15.2Hz), δ 4.79 (br s, 1H), δ 2.21 (dt, 2H, J_1=1.8Hz, J_2=7.1Hz), δ 2.19 (s, 1H), δ 2.03 (q, 2H, J=6.9Hz), δ 1.51 (p, 2H, J=7.0Hz), δ 1.43-1.20 (m, 10H), δ 0.88 (t, 3H, J=7.0Hz), δ 0.87 (t, 3H, J=6.8Hz); ^{13}C NMR (CDCl$_3$) δ 133.5, 129.7, 86.8, 79.9, 63..2, 32.0, 31.5, 31.2, 28.7, 28.4, 22.6, 22.3, 18.8, 14.1, 14.0; HRMS (ES$^+$) calculated (M+Na) 245.1876, observed 245.1882.
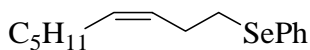
Synthesis of (Z)-1-phenylseleno-3-nonene (31). LiAlH$_4$ (20 mL, 1.0 M/THF, 0.020 mol) was added slowly to a solution of (PhSe)$_2$ (7.50 g, 0.024 mol) in THF (80 mL). The solution turned from dark orange to a cloudy yellow. After 20 min, a solution of (Z)-3-nonen-1-ol methanesulfonate (3.50 g, 0.016 mol) in THF (10 mL) was added. After stirring overnight, the excess (PhSe)$_2$ was reduced by the addition of LiAlH$_4$ until the yellow color dissipated and TLC showed the disappearance of the (PhSe)$_2$. The reaction was quenched with saturated NaHCO$_3$ (100 mL), and extracted with

72

hexanes (3 x 150 mL). The organics were washed with brine and dried over MgSO$_4$. The product was purified by column chromatography (9:1, hexanes:EtOAc) and isolated as a yellow liquid (2.67 g, 60%). ^{1}H NMR (CDCl$_3$) δ 7.41 (m, 2H), δ 7.16 (m, 3H), δ 5.33 (m, 2H), δ 2.82 (t, 2H, J=7.4Hz), δ 2.35 (q, 2H, J=6.8Hz), δ 1.27-1.15 (m, 6H), δ 0.80 (t, 3H, J=6.5Hz); ^{13}C NMR (CDCl$_3$) δ 132.7, 132.0, 130.6, 129.2, 128.0, 126.9, 31.7, 29.5, 28.1, 27.6, 27.5, 22.7, 14.3; HRMS (EI) calculated 282.0881, observed 282.0916.

Synthesis of *trans*-1-bromo-2-octene.[24] NBS (4.28 g, 0.024 mol) was added to a solution of (E)-2-octen-1-ol (3.0 mL, 0.020 mol) and PPh$_3$ (5.77 g, 0.022 mol) in CH$_2$Cl$_2$ (100 mL) at –20 °C, then the reaction mixture was allowed to warm to room temperature. The reaction turned yellow-orange upon warming to rt. After 1.5 h, the reaction mixture was concentrated to half the volume and diluted with hexanes (200 mL) to crash out most of the Ph$_3$P=O, then filtered. The organics were washed with H$_2$O (75 mL), brine, and dried over MgSO$_4$. Chromatography (9:1, hexanes:EtOAc) through a short plug of silica yielded the product (2.91 g, 77%) as a colorless liquid. ^{1}H NMR (CDCl$_3$) δ 5.72 (m, 2H), δ 3.95 (d, 2H, J=7.0Hz), δ 2.06 (q, 2H, J=6.8Hz), δ 1.38 (m, 2H), δ 1.29 (m, 4H), δ 0.89 (t, 3H, J=6.7Hz); ^{13}C NMR (CDCl$_3$) δ 136.9, 126.4, 33.8, 32.2, 31.5, 28.6, 22.7, 14.2; HRMS (EI) calculated 190.0352, observed 190.0340.
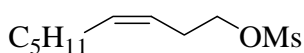
Synthesis of (Z)-3-nonen-1-yl methanesulfonate. Methanesulfonyl chloride (1.1 mL, 0.014 mol) was added dropwise to a solution of *cis*-3-nonen-1-ol (2.0 mL, 0.012 mol) in pyridine (50 mL). After 4 h, the reaction mixture was diluted with H_2O (100 mL) and extracted with ether (3 x 100 mL). The organic layer was washed with 5% HCl (100 mL), saturated $NaHCO_3$ (100 mL), brine, and dried over $MgSO_4$. The product was purified by column chromatography (2:1, hexanes:EtOAc) and isolated as a yellow liquid (2.19 g, 84%). ^1H NMR (CDCl$_3$) δ 5.54 (m, 1H), δ 5.33 (m, 1H), δ 4.19 (t, 2H, *J*=6.9Hz), δ 2.99 (s, 3H), δ 2.49 (1, 2H, *J*=7.5Hz), δ 2.03 (q, 2H, *J*=7.0Hz), δ 1.37-1.24 (m, 6H), δ 0.87 (t, 3H, *J*=6.7Hz); ^{13}C NMR (CDCl$_3$) δ 134.4, 122.7, 69.5, 37.6, 31.6, 29.3, 27.5, 22.7, 14.2; HRMS (ES$^+$) calculated (M+Na) 243.1025, observed 243.1038.

References

(1)   Steinberg, D.; Parhsarathy, S.; Carwe, T. E.; Khoo, J. C.; J.L, W. *New Engl. J. Med.* **1989***, 320*, 915.

(2)   Marnett, L. J. *Carcinogenesis* **2000***, 21*, 361-370.

(3)   Sevanian, A.; Ursini, F. *Free Rad. Biol. Med.* **2000***, 29*, 306-311.

(4)   Spiteller, G.; Spiteller, D.; Jira, W.; Kessling, U.; Dudda, A. et al. *Peroxide Chem.* **2000**, 179.

(5)   Chisolm, G.; Steinberg, D. *Free Rad. Biol. Med.* **2000***, 28*, 1815-1826.

(6)   Chan, H. W.-S.; Levett, G. *Lipids* **1977***, 12*, 99.

(7)   Porter, N. A. *Acc. Chem. Res.* **1986***, 19*, 262-268.

(8)   Porter, N. A.; Caldwell, S. E.; Mills, K. A. *Lipids* **1995***, 30*, 277-290.

(9)   Recknagel, R. O.; Choshal, A. K. *Exp. Mol. Pathol.* **1966**, *5*, 413.

(10)   Slater, T. *Methods in Enzymology*; Academic: Orlando, FL, 1984; 283.

(11)   Nair, V.; Turner, G. A. *Lipids* **1984**, *19*, 804.

(12)   Tagaki, T.; Mitsuno, Y.; Masumura, M. *Lipids* **1978**, *13*, 147.

(13)   Brash, A. R. *Lipids* **2000**, *35*, 047-952.

(14)   Tallman, K. A.; Pratt, D. A.; Porter, N. A. *J. Am. Chem. Soc.* **2001**, *123*, 11827-11828.

(15)   Tallman, K. A.; Roschek, Jr., B; Porter, N. A. *J. Am. Chem. Soc.* **2004**, *126*, 9240-9247.

(16)   Porter, N. A.; Wujek, D. G. *J. Am. Chem. Soc.* **1984**, *106*, 2626-2629.

(17)   Sargis, R. M.; Subbaiah, P. V. *Biochem.* **2003**, *42*, 11533.

(18)   Katan, M. B.; Zock, P. L.; Mensink, R. P. *Annu. Rev. Nutr.* **1995**, *15*, 473.

(19)   Mensink, R. P.; Katan, M. B. *New Engl. J. Med.* **1990**, *323*, 439.

(20)   Ivanov, I. V.; Groza, N. V.; Romanov, S. G.; Kuhn, H.; Myagkova, G. I. *Synthesis* **2000**, 691.

(21)   Dasse, O.; Mahadevan, A.; Han, L.; Martin, B. R.; Di Marzo, V. et al. *Tetrahedron* **2000**, *56*, 9195.

(22)   Jeffery, T.; Gueugnot, S.; Linstrumelle, G. *Tet. Lett.* **1992**, *33*, 5757.

(23)   Brandsma, L.; Nieuwenhuizen, W. F.; Maeorg, U. *Eur. J. Org. Chem.* **1999**, 775.

(24)   Chun, J.; Li, G.; Byun, H.-S.; Bittman, R. *J. Org. Chem.* **2002**, *67*, 2600.

(25)   Capon, R. J.; Barrow, R. A. *J. Org. Chem.* **1998**, *63*, 75.

(26)   Williams, C. M.; Mander, L. N. *Tetrahedron* **2001**, *57*, 425.

(27)   Burton, G. W.; Doba, T.; Gabe, E. J.; Hughes, L.; Lee, F. L. et al. *J. Am. Chem. Soc.* **1985**, *107*, 7053-7065.

(28)   Burton, G. W.; Hughes, L.; Ingold, K. U. *J. Am. Chem. Soc.* **1983**, *105*, 5950.

(29)   Pratt, D. A.; DiLabio, G. A.; Brigati, G.; Pedulli, G.-F.; Valgimigli, L. *J. Am. Chem. Soc.* **2001**, *123*, 4625-4626.

(30) Pratt, D. A.; Mills, J. A.; Porter, N. A. *J. Am. Chem. Soc.* **2003**, *125*, 5801-5810.

(31) Upston, J. M.; Terentis, A. C.; Stocker, R. *FASEB* **1999**, *13*, 977.

(32) Bowry, V. W.; Ingold, K. U. *Acc. Chem. Res.* **1999**, *32*, 27.

(33) Culbertson, S. M.; Vingvist, M. R.; Barclay, L. R. C.; Porter, N. A. *J. Am. Chem. Soc.* **2001**, *123*, 8951.

(34) Bascetta, E.; Gunstone, F. D.; Scrimgeour, C. M.; Walton, J. C. *J. Chem. Soc. Chem. Commun.* **1982**, 110.

(35) Bascetta, E.; Gunstone, F. D.; Walton, J. C. *J. Chem. Soc. Perkin Trans. II* **1983**, 603.

(36) Pratt, D. A.; Porter, N. A. *Org. Lett.* **2003**, *5*, 387-390.

(37) Kranenburg, M.; Ciriano, M. V.; Cherkasov, A.; Mulder, P. *J. Phys. Chem.* **2000**, *104*, 915.

(38) Bayer, E.; Gfrorer, P.; Rentel, C. *Angew. Chem. Intl. Ed.* **1999**, *38*, 992.

(39) Suma, K.; Raju, N. P.; Vairamani, M. *Rapid Comm. Mass Spectrom.* **1997**, *11*, 1939.

(40) Havrilla, C. M.; Hachey, D. L.; Porter, N. A. *J. Am. Chem. Soc.* **2000**, *122*, 8042.

(41) Seal, J. R.; Havrilla, C. M.; Porter, N. A.; Hachey, D. L. *J. Am. Chem. Soc. Mass Spec.* **2003**, *14*, 872.

(42) Hock, H. *Angew. Chem.* **1936**, *49*, 595.

(43) Frimer, A. A. *Chem. Rev.* **1979**, *79*, 359.

(44) Tanigawa, S.; Kajiware, T.; Hatanaka, A. *Phytochemistry* **1984**, *23*, 2439.

(45) Gardner, H. W.; Planter, R. D. *Lipids* **1984**, *119*, 294.

(46) Kenar, J. A.; Havrilla, C. M.; Porter, N. A.; Guyton, J. R.; Brown, S. A. et al. *Chem. Res. Toxicol.* **1996**, *9*, 737.

(47) Guo, C.; Lu, X. *Synlett* **1992**, 405.

(48) Baldwin, J. E.; Reed, N. V.; Thomas, E. J. *Tetrahedron* **1981**, *37*, 263.

(49) Schenck, G. D.; Neumuller, O. A.; Eisfeld, K. C. *Angew. Chem.* **1958**, 595.

(50)   Brill, W. F. *J. Am. Chem. Soc.* **1965***, 87*, 3286.

(51)   Avila, D. V.; Davies, A. G.; Davison, I. G. *J. Chem. Soc. Perkin Trans. II* **1988**, 1847.

(52)   Davies, A. G.; Kinart, W. J. *J. Chem. Res.* **1989**, 22.

(53)   Dang, H.; Davies, A. G.; Davison, I. G.; Schiesser, C. H. *J. Org. Chem.* **1990***, 55*, 5085.

(54)   Porter, N. A.; Kaplan, J. K.; Dussault, P. H. *J. Am. Chem. Soc.* **1990***, 112*, 1266-1267.

(55)   Beckwith, A. L. J.; Davies, A. G.; Davison, I. G.; Maccoll, A.; Mruzek, M. H. *J. Chem. Soc. Chem. Commun.* **1988**, 475.

(56)   Chan, H. W.; Levett, G.; Matthew, J. A. *Chem. Phys. Lipids* **1979***, 24*, 245.

(57)   Olivella, S.; Sole, A. *J. Am. Chem. Soc.* **2003***, 125*, 10641.

(58)   Mills, K. A.; Caldwell, S. E.; Dubay, G. R.; Porter, N. A. *J. Am. Chem. Soc.* **1992***, 114*, 9689-9691.

(59)   Porter, N. A.; Mills, K. A.; Caldwell, S. E.; Dubay, G. R. *J. Am. Chem. Soc.* **1994***, 116*, 6697.

(60)   Porter, N. A.; Mills, K. A.; Carter, R. L. *J. Am. Chem. Soc.* **1994***, 116*, 6690-6696.

(61)   Lowe, J. R.; Porter, N. A. *J. Am. Chem. Soc.* **1997***, 119*, 11534.

(62)   Brill, W. F. *J. Chem. Soc. Perkin Trans. II* **1984**, 621-627.

(63)   Porter, N. A.; Zuraw, P. *J. Chem. Soc. Chem. Commun.* **1985**, 1473.

(64)   Porter, N. A.; Wujek, S. J. *J. Org. Chem.* **1987***, 52*, 5085-5089.

(65)   Boyd, S. L.; Boyd, R. J.; Shi, Z.; Barclay, R. C.; Porter, N. A. *J. Am. Chem. Soc.* **1993***, 115*, 687-693.

(66)   Wijtmans, M.; Pratt, D. A.; Valgimigli, L.; DiLabio, G. A.; Pedulli, G.-F. et al. *Angew. Chem. Intl. Ed.* **2003***, 42*, 4370.

(67)   Hamburg, M.; Su, C.; Oliw, E. *J. Biol. Chem.* **1998***, 273*, 1080.

(68)   Valgimigli, L.; Brigati, G.; Pedulli, G.-F.; DiLabio, G. A.; Mastragostino, M. et al. *Chem. Eur. J.* **2003***, 9*, 4997.

(69)   Gunstone, F. D.; Jacobsberg, F. R. *Chem. Phys. Lipids* **1972***, 9,* 112.

CHAPTER III

ALLYLBENZENE DERIVED PEROXYL RADICAL CLOCKS AND STUDIES
TOWARDS THE ALLYLPEROXYL RADICAL REARRANGEMENT

Introduction

In Chapter I, free radical clocks were discussed as an indirect method for determining radical-molecule reaction kinetics by competition between a unimolecular reaction that has a known rate constant and a bimolecular reaction with an unknown rate constant. Figure I-3 showed the 5-hexenyl radical cyclization clock for determining k_H of abstraction of a hydrogen atom from a substrate A-H by a primary carbon-centered radical, through competition kinetics. The product ratio of non-cyclized to cyclized product is directly proportional to k_H and therefore allows k_H (bimolecular) to be determined as long as k_R (unimolecular) is known.[1]

The first peroxyl radical clock developed in the Porter laboratory was the non-conjugated product of methyl linoleate oxidation seen in Chapter II.[2] Using this non-conjugated β-fragmentation, which has a unimolecular rate for β-fragmentation of 2.6×10^6 s^{-1} (calibrated to α-tocopherol, 3.5×10^6 M^{-1}s^{-1}), the Porter group has been able to determine the inhibition rate constants of antioxidants that donate hydrogen atoms nearly an order of magnitude faster than α-tocopherol (10^6-10^7).[3, 4] Though these initial experiments have proven to be useful in being able to do what EPR and oxygen consumption experiments have not been able to, most commercially useful antioxidants do

not have k_{inh} values so high. Commercial antioxidants typically have a k_{inh} value in the range of 10^4 to 10^5 $M^{-1}s^{-1}$, and because of this, a clock with a unimolecular rate constant of either 10^4 or 10^5 s^{-1} is required for these compounds.

It is well established that phenolic compounds, commonly referred to as chain-breaking antioxidants, act as antioxidants by interrupting the free radical chain process.[5] This chain-breaking occurs by transfer of the phenolic hydrogen atom to a chain-carrying peroxyl radical forming a hydroperoxide and phenoxyl radical:

$$ArO\text{-}H + ROO^\bullet \rightarrow ArO^\bullet + ROO\text{-}H \qquad (1)$$
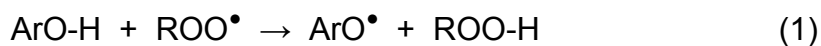
The phenoxyl radical is sufficiently stabilized so that it can no longer propagate the chain reaction by either of the two propagation steps: reaction with another substrate (R-H) to generate a carbon centered radical ($R^\bullet$) or reaction with oxygen to yield an intermediate that reacts with R-H. The rate constant for Equation 1 is commonly referred to as the inhibition rate constant, k_{inh}. These rate constants are typically determined by studying the antioxidant-inhibited autoxidation of an oxidizable substrate.[6] Styrene is the most commonly used substrate for these studies, and the consumption of oxygen is monitored in the presence and absence of an antioxidant.

Unfortunately, these experiments are time-consuming and present some limitations. They require a rather extensive experimental setup (as oxygen consumption is usually monitored by either a pressure transducer or EPR spectroscopy using a nitroxide spin probe).[7-9] Also, for those antioxidants

where no clear induction period exists, a series of autoxidations need to be performed with a wide range of antioxidant concentrations.[10] Given the relative ease with which conventional radical clock methods could be carried out, and the lack of any requirement for specialized equipment, it would be very convenient to have a radical clock approach for the measurement of rate constants for equation 1.

In this chapter, the discussion will focus on the use of allylbenzene as a peroxyl radical clock. Many allylbenzene derivatives were designed in order to determine substituent effects on the peroxyl radical β-fragmentation, but after the experiments were completed, it was found that their was a negligible effect on k_β between allylbenzene and these derivatives.

The following discussion begins with the initial experiments conducted in order to determine α and k_β for the oxidation of allylbenzene, the synthesis of the allylbenzene derivatives, and the initial clocking experiments of allylbenzene and its derivative α-methyl allylbenzene (**10**). When it was discovered that α-tocopherol (as well as the other phenols tested) were being consumed, the calibration and clocking experiments had to be redesigned in order to ensure pseudo-first order kinetics, and as a result, accurate determinations of k_{inh}. The middle of Chapter III discusses the corrected experiments as well as the new, accurate clocking data. The final part of this chapter discusses the use of specific allylbenzene derivatives to give supporting evidence to the allylperoxyl radical rearrangement mechanism.

Design of Allylbenzene as a Peroxyl Radical Clock

Little is known about the thermochemistry of the C-OO$^\bullet$ bond that is made (and eventually broken) in the reaction in equation 2:

$$R^\bullet \; + \; O_2 \; \rightarrow \; ROO^\bullet \qquad\qquad (2)$$

Many groups have worked to address the lack of information regarding this biologically important process. Two of the more recent studies have provided somewhat unexpected results.[11,12] The Knyazev study showed that increasing alkyl substitution at the peroxyl-bearing carbon leads to a stronger C-OO$^\bullet$ bond, favoring the right-hand side of equation 2, which is contrary to the trends in radical stability of carbon-centered radicals. Mulder's data show a modest correlation with the stability of the carbon-centered radical. However, there are many notable exceptions.[11] To account for these differences, the possibility of an anomeric effect has been suggested in structures where a heteroatom is bonded to the peroxyl-bearing carbon, such as in a peroxyl radical derived from triethylamine and tetrahydrofuran.

Pratt and Porter have shown that C-OO$^\bullet$ BDEs are largely unrelated to the stability of the alkyl radical formed by β-fragmentation.[13] Instead, in methyl peroxyls substituted with electron-donating groups, C-OO$^\bullet$ BDEs are affected by substantial hyperconjugative interactions between the substituents on the peroxyl-bearing carbon and the C-O bond.[14] This hyperconjugative effect of electron-donating groups relies on a filled n or π orbital on the substituent, and can have very large effects on the equilibrium between alkyl radicals and their

corresponding peroxyl radicals. In methylperoxyls substituted with electron-withdrawing groups the remaining effect involves the inductive withdrawal of electrons from, and therefore the destabilization of, the polarized C-O bond because there is no interaction with the empty σ_{C-O}^* orbital. Therefore, despite the fact that both electron-withdrawing and electron-donating groups stabilize carbon-centered radicals, they mediate the equilibrium between a peroxyl radical and the parent alkyl radical very differently.

The design of these slower peroxyl radical clocks was aided in large part by theoretical work done by Derek Pratt.[15] From his calculations it was found that peroxyl radical clocks based on the allylbenzene molecule would lower the β-fragmentation of the C-O peroxyl bond by at least one order of magnitude compared to the β-fragmentation of the non-conjugated product from methyl linoleate oxidation. By adding an electron donating substituent to the benzylic position, one should be able to lower the β-fragmentation by an order of magnitude further, down to $10^4 \, s^{-1}$.[13]

Competition kinetics can be applied to the oxidation of allylbenzene (**1**), following the mechanism in Figure III-1. By monitoring the oxidation of allylbenzene and specific derivatives, k_β (the rate of fragmentation of the C-O peroxyl bond) and α (the amount of radical trapped at the benzylic position) were determined using a non-linear least squares analysis (equation 3).

$$\frac{[6]}{[7]} = \left(\frac{\alpha}{1 - \alpha}\right) \frac{k_{inh} \, [\alpha\text{-Toc}]}{k_{inh} \, [\alpha\text{-Toc}] + k_\beta} \tag{3}$$
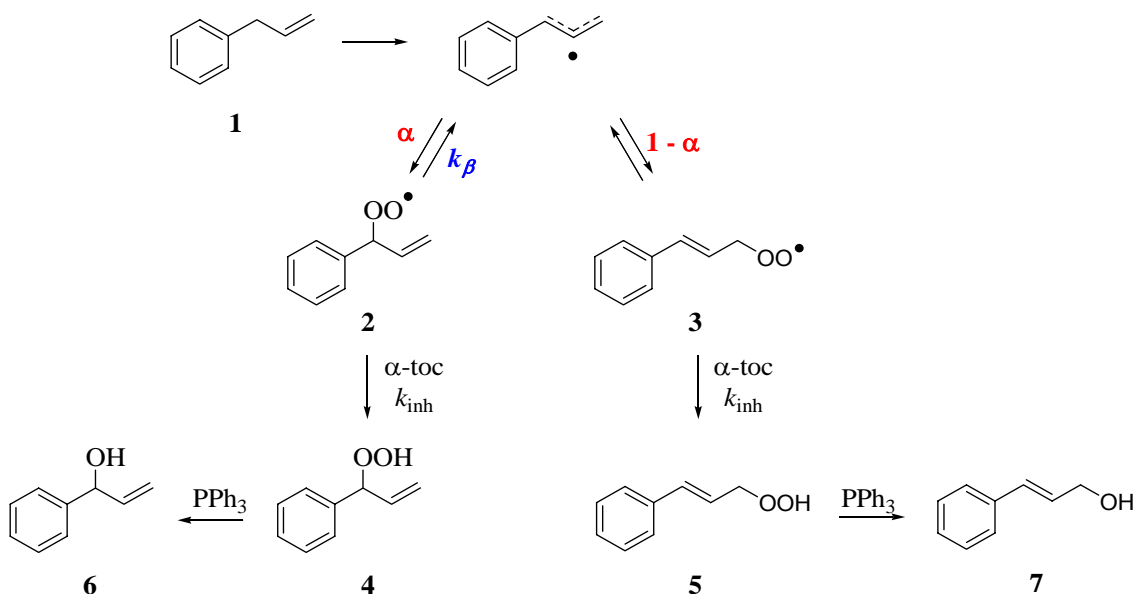
Figure III-1: Mechanism of oxidation of allylbenzene in the presence of α-tocopherol. For our purposes, the product hydroperoxides are reduced with tri-phenylphosphine giving the corresponding alcohols **6** and **7**.

The mechanism for the autoxidation of allylbenzene is very similar to that of methyl linoleate (Figure II-1). Hydrogen atom abstraction from the benzylic position yields an α-vinylbenzyl radical, which is trapped by O_2 generating the nonconjugated and conjugated peroxyl radicals **2** and **3**, respectively.[15] The fraction of α-vinylbenzyl radicals trapped at the benzylic position and leading to the nonconjugated peroxyl radical is defined as α, analogous to the partitioning of O_2 at the central position of the nonconjugated dienes. Similarly, this nonconjugated peroxyl radical (**2**) undergoes β-fragmentation (k_β) in competition with hydrogen atom transfer (k_{inh}), setting up the "intermediate" peroxyl radical clock for hydrogen atom donor processes that occur at or near 10^5 $M^{-1}s^{-1}$. Kinetic analysis of the mechanism in Figure III-1, using equation 3, leads to the same relationship between product ratio, α, k_β, k_{inh}, and

concentration of hydrogen atom donor as defined in Chapter II for the kinetically controlled autoxidation of methyl linoleate.

Synthesis of Allylbenzene Derivatives and Oxidation Products

Allylbenzene (**1**) is a commercially available room temperature liquid, and extremely inexpensive, as are the oxidation products (following triphenylphosphine (PPh$_3$) reduction) α-vinylbenzyl alcohol and cinnamyl alcohol (**6** and **7**, respectively). Allylanisole (**8**) is also commercially available. The other allylbenzene derivatives (Figure III-2), as well as their oxidation products were synthesized. This section briefly describes the synthetic methodology used to obtain the compounds necessary for the oxidation and rearrangement experiments described in this chapter. Detailed synthetic procedures can be found in the *Experimental Methods* section at the end of the chapter.
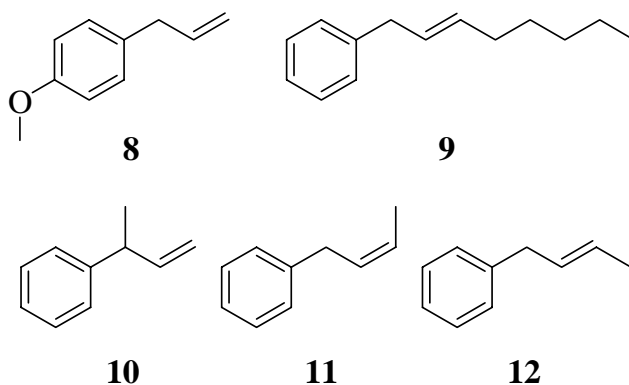
Figure III-2: Allylbenzene derivatives used as peroxyl radical clocks. **8**; allylanisole. **9**; 2-octenylbenzene. **10**; α-MeAB. **11**; 2-*cis*-phenylbutene. **12**; 2-*trans*-phenylbutene.

α-MeAB has been prepared in literature; typically by organometallic reactions involving ethylene to install the terminal olefin,[16] and also by the coupling of α-methyl benzyl magnesium chloride (or the corresponding organozinc reagent) with vinyl bromide.[17] The second coupling procedure afforded very low yields due to the formation of 2, 3-diphenylbutane as a side-product in the preparation of the α-methyl benzyl magnesium chloride precursor. Wittig olefination using 2-phenylpropionaldehyde and methyl triphenylphosphonium bromide however proceeded smoothly in good yield (Figure III-3A). It should be noted that the Wittig reaction was unsuccessful when butyllithium was used to deprotonate the methyl triphenylphosphonium bromide, while the use of potassium t-butoxide proved successful. Distillation of α-MeAB from the reaction mixture yielded a large amount of the isomerized product α, β-dimethylstyrene. However, it was quickly discovered that a short silica gel column eluted with pentane worked much better for purification purposes. 2-octenylbenzene (**9**) was synthesized by a similar Wittig reaction using phenylacetaldehyde and hexyl triphenylphosphonium bromide (Figure III-3B).
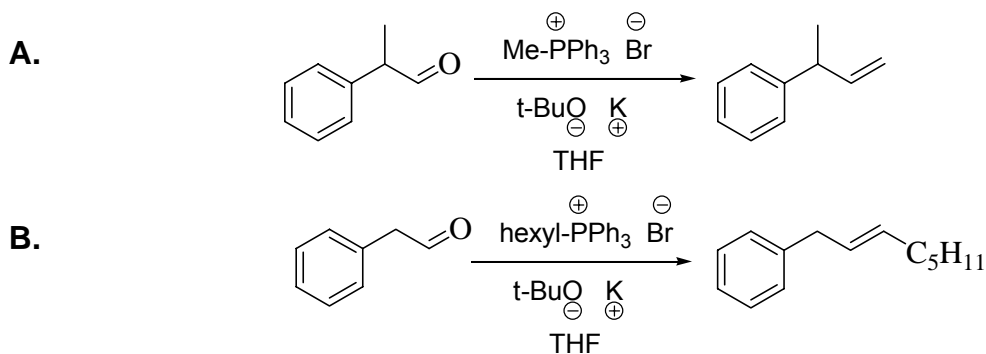
Figure III-3: The synthesis of α-MeAB and 2-octenylbenzene.

Preparation of the phenylbutenes (**11** and **12**) followed a different synthetic route (Figure III-4). **11** and **12** have been reported in the literature for use as mechanistic probes of antibody-catalyzed elimination reactions.[18] The synthetic procedure was quite simple, coupling benzyl bromide to either *cis-* or *trans*-propenylmagnesium bromide using tetrakis(triphenylphosphine)-palladium. However, this synthesis was both time consuming and low yielding for our purposes. An easy alternative route was to switch the reagents, using benzylmagnesium chloride and *cis-* or *trans*-bromopropene. This improved the yields and lowered the reaction times compared to the literature procedure. Changing the palladium catalyst from tetrakis(triphenylphosphine)palladium to Pd(dppf)Cl$_2$ greatly improved the overall yield of the reaction as well as dramatically shortening the reaction times. Although Pd(dppf)Cl$_2$ is not as commonly used at tetrakis(triphenylphosphine)palladium, it is commercially available and not too expensive, allowing this new synthetic procedure to be scaled up quite easily.
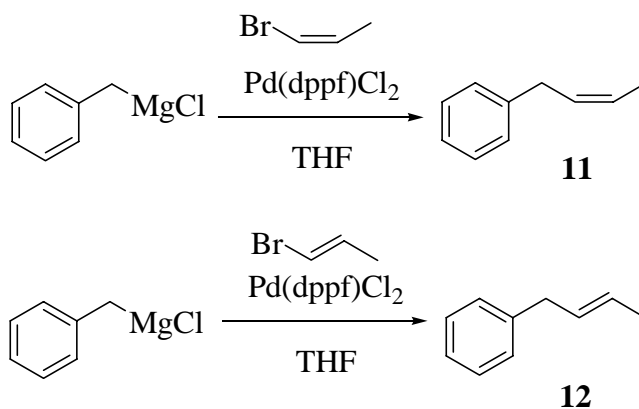
Figure III-4: The synthesis of 2-*cis-* and 2-*trans*-phenylbutene.

In addition to the substrates discussed above, authentic standards of the expected oxidation products were prepared. The oxidation products of 2-octenyl benzene (**13** and **14**, Figure III-5) were easily synthesized, each in one step. The non-conjugated product (**13**) was synthesized through a Grignard reaction of phenylmagnesium bromide and *trans*-2-octenal, while the conjugated product **14** was obtained by the addition of pentylmagnesium bromide to cinnamaldehyde, both in very good yields.
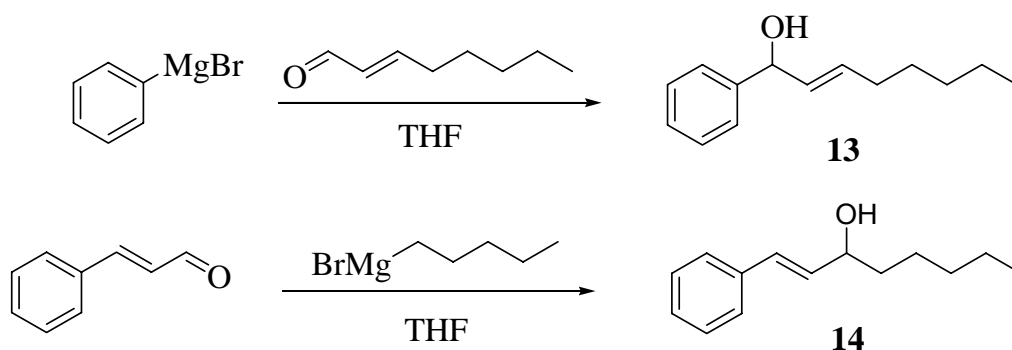
Figure III-5: The synthesis of the oxidation products of 2-octenyl benzene.

The conjugated alcohol product of α-methyl allylbenzene (**16**) was obtained by a Horner-Wadsworth-Emmons reaction between 2-phenyl-propionaldehyde and triphenylphosphonoacetate with sodium hydride in THF. The intermediate ester **15** was then reduced with di-*iso*-butylaluminum hydride (DIBAL) to give the conjugated product **16**. The non-conjugated product (**17**) was synthesized by a Grignard reaction with vinyl magnesium bromide and phenylpropionaldehyde (Figure III-6).
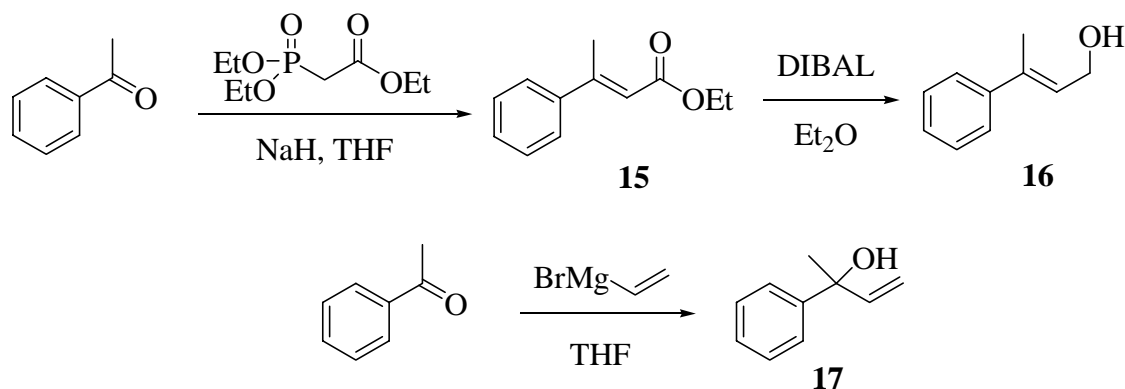
Figure III-6: The synthesis of the oxidation products of α-methylallylbenzene.

The oxidation products of **11** and **12** were synthesized according to Figure III-7 in good yields, and easily purified on a silica gel column. The conjugated product **18** was obtained in one step by a sodium borohydride reduction of the corresponding ketone with cesium chloride in methanol. The *cis-* and *trans-*non-conjugated products, **20** and **21** respectively, were synthesized independently because both products are possible during an oxidation of **11** or **12**. It should be noted that through the course of the oxidation experiments it was found that oxidation of **11** led to **18** and **20** exclusively, while oxidation of **12** led to **18** and **21**. Compounds **20** and **21** were obtained in one step from the intermediate alkynol **19**. Alkynol **19** was obtained from the addition of benzaldehyde to propynylmagnesium bromide in THF. **20** was obtained exclusively by the catalytic hydrogenation using palladium on calcium carbonate, while **19** was reduced with lithium aluminum hydride (LiAlH$_4$) giving the *trans-*product **21**.
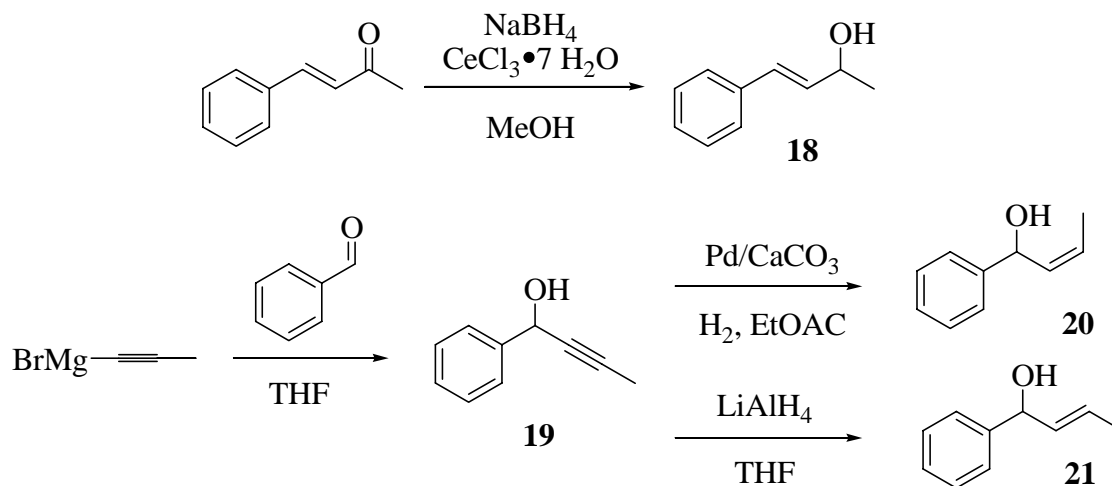
Figure III-7: Synthesis of the *cis-* and *trans*-phenylbutene oxidation products.

The oxidation products of allylanisole (**8**) were quite easy to prepare as well (Figure III-8). The non-conjugated product (**22**) was easily prepared through Grignard reaction in one step using anisaldehyde and vinylmagnesium bromide in THF. The conjugated product **23** was obtained by the reduction of the corresponding aldehyde following the procedure used to obtain **16** in Figure III-6. Both products were obtained in good yields and excellent purity, >98% by GC.
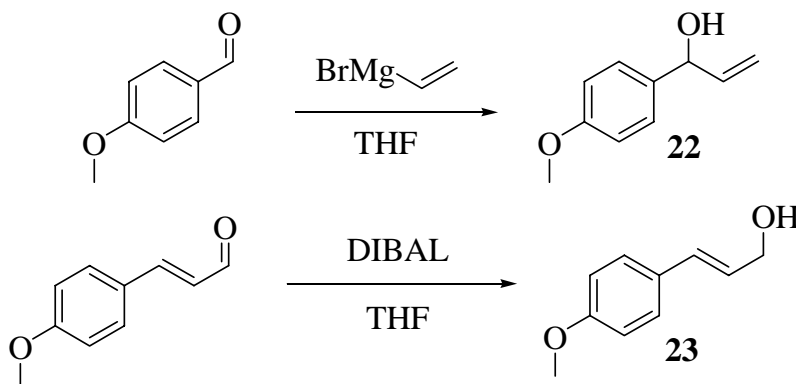
Figure III-8: Synthesis of the allylanisole oxidation products.

With the oxidation products in hand, analysis of the oxidation mixtures was straightforward. All non-conjugated products easily separated from their conjugated isomers on normal phase HPLC, and a common standard (benzyl alcohol) was used in all cases as a reference which allowed for accurate determination of the concentration of the oxidation products. Equation 3 was used to determine α and k_β for allylbenzene and its derivatives **8** through **13** as discussed below.

<center>Calibration of Allylbenzene and Derivatives</center>

Calibration of allylbenzene was initially set-up following the parameters for the oxidation of methyl linoleate[2] discussed in Chapter II with 0.2 M allylbenzene and 0.01 M MeOAMVN in benzene at 37°C for 4 h with the concentration of α-tocopherol ranging from 0.013 to 1.76 M. These reactions were unsuccessful in producing any noticeable amount of oxidation products. The substrate concentration was then increased approximately 10-fold to 2.3 M and the initiator concentration was increased slightly to 0.015 M, while the duration of the oxidation was increased to 6 hours.   Under these new conditions, ample amounts of oxidation products were formed, and were easily detected by normal phase HPLC, and, when reduced with PPh$_3$, by GC as well.

It was immediately clear from the data that β-fragmentation of the intermediate α-vinylbenzyl peroxyl radical (**2**) was much slower than that of the bis-allylic peroxyl radical reported for methyl linoleate (2.6×10^6 s^{-1}) because the ratio of non-conjugated to conjugated oxidation products were unchanged for

most of the data points in the same range of α-tocopherol (0.013 M to 1.76 M).

Decreasing the concentration of α-tocopherol to 0.01 through 0.55 M shown in

Figure III-9 gave $k_\beta = 1.4 \times 10^5 \, s^{-1}$ and $\alpha = 0.69$, when fit using equation 3.
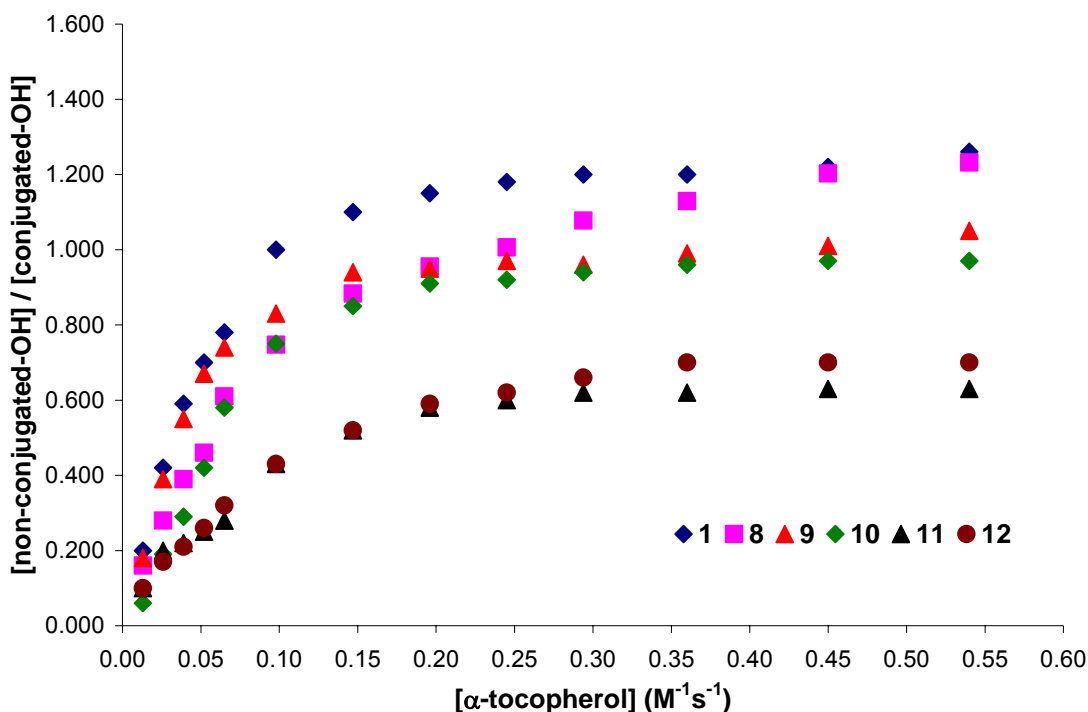
Figure III-9: Calibration of allylbenzene and its derivatives in the presence of α-tocopherol. **1**; allylbenzene. **8**; allylanisole. **9**; 2-octenylbenzene. **10**; α-MeAB. **11**; 2-*cis*-phenylbutene. **12**; 2-*trans*-phenylbutene. [substrate] = 2.3 – 3.4 M; [α-tocopherol] = 0.01 – 0.55 M; [MeOAMVN] = 0.015 M; T = 37°C; t = 6 h.

When it was discovered that α-tocopherol was being consumed in the

calibration experiments, the methodology had to be analyzed and changed

accordingly to allow for pseudo-first order kinetics. Without pseudo-first order

kinetic conditions being met, the peroxyl radical clock method will not allow for

accurate clocking of phenols and other hydrogen atom donors. Therefore, the

data presented in Table III-1 are not necessarily accurate. However, from

Table III-1 it can be seen that the most interesting clocks will be allylbenzene and αMeAB due to the fact that these compounds are the easiest to obtain and analyze, as well as having the greatest difference in k_β.

Table III-1: Calibrated values for allylbenzene derived peroxyl radical clocks.

Clock	α	k_β (s^{-1})
allylbenzene	0.73 (±0.07)	$1.3(\pm0.2)\times10^5$
allylanisole	0.76 (±0.10)	$2.4(\pm0.4)\times10^5$
2-octenylbenzene	0.66 (±0.09)	$1.4(\pm0.3)\times10^5$
αMeAB	0.61 (±0.07)	$1.6(\pm0.4)\times10^4$
2-*cis*-phenylbutene	0.42 (±0.06)	$1.8(\pm0.2)\times10^5$
2-*trans*-phenylbutene	0.44 (±0.05)	$2.7(\pm0.2)\times10^5$

The reaction time, and α-tocopherol concentrations would be the first conditions to adjust in order to make the necessary changes to the allylbenzene calibrations. It turned out that only the α-tocopherol concentration needed to be changed. As can be seen in Figure III-10, when the α-tocopherol concentration is above 0.15 M, less than 5% consumption of hydrogen atom donor is seen, ensuring the necessary condition of pseudo-first order kinetics. Similarly with αMeAB, when α-tocopherol concentration is greater than 0.15 M, almost all of the α-tocopherol (>95%) remains in the oxidation, assuring pseudo-first order kinetics.
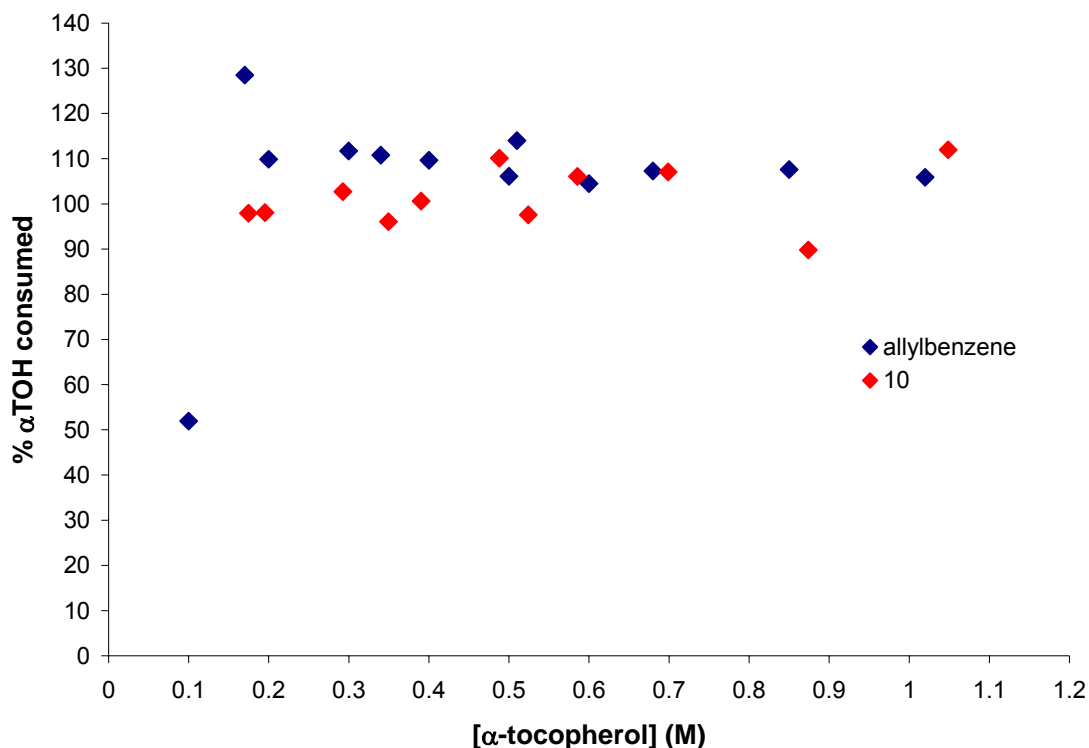
Figure III-10: Consumption of α-tocopherol during the calibration of allylbenzene and αMeAB. [α-tocopherol] = 0.1-1.2 M; [substrate] = 2.3 M; [MeOAMVN] = 0.015 M; T = 37°C; t = 6 h.

Once these appropriate conditions were determined, calibration of allylbenzene and αMeAB proceeded smoothly (Figure III-11). While the α and k_β values had little to no change when calibrating allylbenzene, the calibration of αMeAB showed dramatic change in both α and k_β (Table III-2). This was initially unfortunate due to the fact that αMeAB showed promise to be very useful in clocking slower phenols (10^4 to 10^3 M^{-1}s^{-1}), and now it became obvious that αMeAB would not be an improvement to allylbenzene at these attempts.
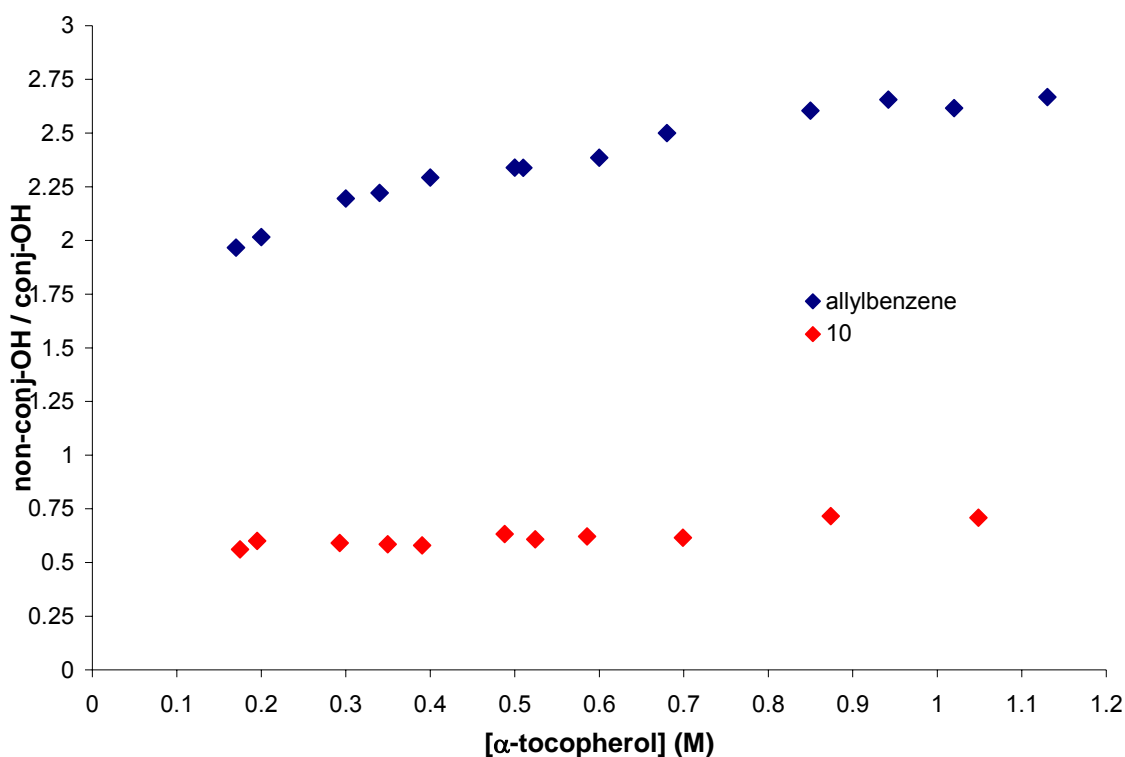
Figure III-11: Calibration of allylbenzene and αMeAB under new conditions. [α-tocopherol] = 0.17-1.17 M; [substrate] = 2.3 M; [MeOAMVN] = 0.015 M; T = 37°C; t = 6 h.

Table III-2: α and k_β values for allylbenzene and αMeAB without consumption of α-tocopherol.

Substrate	α	k_β (M^{-1}s^{-1})
allylbenzene (new)	0.74(±0.12)	2.6(±0.3)x10^5
allylbenzene (original)	0.73(±0.07)	1.3(±0.2)x10^5
αMeAB (new)	0.69(±0.14)	1.7(±0.4)x10^5
αMeAB (original)	0.61(±0.07)	1.6(±0.4)x10^4

Because αMeAB showed little difference in the rate of β-fragmentation when compared to allylbenzene, and because allylbenzene is commercially available, it was decided that allylbenzene would be used for clocking

94

experiments of intermediate hydrogen atom transfer processes, 10^6-10^4 $M^{-1}s^{-1}$. Another reason to exclude αMeAB from further clocking experiments was that the ratio of non-conjugated product versus conjugated product in oxidations of αMeAB showed very little drop off at lower concentrations of α-tocopherol. This trend is a necessity in the calibration experiments and, although not pronounced, the calibration of allylbenzene did show this trend. It was not initially known if the β-fragmentation of allylbenzene would be slow enough to clock hydrogen atom transfer processes in the 10^4-10^3 $M^{-1}s^{-1}$ range, however, as can be seen in the next section, this issue proved to be inconsequential.

Clocking Experiments with Allylbenzene

Autoxidations of allylbenzene, initiated by 2,2'-azobis-(4-methoxy-2,4-dimethylvaleronitrile) (MeOAMVN), were carried out in benzene or chlorobenzene at 37 °C in the presence of varying concentrations of hydrogen atom donor. Appropriate conditions were determined above such that a negligible amount (<5%) of hydrogen atom donor was consumed because the kinetic analysis assumes a constant concentration of hydrogen atom donor. Higher concentrations of substrate and longer reaction times were required for allylbenzene, as compared to autoxidations of methyl linoleate, to obtain sufficient yields of oxidation products for analysis. This is consistent with the higher C-H BDEs predicted for the allylbenzene derived compounds.[19]

In addition to measuring the product ratio derived from each oxidation (Figure III-12), the product ratios (conjugated/nonconjugated) for each clock

were plotted as a function of the hydrogen atom donor concentration (Figure III-13). When the data was fit using equation 3, the values for the rate constants of inhibition (k_{inh}) of the different hydrogen atom donors were determined. The consumption of hydrogen atom donors was also monitored by HPLC (Figure III-14) and presented in Figure III-15.
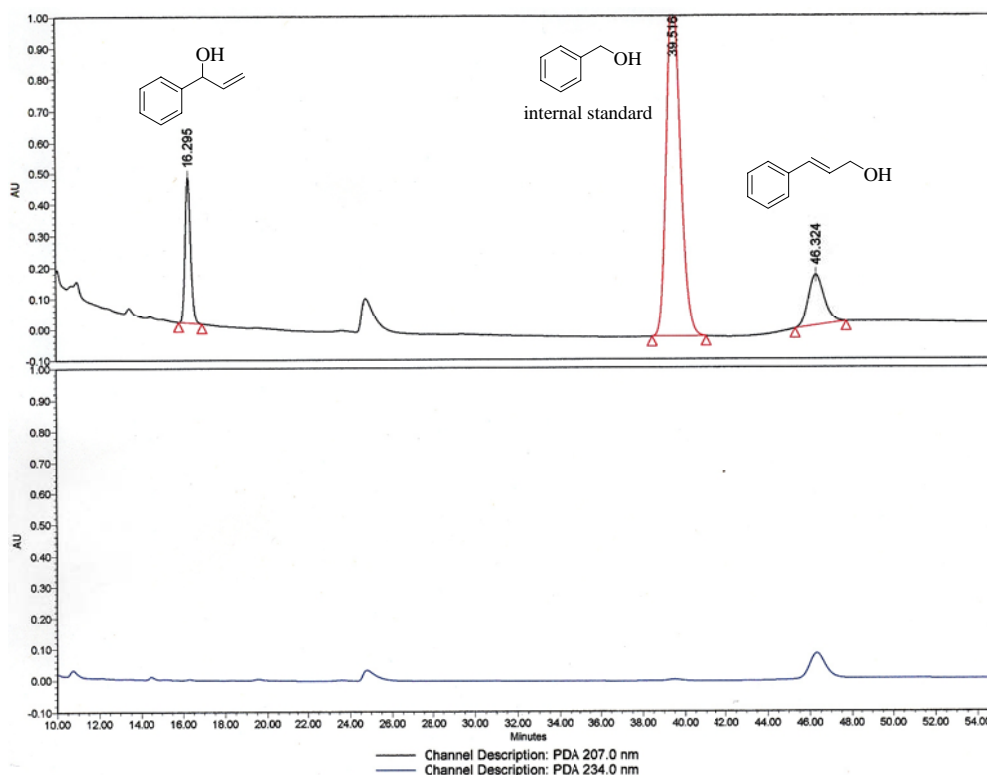
Figure III-12: Representative HPLC chromatogram at 207 (top) and 234 (bottom) nm of an allylbenzene oxidation in the presence of α-tocopherol. Benzyl alcohol (0.01 M) was used as the internal standard. [α-tocopherol] = 0.8 M; [allylbenzene] = 2.3 M; [MeOAMVN] = 0.015 M; T = 37°C; t = 6 h.
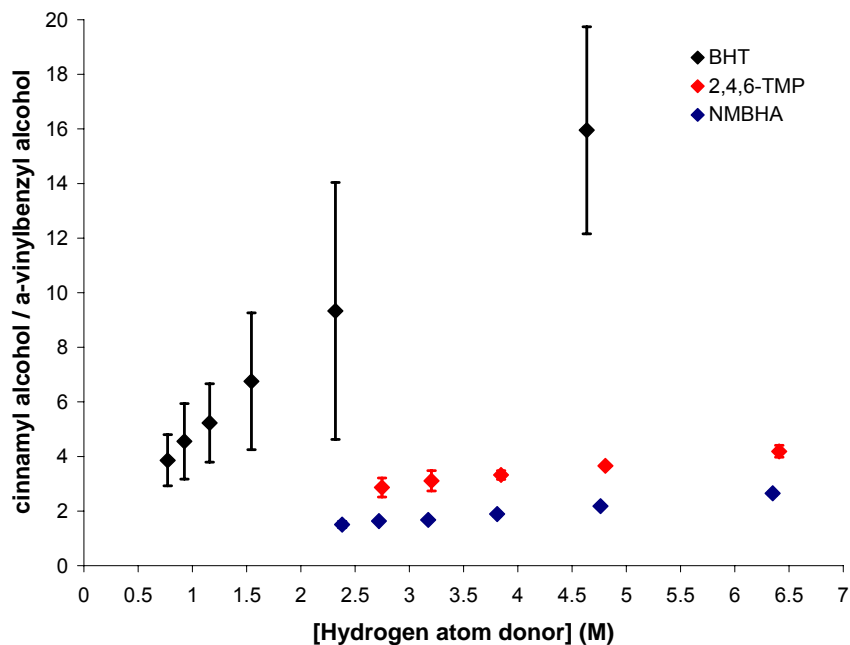
Figure III-13: Plot of hydrogen atom donor vs. product ratio (conjugated/non-conjugated) used for determining k_H's of hydrogen atom donors in allylbenzene clocking experiments. [NMBHA] = 0.02-0.45 M; [2,4,6-TMP] = 0.02-0.45 M; [BHT] = 0.22-1.33 M ; [allylbenzene] = 2.3 M; [MeOAMVN] = 0.015 M; T = 37°C; t = 6 h.
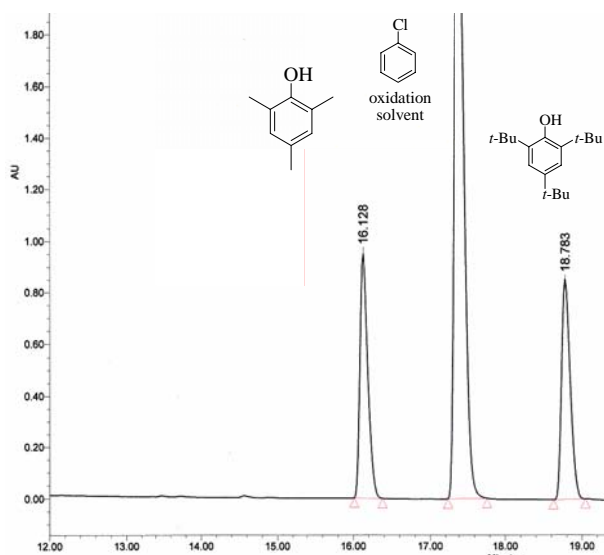
Figure III-14: Representative HPLC chromatogram at 365 nm monitoring 2,4,6-trimethyl phenol consumption in allylbenzene clocking experiments. 2,4,6-tri-*tert*-butyl phenol (0.05 M) was used as the internal standard. [2,4,6-trimethyl phenol] = 0.33 M; [allylbenzene] = 2.3 M; [MeOAMVN] = 0.015 M; T = 37°C; t = 6 h.
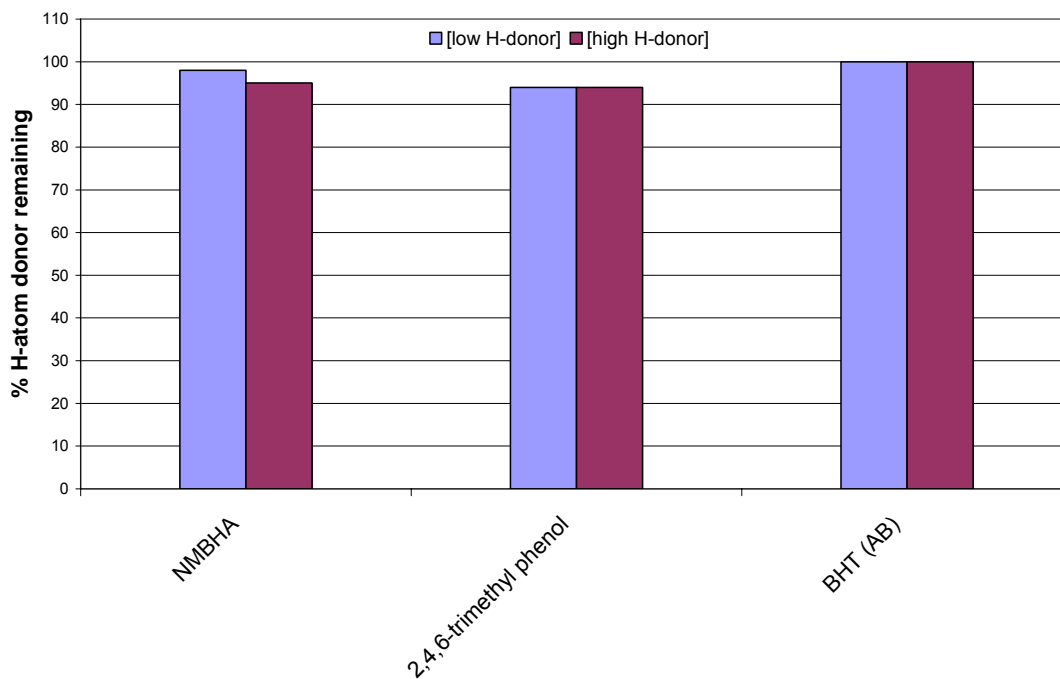
Figure III-15: Consumption plots of allylbenzene clocking experiments in chlorobenzene. [NMBHA] = 0.1 M, 0.3 M; [2,4,6-TMP] = 0.15 M, 0.41 M; [BHT] = 0.11 M, 0.62 M; [allylbenzene] = 2.3 M; T = 37°C; t = 4 h.

The three hydrogen atom donors chosen, represent a range of compounds, as well as a range of k_{inh}'s. These examples show the ability of allylbenzene to determine inhibition rate constants from 10^6 (α-tocopherol) to 10^4 (BHT) M^{-1}s^{-1}.

For those compounds whose inhibition rate constants are available in the literature, those obtained by the allylbenzene peroxyl radical clock method are in good agreement with previously reported values taking into account the temperature differences (Table III-3). While literature values have been measured in experiments that vary widely in solvent, temperature, and method, the values reported here were derived from experiments carried out in benzene

or chlorobenzene at 37°C by a single method. As a result, comparison of the trends in k_{inh} is straightforward and reliable. Furthermore, little is required to determine a rate constant in terms of quantity of antioxidant, equipment, and time investment. Therefore, the allylbenzene peroxyl radical clock method developed here offers several advantages over the traditional methods.

Table III-3: Inhibition rate constants of H-atom donors clocked by allylbenzene.

H-atom donor	k_{inh} (Clock, 303 K)	k_{inh} (Lit.)
N-methylbenzohydroxamic acid	3.1(± 0.6)x10^5 M^{-1}s^{-1}	N/A
2,4,6-tri-methylphenol	2.3(± 0.5)x10^5 M^{-1}s^{-1}	8.5x10^4 M^{-1}s^{-1} [20]
2,6-di-*t*-butyl-4-methylphenol	2.4(± 2.0)x10^4 M^{-1}s^{-1}	1.4x10^4 M^{-1}s^{-1} [20]

Allylperoxyl Radical Rearrangement

In Chapter I, the allylperoxyl radical rearrangement was discussed. This rearrangement can be initiated and inhibited with known radical initiators and radical inhibitors. Peroxyl radicals are known to propagate the free radical chain sequence by hydrogen atom transfer from a parent hydroperoxide to product peroxyl radicals. Therefore, the [1, 3]-allylperoxyl rearrangement is believed to be free radical in nature. The mechanism of the allylperoxyl rearrangement has long been debated with several mechanisms proposed.

The allylperoxyl rearrangement, frequently called the Schenck rearrangement, because it was first described by Schenck and co-workers in 1958 has been studied extensively over the last 40 years. The three most often

suggested mechanisms for the [1, 3]-allylperoxyl rearrangement are shown in Figure III-16.
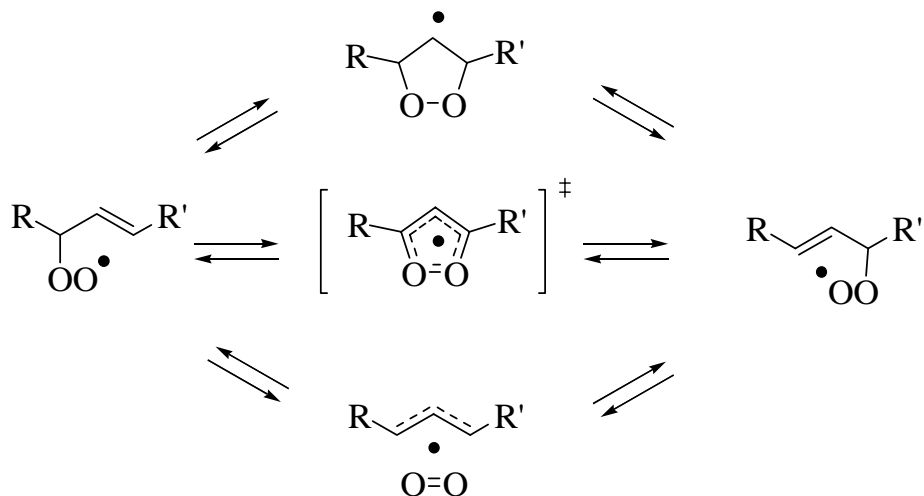
Figure III-16: Suggested mechanisms for the [1, 3]-allylperoxyl rearrangement.

In 1965, Brill made the first concrete proposal for the [1, 3]-allylperoxyl rearrangement mechanism when he suggested a stepwise mechanism involving a 1,2-dioxolan-4-yl radical intermediate.[21] Brill continued his work by looking at the rearrangement of other allylic hydroperoxides such as (*E*)-2-hydroperoxy-2-methyl-3-pentene,[21,22] as well as pinene derived hydroperoxides.[23] Brill's conclusions did not allow for the dioxolanyl radical intermediate. Porter and Zuraw provided additional evidence against the dioxolanyl radical intermediate when they synthesized a localized dioxolanyl radical and demonstrated that it could be trapped with molecular oxygen and did not suffer ring opening to form peroxyl radicals.[24]

Alternative hypotheses to the dioxolanyl radical were advanced for the allylperoxyl rearrangement, and encompass a concerted 1, 3-shift and a β-

fragmentation mechanism giving an allyl radical and dioxygen. Chan has shown that thermal rearrangement of an ^{18}O labeled radical derived from methyl linoleate, undergoes rearrangement under an ^{32}O$_2$ atmosphere to give products that have incorporated atmospheric oxygen.[25] This suggests a fragmentation mechanism to give a pentadienyl radical intermediate. However, a direct expansion to the allylperoxyl rearrangement cannot be assumed because of the fact that the dienyl radical has a much larger driving force for fragmentation by 11-14 kcal/mol more resonance stabilization energy compared to the allyl radical.[26]

$$R_1 = C_7H_{15}, R_2 = (CH_2)_7CO_2H$$
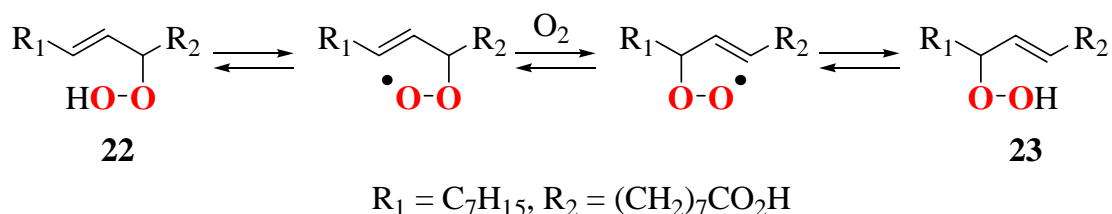
Figure III-17: Porter and Wujek's rearrangement of ^{18}O labeled (E)-9-hydroperoxyoctadec-10-enoic acid under ^{36}O$_2$ atmosphere.[27]

Porter and Wujek, showed that the rearrangement of ^{18}O labeled (E)-9-hydroperoxyoctadec-10-enoic acid under an atmosphere of ^{32}O$_2$ led to no ^{16}O incorporation into the rearrangement product (Figure III-17).[27] Results of these studies are in contrast to those obtained by Chan in the dienyl peroxyl rearrangements, but do not rule out the possibility of a caged radical pair species or a concerted rearrangement mechanism. Further experiments by the Porter group with optically pure methyl oleate hydroperoxides showed that a peroxyl radical, at 40°C in hexane, rearranged with essentially complete retention of

stereochemical integrity.[28]   Based on the observed stereochemistry and the labeling studies, the authors proposed an envelope-type transition state which collapses with complete retention of configuration.

High level molecular orbital calculations by Boyd failed to find a concerted transition state as either minima or maxima on the energy surface of the rearrangement. It was found that dioxolanyl radicals are minima on the energy surface, but the barrier to their formation and opening is prohibitively high. These calculations suggest that the lowest energy pathway is a fragmentation to give an allyl radical and molecular oxygen within a solvent cage.[29]   A more recent theoretical investigation by Olivella and Solé reinforces the findings of Boyd and shows that a loosely-bound radical-dioxygen caged pair is lower in energy than an allyl radical and molecular oxygen.[30]   The transition state to this caged pair however, was calculated to be higher in energy than the free allyl radical and molecular oxygen.

Another piece of evidence which has been obtained on the [1, 3]-allylperoxyl rearrangement was conducted by Porter and Mills who investigated the rearrangements of optically pure *trans*-oleate peroxyl radicals in solvents of differing viscosity under a $^{36}O_2$ atmosphere.[31,32]   The generation of these optically pure allylperoxyl radicals in varying hydrocarbon solvents gave rearranged hydroperoxide products. The products that did not contain ^{18}O were formed with retention of stereochemistry and the products which did contain ^{18}O were formed with random stereochemistry.

The simplest mechanism based on these rather complex yet well-designed experiments, coupled with theoretical calculations, involves an allyl radical-dioxygen caged pair that collapses with stereochemical memory at a rate faster than the diffusion controlled process (Figure III-18). Allyl radicals which diffuse into solution incorporate labeled oxygen with racemization of stereochemistry, suggesting a planar allyl radical which escapes the initial solvent cage. These studies indicate that solvent viscosity affects the partitioning between escape and collapse as the pair collapsed product forms with a high degree of stereoselectivity. Analogous stereochemical and solvent studies performed on *cis*-allyl hydroperoxides gave very similar results.[31]
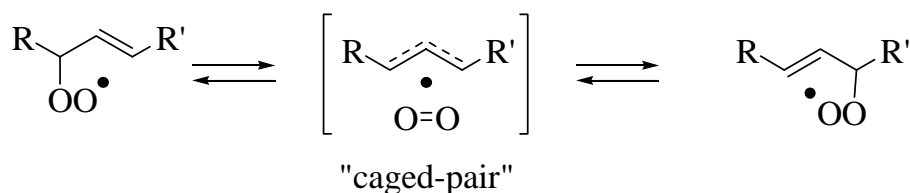
"caged-pair"

Figure III-18: The allyl radical-dioxygen caged pair rearrangement.

The use of unsymmetrically labeled hydroperoxides have also been employed to study the [1, 3]-allylperoxyl rearrangement. Results of these studies show that a competition exists between a concerted [1, 3] transfer of oxygen, and an allyl-dioxygen pair. Solvent studies with unsymmetrically labeled hydroperoxides indicated that solvent viscosity affects the partitioning between escape and cage collapse of the allyl-dioxygen caged pair. An increase in solvent viscosity results in a decrease in escape product and an increase in radical pair collapse.[33]

An understanding of allylperoxyl radicals is of significant value because of their propensity to form from the autoxidation of PUFA chains and in cholesterol head groups.[34] Due to a difference in β-fragmentation of methyl linoleate isomers and 9, 12-pentadecadiene isomers[35] it became necessary to try to determine to what extent rearrangement is occurring across both *cis*- and *trans*-double bonds. Even with the number of studies that exist looking into the mechanism of the allylperoxyl rearrangement, there is continued interest to study the behavior of this intermediate when generated on a lipid chain. Both the autoxidation of oleate and linoleate have shown that allylic hydroperoxides do form.[2,36,37] A more detailed and involved study of the rearrangement of the allylic hydroperoxides and allylperoxyl radicals is necessary to determine the likely mechanism of rearrangement.

To do this, it became necessary to synthesize substrates that, upon oxidation, would lead to unsymmetrical allylic hydroperoxides neighboring either a *cis*- or *trans*-double bond, but not both. The simplest compound with these characteristics seemed to be 1-phenyl-2-butene. Referring back to Table III-1, it can be seen that the oxidation of 2-*cis*-phenylbutene and 2-*trans*-phenylbutene do have slightly different kinetics. That is, while the α values (0.42, 0.44 respectively) do not vary, the k_β value for 2-*trans*-phenylbutene (2.7×10^5 s^{-1}) is 1.5 times faster than 2-*cis*-phenylbutene (1.8×10^5 s^{-1}). The allylbenzene derived substrates without a functional group at the benzylic position (allylanisole and 2-octenylbenzene) do not have k_β values that differ greatly from allylbenzene (Table III-1). The question then arises: Is the

difference between the k_β values of 2-*cis*-phenylbutene and 2-*trans*-phenylbutene due to the expected faster allylperoxyl rearrangement across a *trans*-double bond? (Figure III-19).
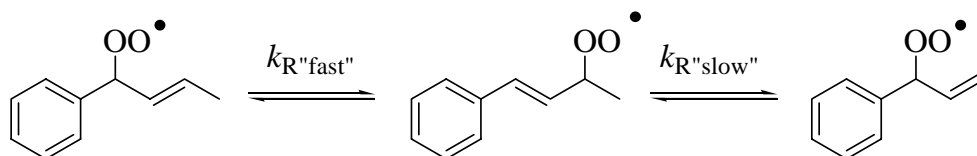
Figure III-19: Allylperoxyl rearrangement in 2-*cis*- and 2-*trans*-phenylbutene.

In order to study the rearrangement of the allylperoxyl radical, a single enantiomer of the benzylic hydroperoxide of 2-*cis*-phenylbutene and 2-*trans*-phenylbutene needed to be synthesized. Despite the importance of unsaturated hydroperoxides in chemistry, biology, and medicine, no general method for the preparation of these compounds have been reported. Chemical synthesis of optically pure hydroperoxides have been attempted,[38-40] but no general chemical approach has been found to prepare allylic and dienylic hydroperoxides like those formed from lipoxygenase enzymes. For example, nucleophilic displacement of mesylates or tosylates by hydrogen peroxide has been reported in the synthesis of 2-octyl hydroperoxide, but allylic and dienylic mesylates are unstable and reactions with these compounds give racemic hydroperoxide products.

The hydroperoxides **24** and **25** were obtained by using a modified version of the procedure published by Nagata *et al* (Figure III-20), beginning with the *trans*-non-conjugated alcohol.[41] Chlorodiethylphosphite and

triethylamine, in a 2 to 3 ratio respectively, were added to 1-phenyl-1-hydroxy-*trans*-2-butene in hexanes at -78°C. After 30 minutes, the hexanes were removed and the filtrate was allowed to react with anhydrous hydroperoxide extracted from a 30% H_2O_2 solution in water with methylene chloride. It was found that the use of methylene chloride afforded no conversion of the intermediate phosphite to product hydroperoxide. Changing the solvent to diethyl ether allowed the reaction to proceed as expected giving products **24** and **25** in combined yields near 40%.
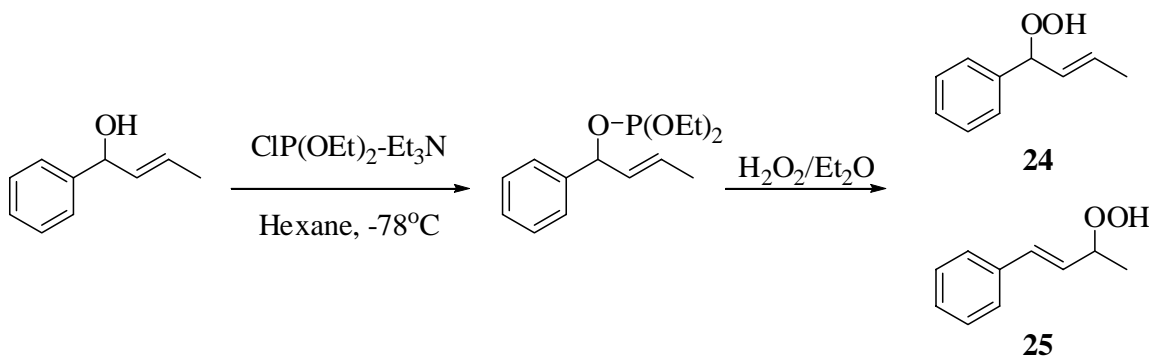
Figure III-20: Synthesis of hydroperoxides **24** and **25**.

It was also seen that, regardless of the alcohol (the non-conjugated 1-phenyl-1-hydroxy-*trans*-2-butene or the conjugated 1-phenyl-3-hydroxy-*trans*-1-butene) used as starting material for the hydroperoxidation reaction, the products **24** and **25** were always formed in a 5:1 ratio (**25**:**24**, by NMR), indicating the hydroperoxidation reaction proceeds via an Sn1 nucleophilic substitution mechanism with the cation delocalized throughout the intermediate compound. Addition of hydroperoxide to the γ-position of 2-*trans*-phenylbutene would give the most stable hydroperoxide product, **25**. However, the benzylic

106

position possesses the most spin resonance energy,[15] which leads to addition of hydroperoxide at this position, giving compound **24**.

The resolution of unsaturated hydroperoxide enantiomers by liquid chromatography of diastereomeric derivatives reported by Porter and Dussault offers a general solution to this problem.[42] This method allows for the non-enzymatic preparation of optically pure allylic or dienylic hydroperoxide natural products through conversion of the racemic hydroperoxide to diastereomeric perketals by the reaction with the vinyl ether **28** (Figure III-21), followed by separation of the perketal diastereomer by liquid chromatography, and deprotection of the separated perketals giving the optically pure hydroperoxides.
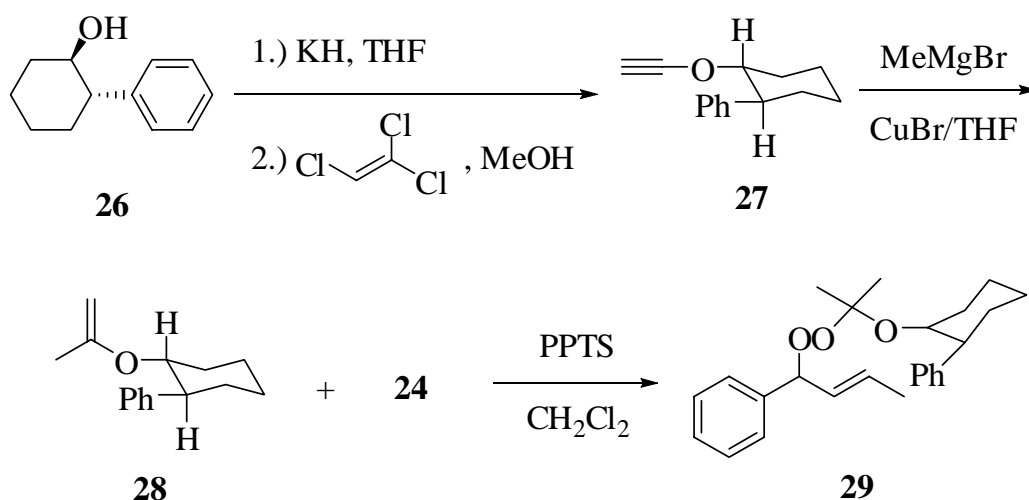
Figure III-21: Synthesis of the diastereomeric perketal **29**.

The method described by Porter and Dussault has been used to resolve a racemic mixture of α-phenethyl hydroperoxide,[42] a compound that shares

structural similarities with 1-hydroperoxy-1-phenyl-*trans*-2-butene (**24**). The starting ethynyl ether (**27**) was synthesized by the addition of (-)-*trans*-2-phenylcyclohexanol (**26**) to a solution of potassium hydride in THF. Trichloroethylene was then added and the reaction was quenched with methanol giving **27** in excellent yield. Addition of methylmagnesium bromide to a solution of copper bromide in THF, followed by the slow addition of **27** gave **28** in very good yield. The final step in the perketal formation is the addition of **28** and pyridinium *p*-toluenesulfonate to the hydroperoxide **24** in methylene chloride, which gave the desired perketal **29** in quantitative yield.

This technique will be especially useful for our purposes because the hydroperoxide oxidation products of 2-*cis*- and 2-*trans*-phenylbutene cannot be prepared enzymatically. Therefore, chemical synthesis of the racemic hydroperoxide mixture, followed by diastereomeric separation is needed to obtain the optically pure benzylic hydroperoxides of 2-*cis*- and 2-*trans*-phenylbutene. The optically pure hydroperoxides were analyzed on a chiral HPLC column (discussed further in *Experimental Methods*) to determine the extent of rearrangement as well as the stereochemical integrity of the oxidation mixture.

With compound **29** (as well as the corresponding perketal of hydroperoxide **25**) in hand, separation of the diastereomers on reverse phase HPLC as described by Porter and Dussault was attempted.[42] The perketals were isolated on a silica gel column treated with triethylamine, and fractions containing ~20mg of perketal were injected on a Supelco Discovery C-18

column beginning with neat acetonitrile at 10mL/min as the mobile phase. Increasing the concentration of water in the mobile phase up to 50% did not improve the separation of the diastereomers. Methanol was used as the primary mobile phase with an increasing concentration of water. This proved to be unsuitable for separation of the diastereomers as well. Using the best (although not sufficient) separation conditions (70:30 acetonitrile:water) determined on a semi-preparative column, an analytical Discovery C-18 column was used in an attempt to purify any amount of the diastereomers. This failed to be sufficient for our purposes, and although the diastereomers could be separated on an analytical column, the time frame needed to collect enough material to be used in the rearrangement studies was extremely prohibitive.

Knowing that the hydroperoxides **24** and **25** formed from the reaction in Figure III-21 would give a racemic mixture of enantiomers, an attempt was made to separate these enantiomers directly on a chiral-HPLC column. The chiral-HPLC columns tested were a CHIRALCEL-OJ and a CHIRALPAK-AD analytical column from Daicel Chemical, Ind., Ltd. Because of the specialized packing material in each column, typical normal phase conditions could not be used. 1% methanol in hexanes was used as the mobile phase and gave separation of the conjugated hydroperoxide enantiomers **25-A** and **25-B**, and near baseline separation of the nonconjugated hydroperoxide enantiomers **24-A** and **24-B** (Figure III-22).
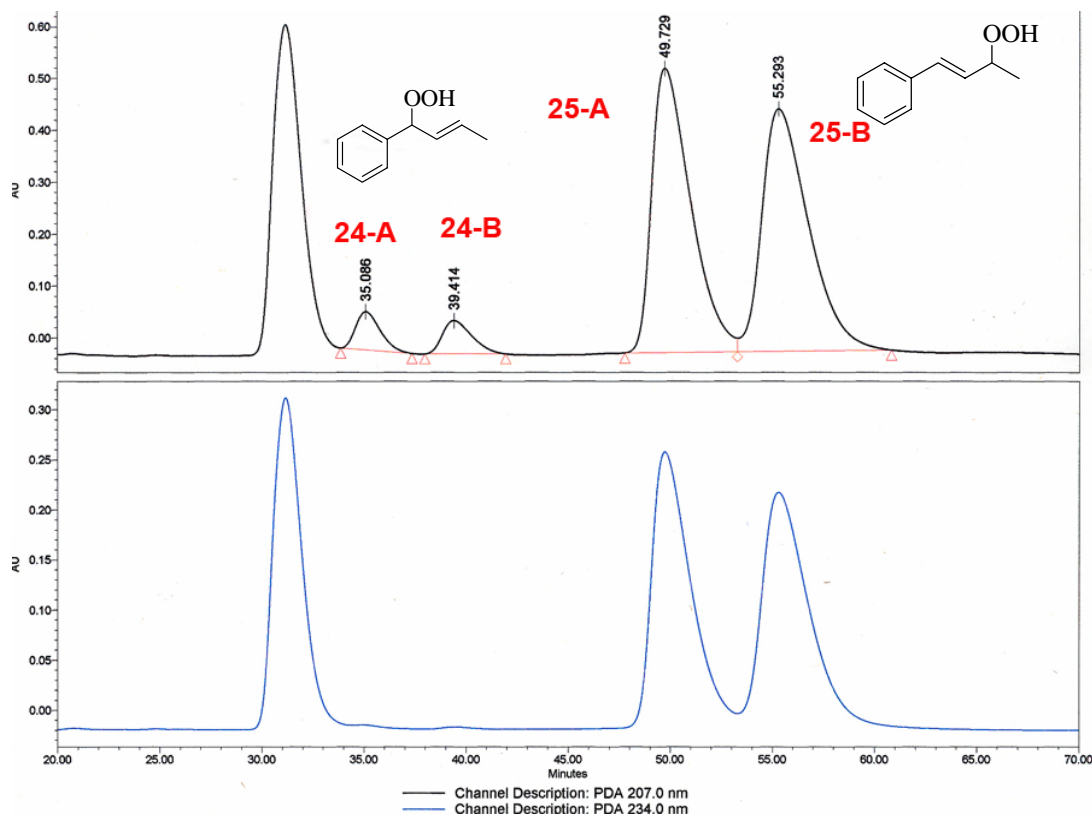
Figure III-22: Separation of the enantiomers of hydroperoxides **24** and **25** on a CHIRALPAK-AD chiral HPLC column using 1% methanol in hexanes as the mobile phase at 207 (top) and 234 (bottom) nm.

Because all four enantiomers produced in the hydroperoxidation reaction from Figure III-21 could be isolated from a chiral HPLC analytical column after multiple injections, a CHIRALPAK-AD semi-preparative column was purchased and used to isolate each hydroperoxide enantiomer. The fractions containing the enantiomers of **24** were combined, concentrated and re-injected to provide the enantiomers **24-A** and **24-B** (*R* and *S* were never assigned, therefore **A** and **B** denotes the retention of each enantiomer, i.e. **A** came off the column before **B**) in greater than 98% enantiomeric excess. The enantiomers **25-A** and **25-B**

did not need to be re-injected after the combining of fractions because they were easily obtained in greater than 98% e.e.

The first experiments on the allylperoxyl radical rearrangement were set-up to determine suitable conditions. The racemization of **25**-**A** was examined with varying concentrations of initiator, with and without α-tocopherol (Figure III-23). From these experiments it was determined that the rearrangement studies should be conducted at both room temperature and 37°C with 0.1mM MeOAMVN, 1mM α-tocopherol, and >10mM substrate. The enantiomer **24-B** was used as the substrate because it was the easiest non-conjugated hydroperoxide to obtain in high e.e.
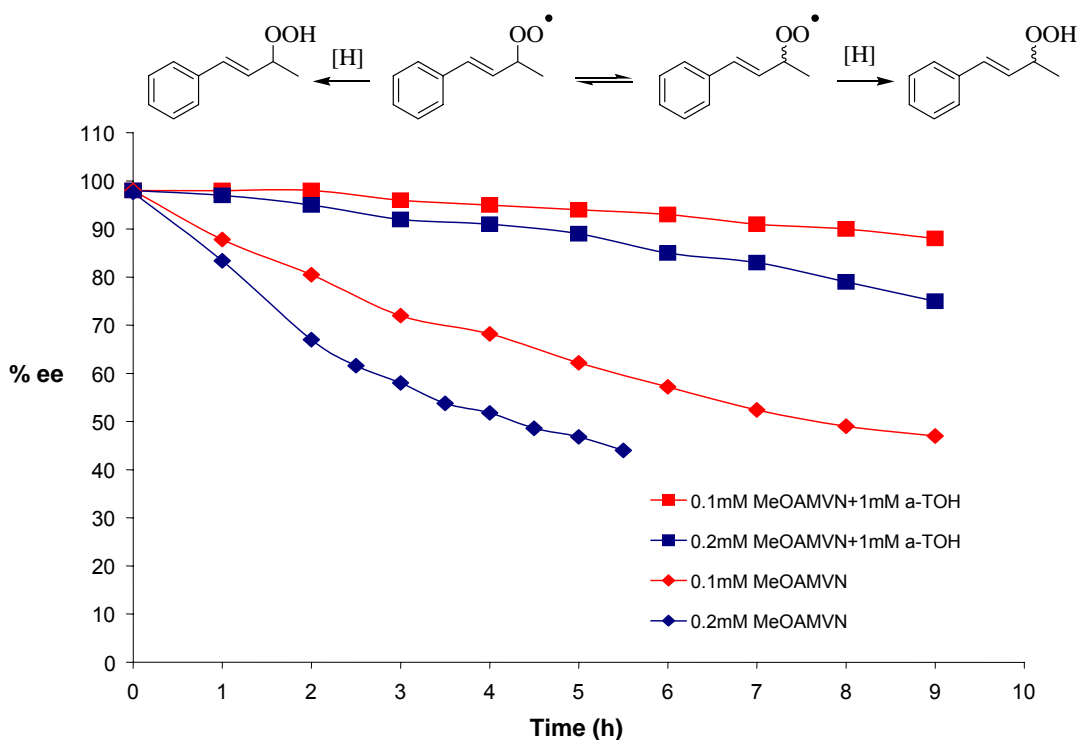
Figure III-23: Racemization of **25-A** at 37°C in chlorobenzene. [**25-A**] = 10 mM; [MeOAMVN] = 0.1-0.2 mM; [α-tocopherol] = 0 mM or 1 mM; T = 37°C; t = 1-9 h.

The initial rearrangement experiments were conducted on **24-B** at room temperature over 36 hours. Aliquots were taken every 2 hours for the first 12 hours and then at 12 hour intervals up to 36 hours. It can be seen in Figure III-24 that, without α-tocopherol, the non-conjugated enantiomer **24-B** readily rearranges to both conjugated enantiomers **25-A** and **25-B**. Although there is an initial 2 hour lag time before rearrangement occurs, after 36 hours an equal amount of **25-A** and **25-B** (~60% combined product composition) is formed. It can also be seen that none of the other non-conjugated enantiomer **24-A** is formed during the oxidation which indicates that β-fragmentation is occurring when there is not a sufficient hydrogen atom donor present to trap the benzylic peroxyl radical, or prevent rearrangement to the conjugated hydroperoxides.
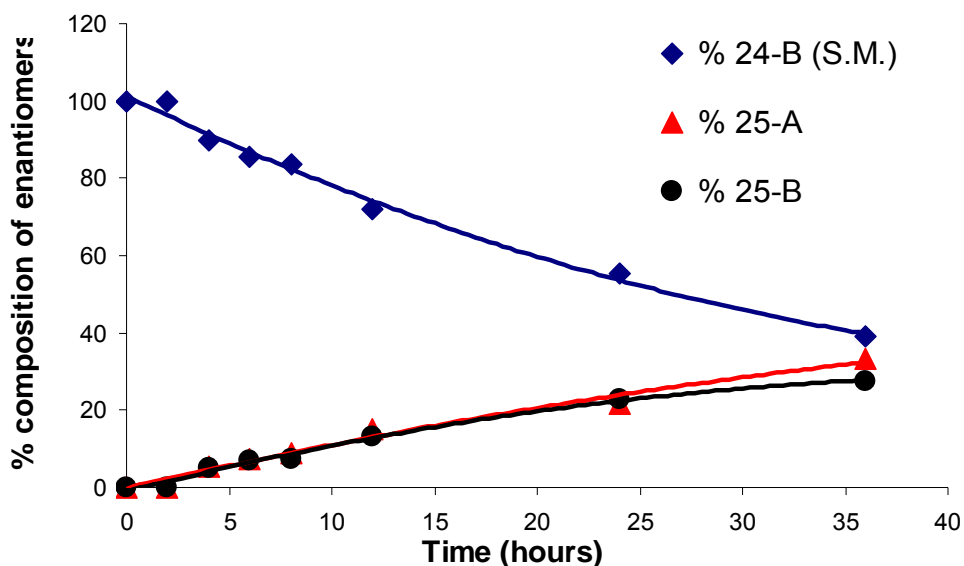
Figure III-24: Rearrangement of the non-conjugated hydroperoxide **24-B** at room temperature with no α-tocopherol in chlorobenzene. [**24-B**] = 16 mM; [MeOAMVN] = 0.1 mM; T = room temperature. Aliquots taken at 0, 2, 4, 6, 8, 12, 24 and 36 hours.

Figure III-25 shows similar experiments conducted at 37°C. It can be seen here that similar results to the rearrangement experiments at room temperature are obtained. First, there is no **24-A** being formed in the product mixture, which is to be expected from the lack of any sufficient hydrogen atom donor present in the oxidation. Second, **25-A** and **25-B** are still being formed in relatively equal amounts throughout the entire 24 hours. However, the relative % of each enantiomer in the product mixture is increased (~40%) compared to the oxidations at room temperature (~30%) which is to be expected due to the increase in reaction temperature. Lastly, there is no noticeable lag time at the beginning of the oxidation as was seen during the oxidations at room temperature showing the oxidation proceeds rapidly at a higher temperature.
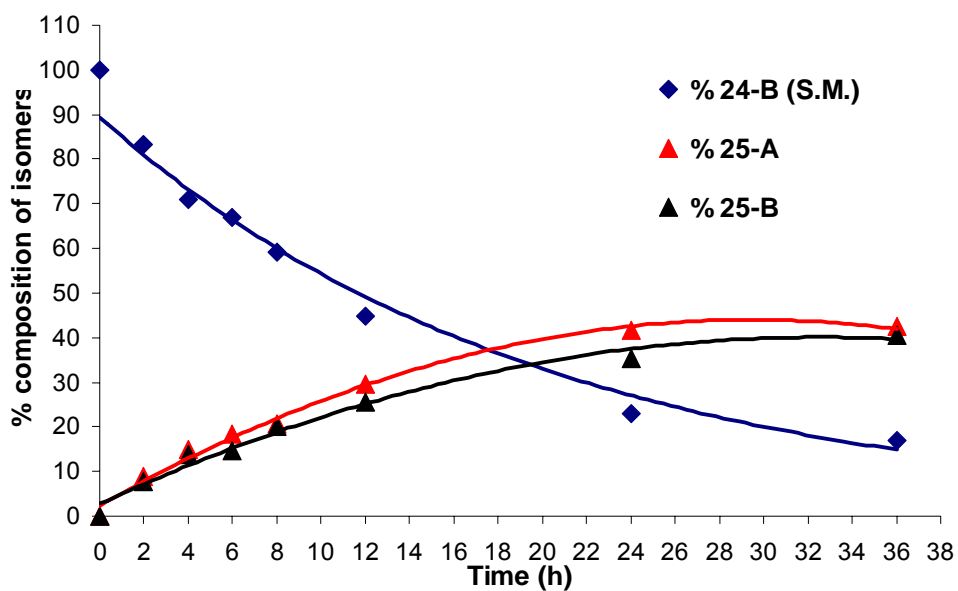
Figure III-25: Rearrangement of the non-conjugated hydroperoxide **24-B** at 37°C with no α-tocopherol in chlorobenzene. **[24-B]** = 16 mM; [MeOAMVN] = 0.1 mM; T = 37°C. Aliquots taken at 0, 2, 4, 6, 8, 12, 24 hours.

Finally, the rearrangement of **24-B** was carried out at room temperature in the presence of 1mM α-tocopherol (Figure III-26). It can be seen here, that some of the non-conjugated enantiomer **24-A** (~7%) is being formed in the early stages of the oxidation (<5 h), which is expected due to the fact that a sufficient hydrogen atom donor is available to trap the non-conjugated peroxyl radicals. The amount of **25-A** or **25-B** formed during this reaction (~15%) is much lower than the amount of **25-A** or **25-B** formed (~30%) when there is no α-tocopherol present and the amount of **24-B** lost to rearrangement (~35%) is also much lower when compared to the results seen in Figure III-25.

Figure III-26: Rearrangement of the non-conjugated hydroperoxide **24-B** at room temperature with 1mM α-tocopherol in chlorobenzene. [**24-B**] = 20 mM; [α-tocopherol] = 1 mM; [MeOAMVN] = 0.1 mM; T = 37°C. Aliquots taken at 0, 1, 2, 3, 4, 16, and 24 hours.
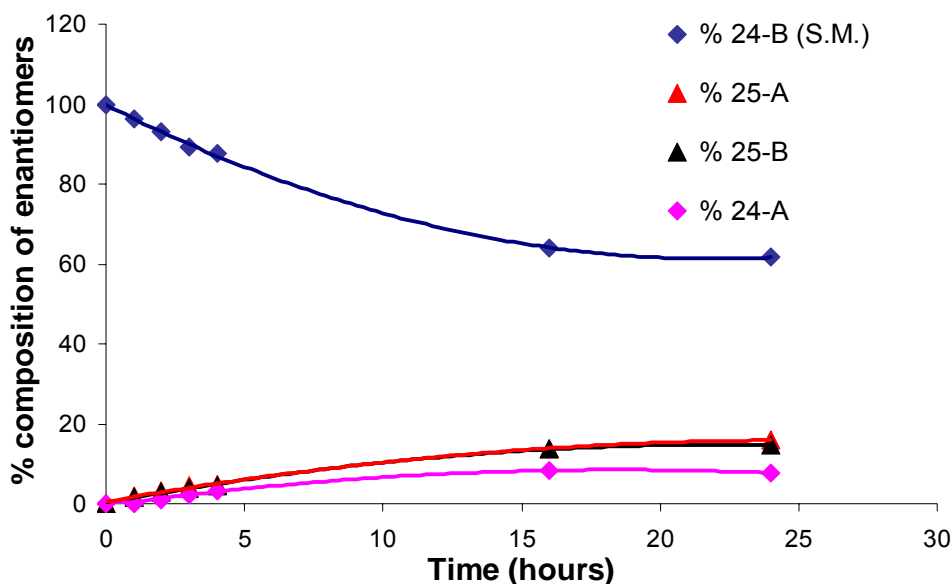
These experiments seem to support the theory that the rearrangement of the allylperoxyl radical proceeds via a β-fragmentation pathway (Figure III-27). However, some other conclusions can be drawn:

1. The temperature of the reaction plays a vital role in the control of the rearrangement. That is, the higher the temperature, the more likely the rearrangement will occur at a faster rate and to a greater extent.

2. Antioxidants such as α-tocopherol not only impede the extent of oxidation, but also inhibit the peroxyl radical rearrangement. Perhaps due to the rapid hydrogen atom transfer, trapping the kinetic products.
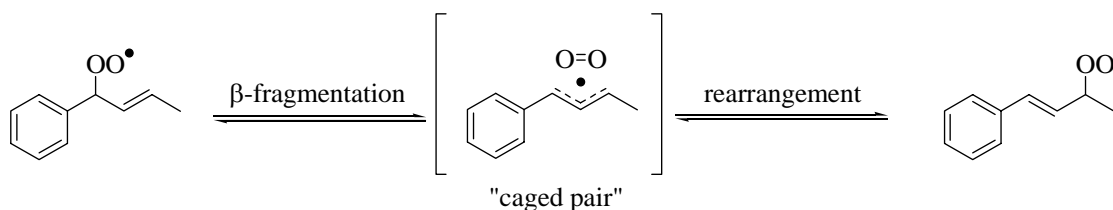
Figure III-27: The β-fragmentation pathway of the allylperoxyl radical rearrangement in a phenylbutene system.

Finally, the results here closely parallel the theoretical investigations of Olivella and Solé who showed that an allyl radical oxygen pair was lower in energy than any possible transition states leading to the rearranged allylperoxyl radical.[30] The experimental work by Porter and Mills[31-33] with symmetrically ^{18}O labeled hydroperoxides as well as Lowe's unsymmetrically labeled hydroperoxides (Figure III-28)[33,43], coupled with the theoretical work of Olivella and Solé, and the experimental work presented here, strongly suggest the β-

fragmentation of the peroxyl radical, leading to a caged pair of molecular oxygen and an allyl radical as the most plausible mechanism for allylperoxyl radical rearrangement.

Experimental Methods

General methods

^{1}H and ^{13}C NMR spectra were collected on a 300 or 400 MHz NMR, using Bruker software. HPLC analyses were carried out with a Waters 600 liquid chromatograph interfaced to a Waters 996 PDA detector. Oxidation products were separated on a Beckman Ultrasphere silica column (0.46 x 25 cm). The mobile phase was either 0.4% *iso*-propanol in hexanes or 0.5% *iso*-propanol in hexanes. The absorbance for the alcohols and hydroperoxides that formed during the oxidations was corrected based upon the oxidation products that were synthesized and their response factor to an internal standard (benzyl alcohol) at 207nm. GC analyses were carried out with a Hewlett-Packard 5890 or 6890 mass spectrometer (flame ionization detection) equipped with a DB-5 (30 m x 0.32 mm x 0.25 μm) fused silica column from J&W Scientific.

Materials

All solvents were bulk solvents from Fisher Scientific except for HPLC hexanes (Burdick and Jackson) and THF (Solv-Tek Inc.). HPLC solvents were filtered before use. All chemicals were purchased from Aldrich Chemicals

unless otherwise noted. Vitamin-E (Fluka) was purified a day before use by flash column chromatography in 5-7% ethyl acetate in hexanes under nitrogen and stored *in vacuo* overnight. All glassware was cleaned and dried overnight in either a 60°C or 200°C constant temperature oven.

The initiator, 2,2'-azobis-(4-methoxy-2, 4-dimethylvaleronitrile) (MeOAMVN), was obtained from Wako and dried under high vacuum for 2 h. Benzene and chlorobenzene were passed through a column of neutral alumina and stored over 4Å molecular sieves. Hexanes used in HPLC analysis and column chromatography was HPLC grade from Burdick & Jackson. Allylbenzene (**1**), allylanisole (**8**), α-vinylbenzyl alcohol (**6**), and cinnamyl alcohol (**7**) were purchased from Aldrich. **1** and **8** were chromatographed on silica in hexanes immediately before use to remove any oxidation products. NMBHA (**32**) was synthesized by literature procedures. All other antioxidants used in this study were purchased from Aldrich and were used as received.

General procedure for allylbenzene clock calibrations

The oxidations were carried out with allylbenzene (2.26 M), MeOAMVN (0.02 M), and α-tocopherol (0.20–1.07 M) in chlorobenzene. The samples were incubated at 37 °C for 6 h. The oxidations were stopped by the addition of excess BHT, followed by the addition of the internal standard (10 mM benzyl alcohol). The hydroperoxides were reduced to their corresponding alcohols with PPh$_3$ and the samples were diluted with hexanes (1.8 mL). HPLC analyses were carried out with a Waters 600 liquid chromatograph interfaced to

a Waters 996 PDA detector with using a Beckman Ultrasphere silica column (0.46 x 25 cm) using 0.5% *iso*-propanol/hexanes at 1.0 mL/min and detected at 207 nm for BHT (**26**) and NMBHA (**32**). GC analysis was carried out for BHT (**26**) and 2,4,6-tri-methyl phenol (**31**) on a Hewlett-Packard 5890 or 6890 mass spectrometer (flame ionization detection) equipped with a DB-5 (30 m x 0.32 mm x 0.25 μm) fused silica column from J&W Scientific using the following temperature program: 75 ºC, 5 min-150 ºC @ 5 º/min, 150-280 ºC @ 25 º/min, 2.8 min. The values for α and k_β are derived from the y-intercept and slope, respectively, using Equation 3.

General procedure for hydrogen atom donor consumption experiments

The oxidations were carried out with allylbenzene (2.26 M) or αMeAB (3.43 M), MeOAMVN (0.02 M), and hydrogen atom donor (0.20–1.07 M) in chlorobenzene. The samples were incubated at 37 ºC for 6 h. The oxidations were stopped by the addition of excess 2, 4, 6-tri-*t*-butylphenol followed by the addition of the internal standard (10 mM of 4-methoxyphenol). The hydroperoxides were reduced to their corresponding alcohols with excess trimethylphosphite and the samples were diluted with methanol (1.8 mL). HPLC analyses were carried out with a Waters 600 liquid chromatograph interfaced to a Waters 996 PDA detector with a SUPELCO Discovery C-18 (25cm x 4.6mm, 5 μm) RP-HPLC column. Methanol and water were used as the mobile phase and the gradient was: (Methanol:water) 90:10 for 5 min, ramp to 75:25 in 10 min, ramp to 20:80 in 15 min, ramp to 90:10 in 10 min.

Consumption was monitored at a wavelength >260 nm to ensure no peak contamination from the oxidation products. When consumption of *N*MBHA was monitored, acetonitrile was used instead of methanol in the mobile phase and sample preparation due to solubility issues.

General procedure for clocking experiments

The samples were prepared as described above for each clock in benzene or chlorobenzene and varying the hydrogen atom donor concentration. The samples were incubated at 37 ºC for 6 h. Following the oxidation, BHT (50 mM) and 5 mM benzyl alcohol were added to each sample. Oxidation mixtures of allylbenzene were reduced with PPh_3 (50 mM) and analyzed by HPLC: Beckman Ultrasphere silica column (0.46 x 25 cm) using 0.5% *iso*-propanol/hexanes at 1.0 mL/min and detected at 207 nm, or by GC: 75 ºC, 5 min-150 ºC @ 5 º/min, 150-280 ºC @ 25 º/min, 2.8 min. The rate constants k_H were derived from Equations 3 and presented in Table III-3.

Error analysis

All errors reported are 95% confidence limits of the rate constant as determined by t tests, i.e. best fit ± (standard error)(t*). The standard error was determined from SigmaPlot or Origin and multiplied by t*. The value for t* was calculated in Excel using the equation TINV (0.05, df), where df is the degrees of freedom. The degrees of freedom were calculated by subtracting the

number of parameters (2) from the total number of data points. The error in literature values for α-TOH (±10%) was also propagated into the error.

Allylperoxyl Rearrangement Experimental Conditions

A 0.1mM solution of MeOAMVN azo-initiator was added to a 10-20 mM solution of a single enantiomer of the conjugated hydroperoxide **25** isolated from the method above. Aliquots were removed every 30 minutes after the first hour to determine the extent of β-fragmentation of **25**. After suitable conditions were determined, similar experiments were conducted at both room temperature and 37°C using a single enantiomer of hydroperoxide **24** in the presence of either 1 mM or no α-tocopherol, described below.

24-B (16 mM) was oxidized with MeOAMVN (0.1 mM) at room temperature and at 37°C in the presence and absence of α-tocopherol Separation of the enantiomers of **24** and **25** was achieved using a CHIRALPAK-AD semi-preparative chiral HPLC column (1cm x 25cm) with 1% methanol in hexanes as the mobile phase at 5 mL/min, and analyzed at 207 nm. Relative product ratios were determined by integration of the enantiomer peaks for **24-A, 24-B, 25-A,** and **25-B** respectively. **24-B** was always the oxidation substrate because it was the nonconjugated hydroperoxide most readily available in the greatest quantity and purity. Aliquots were removed every 2 hours for the first 12 hours and then again at 24 and 36 hours. Analytical chiral-HPLC analysis described above was used to determine the extent of rearrangement of a single enantiomer of **24** to any of the other three

possible isomers (one more from **24** and two from **25**). Relative product ratios were plotted as a function of time.

Synthetic Procedures

Analytical Data: All known compounds that were synthesized below compare favorably with previously reported ^{1}H and ^{13}C NMR spectra. Only commercially available materials were ultimately used for publication purposes, therefore full analytical characterization (elemental analysis, high resolution mass spectrometry) was not fulfilled on the unknown compounds synthesized in this section. The unknown compounds were not fully characterized due to the fact that they were not ultimately used in the resulting publication. All known compounds compare favorably with previously published NMR spectra.
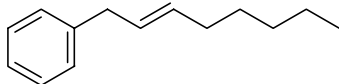
2-octenylbenzene (9):[44] Hexyltriphenylphosphonium bromide (4.7 g, 11 mmol) was dissolved in 100 mL THF, and potassium *t*-butoxide (11 mL, 11 mmol) was added slowly. After 1 hour, phenylacetaldehyde (1.12 mL, 10 mmol) was added slowly and stirred for an additional 2 hours at room temperature under argon. The solvent was evaporated, the residue was washed with hexanes and filtered over silica gel. Evaporation of the hexanes gave 1.34 g (71%) of a clear and colorless liquid. NMR (CDCl$_3$) 300 MHz; ^{1}H: δ 7.27-7.16 (m, 5H, C$_6$H$_5$), δ 6.08-5.41 (m, 2H, CH=CH), δ 3.22 (d, *J*=6.1Hz, 2H, PhCH$_2$), δ 1.96 (m, 2H, CH$_2$), 1.33-1.29 (m,

6H, 3xCH_2), 0.96 (t, J=6.9Hz, 3H, CH_3). ^{13}C: δ 137.4, 132.1, 129.0 (2C), 128.7 (2C), 126.1, 125.8, 47.9, 33.7, 31.9, 29.6, 22.8, 14.1.
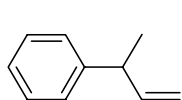
3-phenyl-1-butene (10):[45] Methyl triphenylphosphonium bromide (3.0 g, 8.3 mmol) was dissolved in 25 mL THF, and 8.3 mL of a 1.0 M solution of potassium t-butoxide (8.3 mmol) was added slowly. When solution changed from red to milky-white, 2-phenylpropionaldehyde (1.0 mL, 7.5 mmol) was added and allowed to stir at room temperature under argon for 2 hours. The solvent was then evaporated, and the residue was washed with pentane and filtered through silica. Evaporation of the pentane gave 904 mg (91%) of a clear liquid. NMR (CDCl$_3$) 300 MHz; ^{1}H: δ 7.35-7.12 (m, 5H, C$_6$$H_5$), δ 6.30 (m, 1H, PhC$H$), δ 4.94 (m, 2H, CH=C$H_2$), δ 3.63 (m, 1H, C$H$=CH$_2$), δ 1.44 (d, J=6.7Hz, 3H, CH_3). ^{13}C: δ 140.7, 139.4, 128.7 (2C), 127.7 (2C), 126.0, 116.4, 47.7, 21.0.

1-phenyl-cis-2-butene (11):[18] Pd(dppf)Cl$_2$ (482 mg, 0.59 mmol) was added to 20 mL THF. To this, 1.0 mL (11.8 mmol) of cis-bromopropene and 6 mL (12.0 mmol) of a 2.0 M solution of benzyl magnesium chloride were added. The reaction stirred under nitrogen at room temperature for 48 h. The reaction was filtered through celite washed with saturated NH$_4$Cl, NaHCO$_3$, water, and NaCl. A column in hexanes afforded 692.4 mg (45%) of a clear colorless liquid. NMR (d$_6$-DMSO) 300 MHz; ^{1}H: δ 7.29-7.14 (m, 5H, C$_6$$H_5$), δ 5.59-5.49 (m, 2H, C$H$=C$H$), δ 3.35 (d, J=5.5Hz, 2H, CH_2), δ 1.68 (d,
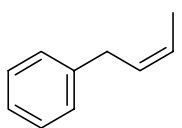
J=4.9Hz, 3H, CH_3). ^{13}C: δ 140.8, 129.1, 128.4, 128.2, 125.8, 124.4, 32.50,

12.7.
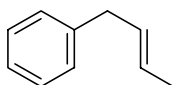
1-phenyl-*trans*-2-butene (12):[18] Pd(dppf)Cl$_2$ (2.4 g, 2.07 mmol), was added to a solution of trans-bromopropene (5.0 g, 41.33 mmol) in THF (100 mL).   To this, 43.4 mL (43.4 mmol) of a 1.0 M solution of benzyl magnesium chloride was added and stirred at room temperature for 24 h under nitrogen. The reaction was filtered through celite washed with saturated NH$_4$Cl, NaHCO$_3$, water, and NaCl. A column in hexanes afforded 3.82 g (70%) of a clear liquid.   NMR (d$_6$-DMSO) 300 MHz; ^{1}H: δ 7.29-7.14 (m, 5H, C$_6$H$_5$), 5.59-5.43 (m, 2H, CH=CH), δ 3.27 (d, J=5.8, 2H, CH_2), δ 1.63 (d, J=6.2 Hz, 3H, CH_3). ^{1}H decoupled NMR (d$_6$-DMSO, 500 MHz): irradiating –CH$_2$- protons (δ = 3.27); δ 5.52 (d, 1H, J=15.2Hz, CH$_2$CH), δ 5.49-5.43 (dq, 1H, J_1= 15.2Hz, J_2=6.2Hz, CHCHCH$_3$). ^{13}C: δ 140.6, 130.3, 128.3, 128.2, 125.8, 125.7, 38.3, 17.6.
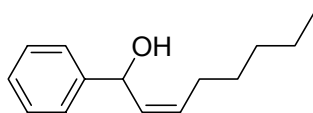
1-phenyl-2-octen-1-ol (13):[46]   2-*t*-octenal (1 mL, 6.7 mmol)   was   dissolved   in   10   mL   THF. Phenylmagnesium bromide (2.5 mL, 7.4 mmol) was added slowly and allowed to stir under argon at room temperature for 1 hour. The reaction was quenched with saturated ammonium chloride and extracted with diethyl ether. The ether layer was washed with water and saturated sodium chloride and dried over magnesium sulfate.   Column chromatography with 10% ethyl acetate in

123

hexanes yielded 1.01 g (67%) of a pale-yellow liquid. NMR (CdCl$_3$) 300 MHz;

^{1}H: δ 7.37-7.19 (m, 5H, C$_6$H$_5$), δ 5.41 (m, 2H, CH=CH), δ 5.19 (dd, J_1=6.0Hz,

J_2=2.5Hz, 1H, ArCH), δ 2.08 (d, J=2.9Hz, 1H, OH), δ 1.99 (m, 2H, CHCH$_2$), δ

1.33-1.29 (m, 6H, 3xCH$_2$), δ 0.96 (t, J=6.6Hz, 3H, CH$_3$). ^{13}C: δ 141.6, 131.3,

129.0 (2C), 128.6, 127.7, 127.1 (2C), 73.2, 34.0, 31.9, 29.6, 22.8, 14.1.
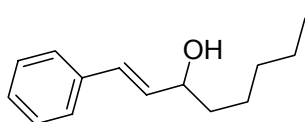
1-phenyl-1-octen-3-ol (14):[48] Cinnamaldehyde (1 mL, 7.9 mmol) was dissolved in 25 mL THF. Pentylmagnesium bromide (4.4 mL, 8.7 mmol) was added slowly and the reaction was allowed to stir for 2 hours under argon at room temperature. The reaction was quenched with saturated ammonium chloride and extracted with diethyl ether. The ether layer was washed with water and saturated sodium chloride and dried over magnesium sulfate. Column chromatography with 10% ethyl acetate in hexanes yielded 1.11 g (69%) of a pale-yellow liquid. NMR (CDCl$_3$) 300 MHz; ^{1}H: δ 7.37-7.19 (m, 5H, C$_6$H$_6$), δ 6.08 (d, J=16.0Hz, 1H, PhCH), δ 5.41 (dd, J_1=16.0Hz, J_2=6.8Hz, 1H, PhCH=CH), δ 5.19 (dt, J_1=6.3Hz, J_2=6.3Hz, 1H, PhCH=CHCH), δ 1.99 (m, 3H), δ 1.33-1.29 (m, 6H), δ 0.96 (t, J=6.6Hz, 3H, CH$_3$). ^{13}C: δ 135.2, 129.0, 128.7 (2C), 128.5, 128.0, 126.4 (2C), 72.7, 37.5, 32.2, 23.2, 22.7, 14.1.
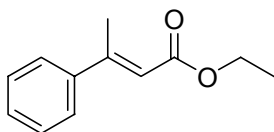
Ethyl-3-phenyl-2-butenoate (15):[47] Sodium hydride (377 mg, 9.4 mmol) was added to a 100mL RBF and dissolved in 40 mL THF. Solution was cooled to 0°C and triphenylphosphonoacetate (2.1

mL, 10.3 mmol) was added dropwise. Acetophenone (1 mL, 8.6 mmol) was diluted in 5 mL THF and added slowly. Reaction was allowed to stir overnight at room temperature under Argon. The reaction was washed with saturated sodium bicarbonate and saturated sodium chloride and dried over magnesium sulfate. Both the E- and Z-isomers are formed in this reaction, however, column chromatography on silica gel with 10% ethyl acetate in hexanes yielded 1.4 g (86%) of a yellowish liquid. According to NMR data, this isolated compound was the E-isomer. NMR (CDCl$_3$) 300 MHz; ^{1}H: δ 7.41-7.20 (m, 5H, C$_6$H$_5$), δ 6.11 (s, 1H, C=CH), δ 4.19 (q, J=7.0Hz, 2H, OCH$_2$CH$_3$), δ 1.71 (s, 3H, CH$_3$), δ 1.30 (t, J=7.0, 3H, OCH$_2$CH$_3$). ^{13}C: δ 166.5, 155.4, 139.4, 128.7 (2C), 128.0, 126.4 (2C), 117.5, 61.4, 15.1, 14.2.
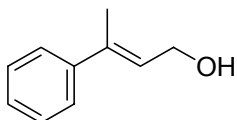
3-phenyl-2-buten-1-ol (16):[46] Ethyl-3-phenyl-2-butenoate (850 mg, 4.5 mmol) was dissolved in 25 mL diethyl ether. Di-*iso*-butyl aluminum hydride (9 mL, 8.9 mmol) was added slowly and the reaction was allowed to stir overnight at room temperature under an argon atmosphere. Brine was added slowly until the aluminum was quenched. Once the reaction was quenched, concentrated hydrochloric acid was added dropwise until phase separation occurred. The reaction mixture was extracted with diethyl ether, washed with saturated sodium chloride, and dried over anhydrous magnesium sulfate. Column chromatography on silica gel with 10% ethyl acetate in hexanes yielded 550 mg (82%) of a white solid. NMR (CDCl$_3$) 300 MHz; ^{1}H: δ 7.30-7.14 (m, 5H, C$_6$H$_5$), δ 5.97 (dt, J$_1$=6.7Hz,

J_1=1.5Hz, 1H, C=C*H*CH$_2$), δ 4.20 (d, *J*=6.8Hz, 2H, C*H$_2$*OH), δ 1.92 (bs, 1H, O*H*), δ 1.41 (s, *J*=6.5Hz, 3H, C*H$_3$*). ^{13}C: δ 139.4, 134.1, 128.7 (2C), 127.2, 126.4 (2C), 58.5, 15.7.
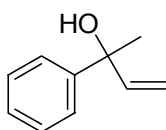
2-phenyl-3-buten-2-ol (17):[46] Vinyl magnesium bromide (10.3 mL, 10.3 mmol) was dissolved in 10 mL THF and cooled to 0°C. Acetophenone (1 mL, 8.6 mmol) was dissolved in 5 mL THF and added slowly to the vinyl magnesium bromide solution. The reaction was allowed to stir overnight at room temperature under an argon atmosphere. The reaction was quenched with saturated ammonium chloride and extracted with diethyl ether. The organic layer was washed with water and saturated sodium chloride and then dried over anhydrous magnesium sulfate. Silica gel column with 10% ethyl acetate in hexanes afforded 0.99 g (78%) of a clear, pale-orange liquid. NMR (CDCl$_3$) 300 MHz; ^{1}H: δ 7.37-7.190 (m, 5H, C$_6$*H$_5$*), δ 6.30 (dd, J_1=17.1Hz, J_2=10.9Hz, 1H, C*H*=CH$_2$), δ 4.96 (dd, J_1=17.2Hz, J_2=1.4Hz, 2H, CH=C*H$_2$*), δ 4.93 (m, 1H, O*H*), δ 1.69 (s, 3H, C*H$_3$*). ^{13}C: δ 144.0, 140.5, 129.0 (2C), 127.7, 127.1 (2C), 116.4, 75.4, 29.2.
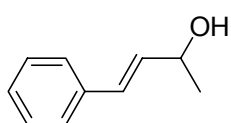
1-phenyl-3-hydroxy-*trans*-1-butene (18):[48] 4-phenyl-3-butene-2-one (731 mg, 5 mmol) and cerium trichloride heptahydrate (1.86 g, 5 mmol) were dissolved in 13 mL MeOH. Sodium borohydride (189 mg, 5 mmol) was added in one portion while stirring. Reaction quenched after 5 minutes with the addition of dilute HCl to a pH of

7.0. The solution was extracted with ether and passed through a plug of alumina to give 355.7 mg (48%) of a clear liquid that becomes a white solid once cooled. NMR (d$_6$-DMSO) 300 MHz; ^{1}H: δ 7.41-7.20 (m, 5H, *Ph*), δ 6.48 (d, 1H, J=16.7 Hz, PhC*H*CH), δ 6.29 (dd, 1H, J_1= 16.0Hz, J_2=5.4Hz, C*H*CHOH), δ 4.87 (d, 1H, J=5.6Hz, O*H*), δ 4.33-4.24 (m, 1H, C*H*OH), δ 1.21 (d, 3H, J=6.3Hz, C*H$_3$*). ^{13}C (CDCl$_3$): δ 137.9, 133.8, 130.1 (2C), 129.2, 127.8 (2C), 126.5, 69.2, 23.9.
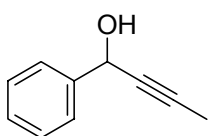
1-phenyl-1-hydroxy-2-butyne (19):[49] 4.4 mL (43.3mmol) of benzaldehyde in THF (25mL) was added to 94 mL (47mmol) of a 0.5 M solution of propynyl magnesium bromide in THF. The reaction was stirred overnight under nitrogen and was quenched with saturated ammonium chloride yielding viscous yellow oil. A silica column with 20% EtOAc in hexanes as the mobile phase yielded 5.23 g (83%) of 1-phenyl-1-hydroxy-2-butyne as a pale yellow liquid. NMR (d$_6$-DMSO) 300 MHz; ^{1}H: δ 7.46-7.23 (m, 5H, Ph), δ 5.84 (d, 1H, J=7.9Hz, O*H*), δ 5.32-5.28 (m, 1H, PhC*H*), δ 1.83 (d, 3H, J=2.3Hz, C*H$_3$*). ^{13}C: δ 142.8, 128.1, 127.3, 126.3, 81.3, 81.0, 62.7, 3.2.
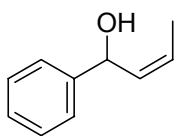
1-phenyl-1-hydroxy-*cis*-2-butene (20):[50] Quinoline (1.35 mL, 38%/wt) and Pd/CaCO$_3$ (100 mg, 20%/wt) was added to 1-phenyl-1-hydroxy-2-butyne (500 mg, 3.42 mmol) in 25 mL of ethyl acetate. The reaction was charged with H$_2$ and stirred for 4 hrs. at room

temperature. The reaction was filtered through celite, washed with HCl, NaHCO$_3$, and NaCl. A column of 20% EtOAc/hex yielded 390.6 mg (77%) of an orange-yellow liquid. NMR (d$_6$-DMSO) 300 MHz; ^{1}H: δ 7.35-7.20 (m, 5H, *Ph*), δ 5.52-5.32 (m, 4H) δ 1.71 (d, 3H, *J*=5.5Hz, C*H*$_3$). ^{13}C: δ 145.3, 134.8, 128.0, 126.6, 125.7, 123.2, 67.7, 13.1.
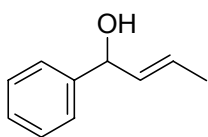
1-phenyl-1-hydroxy-*trans*-2-butene (21):[50] LAH (130 mg, 3.42 mmol) was added to 1-phenyl-1-hydroxy-2-butyne (250 mg, 1.71 mmol) in 10 mL THF and allowed to reflux for 30 minutes. After cooling to room temperature, the reaction was quenched with water and 10% NaOH and extracted with hexanes. A column of 20% EtOAc in hexanes yielded 97.9 mg (39%) of yellow oil. An alternative method began with 4.7 mL (57 mmol) of crotonaldehyde dissolved in 25 mL THF that was added slowly to 20 mL (60 mmol) of a 3.0 M (THF) solution of phenyl magnesium bromide in 100 mL THF after being cooled to 0°C. Reaction was allowed to stir overnight under nitrogen and was quenched with saturated ammonium chloride, extracted with diethyl ether and chromatographed in 20% EtOAc/hexanes to yield 6.31 g (75%) of a pale-yellow liquid. Both methods gave the identical NMRs once purified by column chromatography. NMR (d$_6$-DMSO) 300 MHz; ^{1}H: δ 7.30-7.15 (m, 5H, *Ph*), δ 5.65-5.50 (m, 2H, C*H*=C*H*CH$_3$), δ 5.31 (d, 1H, *J*=4.4Hz, O*H*), δ 4.96-4.99 (m, 1H, PhC*H*), δ 1.62 (d, 3H, *J*=5.5Hz, C*H*$_3$). ^{13}C: δ 143.3, 133.6, 128.4, 127.4, 127.3, 126.1, 75.12, 17.7.
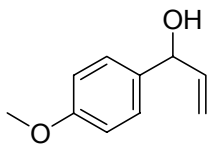
1-(4-methoxyphenyl)-2-propen-1-ol (22):[51]   Anisaldehyde (0.5 mL, 4.1 mmol) was dissolved in 25 mL THF and cooled to 0°C. Vinyl magnesium bromide (5.0 mL, 5.0 mmol) was added slowly and the reaction was allowed to stir at room temperature under argon for 3 hours. The reaction mixture was quenched with saturated ammonium chloride and extracted with diethyl ether. The ether layer was then washed with water and saturated sodium chloride and dried over anhydrous magnesium sulfate. Silica gel chromatography with 10% ethyl acetate in hexanes as the mobile phase yielded 557 mg (82%) of a pale yellow liquid. NMR (CDCl$_3$) 300 MHz; ^{1}H: δ 7.37 (d, J=8.6Hz, 2H), δ 6.91 (d, J=8.7Hz, 2H), δ 6.09 (m, 1H, CH=CH$_2$), δ 5.30 (dd, J_1=17.2Hz, J_2=1.6Hz, 1H), δ 4.96 (dd, J_1=11.8Hz, J_2=1.6Hz, 1H), δ 4.93 (s, 1H, OH), δ 3.69 (s, 3H, OCH_3), δ 1.81 (m, 1H, PhCH). ^{13}C: δ 159.5, 138.6, 133.9, 128.1 (2C), 116.4, 114.5 (2C), 73.4, 55.8.
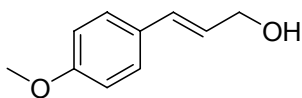
3-(4-methoxyphenyl)-2-propen-1-ol (23):[52]   4-meth-oxycinnamaldehyde (500 mg, 3.1 mmol) was dissolved in 50 mL THF. DIBAL (6.5 mL, 6.2 mmol) was added slowly and the reaction mixture stirred overnight at room temperature under argon. Brine was added slowly to the reaction mixture forming a cloudy gel. When the aluminum was quenched, concentrated hydrochloric acid was added dropwise until phase separation occurred. The reaction mixture was extracted with diethyl ether, and the ether layer was washed with water and saturated sodium chloride, and dried over magnesium sulfate. Column chromatography on silica gel with 10%

ethyl acetate in hexanes gave 258 mg (51%) of an off-white powder. NMR

(CDCl$_3$) 300 MHz; ^{1}H: δ 7.19 (d, *J*=8.5Hz, 2H), δ 7.09 (d, *J*=8.4Hz, 2H), δ 6.62

(d, *J*=16.2Hz, 1H, ArC*H*), δ 6.25 (m, 1H, ArCH=C*H*), δ 5.56 (bs, 1H, O*H*), δ 4.20

(d, *J*=3.5Hz, 2H, C*H$_2$*OH), δ 3.85 (s, 3H, OC*H$_3$*). ^{13}C: δ 159.8, 129.7, 127.5,

127.4 (2C), 123.8, 114.2 (2C), 65.0, 55.8.
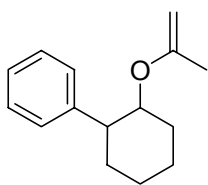
(2-(1-propen-2-yloxy)cyclohexyl)benzene (24):[42]   CuBr

(985.5 mg, 6.87 mmol) was added to THF (15 mL) and cooled

to -40°C. 3.6 mL of 1.4 M MeMgBr in 3:1 toluene/THF was

added. After 10 minutes, (2-(ethynyloxy)cyclohexyl)benzene was added. After

30 minutes the solution was warmed to 0°C and stirred for 1 hr. The reaction

was quenched with 1:1 (NH$_4$Cl: 2 M NH$_4$OH) and stirred for an additional hour.

The reaction was diluted with pet ether and washed with ammonia buffer. The

aqueous layers were extracted with pet ether, dried over MgSO$_4$ and distilled in

a Kugelrohr apparatus to give 657.2 mg (66%) of clear-colorless oil. ^{1}H NMR

(300 MHz, CD$_2$Cl$_2$): δ 7.33-7.20 (m, 5H, Ph); δ 4.10 (m, 1H, *H*CO); δ 3.87, 3.81

(s, 2H, C*H$_2$*=CCH$_3$); δ 2.72 (m, 1H, PhC*H*); δ 1.97-1.86 (m, 4H); δ 1.56 (s, 3H,

C*H$_3$*); δ 1.45-1.34 (m, 4H). ^{13}C NMR (300 MHz, CD$_2$Cl$_2$): δ 158.7, 144.8,

128.4, 127.8, 126.4, 81.5, 78.6, 50.7, 34.7, 31.5, 26.6, 25.2, 21.4.
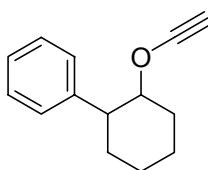
(2-(ethynyloxy)cyclohexyl)benzene (26):[42] To a suspension

of 1.5 g of KH (30% in oil) in THF (30 mL) was added two

crystals of imidazole and 1.0 g (5.67 mmol) of (-)-*trans*-2-

phenylcyclohexanol (**25**) in ~200 mg portions over 30 minutes. The solution

was cooled in an ice bath and trichloroethylene (510 μL, 5.67 mmol) was added

resulting in an immediate brown color. The cooling bath was removed and the

reaction mixture became a deep brown suspension. A small amount of THF

had to be added to aid stirring. After 30 minutes, the reaction was cooled to -

78°C and 6.14 mL of 2.4 M BuLi/hexane (14.7 mmol) was added. The reaction

was warmed to -40°C and quenched with MeOH. The suspension was diluted

with water, warmed to room temperature and extracted 2x with pet ether. The

aqueous extract was washed with saturated NaCl and the organic washes were

dried over $MgSO_4$. A column of 5% EtOAc/1% Et_3N/Pet Ether on Silica gel

equilibrated in 2.5% v/v Et_3N gave 917.5 mg (81%) of yellow oil. ^{1}H NMR (300

MHz, CD_2Cl_2): δ 7.36-7.22 (m, 5H, Ph); δ 4.14 (dt, 1H, J_1=4.5Hz, J_2=6.4Hz,

*H*CO); δ 2.76 (dt, 1H, J_1=2.7Hz, J_2=6.4Hz, PhC*H*); δ 2.41 (m, 1H, C≡C*H*); δ

1.95-1.90 (m, 2H, OCHC*H$_2$*); δ 1.81-1.32 (m, 6H, 3xC*H$_2$*). ^{13}C NMR (300 MHz,

CD_2Cl_2): δ 143.0, 128.8, 127.8, 127.0, 90.2, 89.2, 49.3, 34.3, 31.1, 28.0, 25.8,

25.0.
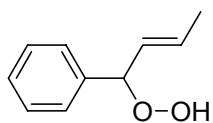
 (*E*)-(1-Hydroperoxy-2-butenyl)benzene (27): 430 mg (2.90

mmol) of 1-hydroxy-1-phenyl-*trans*-2-butene was added to

hexane at cooled to -78°C. Diethylchlorophosphite (671 μL, 4.64 mmol), and

triethylamine (687 μL, 4.93 mmol) was added and allowed to stir for 1 hr at -

78°C. Hydrogen peroxide (extracted in ether from 30% in water) was added

and the reaction was allowed to warm to room temperature and stirred for 2

hrs. The reaction was diluted with hexanes, washed with water and saturated NaCl, dried over $MgSO_4$. A column of 5% EtOAc/1% Et_3N/Pet Ether yielded 103.2 mg (22%) of clear oil. ^1H NMR (300 MHz, CD_2Cl_2): δ 7.37-7.19 (m, 5H); δ 6.08 (dd, 1H, J); δ 5.41 (m, 1H); δ 5.19 (d, 1H); δ 2.00 (bs, 1H); δ 1.71 (d, 3H). ^{13}C NMR (300 MHz, CD_2Cl_2): δ 141.6, 130.1, 129.0 (2C), 127.7, 127.1 (2C), 125.9, 84.2, 19.5. PPh_3 was added to the pure product in order to reduce the hydroperoxide to the corresponding alcohol.[50] NMR (d_6-DMSO) 300 MHz; ^1H: δ 7.30-7.15 (m, 5H, *Ph*), δ 5.65-5.50 (m, 2H, C*H*=C*H*CH_3), δ 5.31 (d, 1H, *J*=4.4Hz, O*H*), δ 4.98 (m, 1H, PhC*H*), δ 1.62 (d, 3H, *J*=5.5Hz, C*H_3*). ^{13}C: δ 143.3, 133.6, 128.4, 127.4, 127.3, 126.1, 75.12, 17.7.
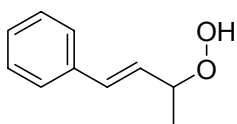
 (*E*)-(3-Hydroperoxy-1-butenyl)benzene (28): 430 mg (2.90 mmol) of 1-hydroxy-1-phenyl-*trans*-2-butene was added to hexane at cooled to -78°C. Diethylchlorophosphite (671 μL, 4.64 mmol), and triethylamine (687 μL, 4.93 mmol) was added and allowed to stir for 1 hr at -78°C. Hydrogen peroxide (extracted in ether from 30% in water) was added and the reaction was allowed to warm to room temperature and stirred for 2 hrs. The reaction was diluted with hexanes, washed with water and saturated NaCl, dried over $MgSO_4$. A column of 5% EtOAc/1% Et_3N/Pet Ether yielded 103.2 mg (22%) of clear oil. ^1H NMR (300 MHz, CD_2Cl_2): δ 7.39-7.24 (m, 5H); δ 6.62 (d, 1H, J); δ 6.25 (dd, 1H); δ 4.08 (m, 1H); δ 2.00 (bs, 1H); δ 1.31 (d, 3H). ^{13}C NMR (300 MHz, CD_2Cl_2): δ 135.2, 129.7, 128.7 (2C), 128.0, 126.4 (2C), 125.4, 77.4, 17.4. PPh_3 was added to the pure product in order to

reduce the hydroperoxide to the corresponding alcohol.[48] NMR (d_6-DMSO) 300

MHz; [1]H: δ 7.41-7.20 (m, 5H, *Ph*), δ 6.48 (d, 1H, J=16.7 Hz, PhC*H*CH), δ 6.29

(dd, 1H, J_1= 16.0Hz, J_2=5.4Hz, C*H*CHOH), δ 4.87 (d, 1H, *J*=5.6Hz, O*H*), δ 4.33-

4.24 (m, 1H, C*H*OH), δ 1.21 (d, 3H, *J*=6.3Hz, C*H$_3$*). [13]C (CDCl$_3$): δ 137.9, 133.8,

130.1 (2C), 129.2, 127.8 (2C), 126.5, 69.2, 23.9.

The desired racemic mixture of hydroperoxides **27** and **28** were synthesized

from the same reaction in a 5:1 ratio (**28:27**, by NMR). The yields reported

here are the overall yields of the reaction, not of each specific hydroperoxide.
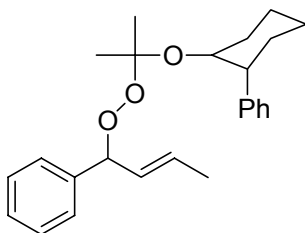
(E)-(2-(2-(1-phenylbut-2-enylperoxy)propan-2-yloxy) cyclohexyl)benzene formation (29): 78.2 mg (0.48 mmol) of hydroperoxide was dissolved in 1 mL of CH$_2$Cl$_2$. 3 mg (2.5 mol %) of pyridinium *p*-toluenesulfonate and 114.6 mg (0.53 mmol) of (2-(1-propen-2-yloxy)cyclohexyl)benzene was added. After 5 min, an additional 20 μL of (2-(1-propen-2-yloxy)cyclohexyl)benzene was added and the reaction was diluted with CCl$_4$. The methylene chloride was removed by a nitrogen stream and a flash column on 20 g of silica gel (5% EtOAc/Pet Ether) yielded 148.1mg (81.3%) of a colorless liquid with some solid white specs. Semi-Prep HPLC (95 acetonitrile: 5 water: 1 triethylamine) was used to attempt to separate the diastereomers. ^{1}H NMR (300 MHz, CD$_2$Cl$_2$): δ 7.37-7.13 (m, 5H,); δ 6.08 (dd, 1H); δ 5.41 (m, 1H); δ 5.19 (d, 1H); δ 3.17-3.04 (m, 2H); δ 1.86-1.39 (m, 14H).

^{13}C NMR (300 MHz, CD$_2$Cl$_2$): δ 144.6, 141.6, 130.1, 129.0 (2C), 128.5 (2C), 127.7, 127.1 (2C), 126.5 (2C), 126.0, 125.9, 104.4, 82.6, 81.4, 49.2, 32.3, 27.4, 25.7, 22.4, 23.1, 19.5. Perketal **29** was not useful for our purposes, therefore the exact mass was not determined. However, both ^{1}H and ^{13}C NMR are similar to both (*E*)-(1-hydroperoxy-2-butenyl)benzene (**27**) and (2-(1-propen-2-yloxy)cyclohexyl)benzene (**24**).

References

(1)   Newcomb, M. *Tetrahedron* **1993***, 49*, 1151-1176.

(2)   Tallman, K. A.; Pratt, D. A.; Porter, N. A. *J. Am. Chem. Soc.* **2001***, 123*, 11827-11828.

(3)   Pratt, D. A.; DiLabio, G. A.; Brigati, G.; Pedulli, G.-F.; Valgimigli, L. *J. Am. Chem. Soc.* **2001***, 123*, 4625-4626.

(4)   Wijtmans, M.; Pratt, D. A.; Valgimigli, L.; DiLabio, G. A.; Pedulli, G.-F. et al. *Angew. Chem. Intl. Ed.* **2003***, 42*, 4370.

(5)   Bolland, J. L.; Ten Haave, P. *Trans. Faraday Soc.* **1947***, 43*, 201.

(6)   Ingold, K. U. *Acc. Chem. Res.* **1969***, 2*, 1-9.

(7)   Cipollone, M.; Di Palma, C.; Pedulli, G.-F. *Appl. Magn. Res.* **1992***, 3*, 99.

(8)   Pedulli, G.-F.; Lucarini, M.; Pedrielli, P.; Sagrini, M.; Cipollone, M. *Res. Chem. Intermed.* **1996***, 22*, 1.

(9)   Lucarini, M.; Pedulli, G.-F.; Valgimigli, L. *J. Org. Chem.* **1998***, 63*, 4497-4499.

(10)   Darlay-Usmar, V. M.; Hersey, A.; Garland, L. G. *Biochem. Pharmacol.* **1989***, 38*.

(11)   Kranenburg, M.; Ciriano, M. V.; Cherkasov, A.; Mulder, P. *J. Phys. Chem.* **2000***, 104*, 915.

(12)   Knyazev, V. D.; Slagle, I. R. *J. Phys. Chem. A* **1998***, 102*, 1770.

(13)   Pratt, D. A.; Porter, N. A. *Org. Lett.* **2003***, 5*, 387-390.

(14) Hoffmann, R.; Radom, L.; Pople, J. A.; Schleyer, P. v. R.; Hehre, W. J. et al. *J. Am. Chem. Soc.* **1972***, 94*, 6221.

(15) Pratt, D. A.; Mills, J. A.; Porter, N. A. *J. Am. Chem. Soc.* **2003***, 125*, 5801-5810.

(16) Yi, C. S.; He, Z.; Lee, D. W. *Organometallics* **2001**, 802-804.

(17) Cross, G. A.; Kellogg, R. M. *J. Chem. Soc. Chem. Commun.* **1987**, 1746-1747.

(18) Romesberg, F. E.; Flanagan, M. E.; Uno, T.; Schultz, P. G. *J. Am. Chem. Soc.* **1998***, 120*, 5160-5167.

(19) Pratt, D. A. Ph.D. Dissertation; Vanderbilt University: Nashville TN, 2003.

(20) Burton, G. W.; Doba, T.; Gabe, E. J.; Hughes, L.; Lee, F. L. et al. *J. Am. Chem. Soc.* **1985***, 107*, 7053-7065.

(21) Brill, W. F. *J. Am. Chem. Soc.* **1965***, 87*, 3286.

(22) Brill, W. F. *Adv. Chem. Ser.* **1968***, 75*, 93.

(23) Brill, W. F. *J. Chem. Soc. Perkin Trans. II* **1984**, 621-627.

(24) Porter, N. A.; Zuraw, P. *J. Chem. Soc. Chem. Commun.* **1985**, 1473.

(25) Chan, H. W.; Levett, G.; Matthew, J. A. *Chem. Phys. Lipids* **1979***, 24*, 245.

(26) Korth, H.-G.; Heinrich, T.; Sustmann, R. *J. Am. Chem. Soc.* **1981***, 103*, 4483.

(27) Porter, N. A.; Wujek, S. J. *J. Org. Chem.* **1987***, 52*, 5085-5089.

(28) Porter, N. A.; Kaplan, J. K.; Dussault, P. H. *J. Am. Chem. Soc.* **1990***, 112*, 1266-1267.

(29) Boyd, S. L.; Boyd, R. J.; Shi, Z.; Barclay, R. C.; Porter, N. A. *J. Am. Chem. Soc.* **1993***, 115*, 687-693.

(30) Olivella, S.; Sole, A. *J. Am. Chem. Soc.* **2003***, 125*, 10641-10650.

(31) Mills, K. A.; Caldwell, S. E.; Dubay, G. R.; Porter, N. A. *J. Am. Chem. Soc.* **1992***, 114*, 9689-9691.

(32) Porter, N. A.; Mills, K. A.; Caldwell, S. E.; Dubay, G. R. *J. Am. Chem. Soc.* **1994***, 116*, 6697-6705.

(33) Lowe, J. R.; Porter, N. A. *J. Am. Chem. Soc.* **1997***, 119*, 11534.

(34)   *Peroxyl Radicals*; John Wiley & Sons: Chichester UK, 1997.

(35)   Tallman, K. A.; Roschek, J., B; Porter, N. A. *J. Am. Chem. Soc.* **2004**, *126*, 9240-9247.

(36)   Brash, A. R. *Lipids* **2000**, *35*, 047-952.

(37)   Porter, N. A.; Mills, K. A.; Carter, R. L. *J. Am. Chem. Soc.* **1994**, *116*, 6690-6696.

(38)   Williams, H. R.; Mosher, H. S. *J. Am. Chem. Soc.* **1954**, *76*, 2987-2990.

(39)   Johnson, R. A.; Nidy, E. G.; Merritt, M. V. *J. Am. Chem. Soc.* **1978**, *100*, 7960-7966.

(40)   Porter, N. A.; Ziegler, C. B., Jr.; Khouri, F. F.; Roberts, D. H. *J. Org. Chem.* **1985**, *50*, 2252-2258.

(41)   Nagata, R.; Kawakami, M.; Matsuura, T.; Saito, I. *Tet. Lett.* **1989**, *30*, 2817-2820.

(42)   Porter, N. A.; Dussault, P. H.; Breyer, R. A.; Kaplan, J. K.; Morelli, J. *Chem. Res. Toxicol.* **1990**, *3*, 236-243.

(43)   Lowe, J. R. In *Chemistry*; Duke University: Durham, NC, 1998; pp 201.

(44)   Lipshutz, B. H.; Bulow, G.; Lowe, R. F.; Stevens, K. L. *Tetrahedron* **1996**, *52*, 7265-7276.

(45)   Fassina, V.; Ramminger, C.; Seferin, M.; Monteiro, A. L. *Tetrahedron* **2000**, *56*, 7403-7409.

(46)   Morrill, C.; Grubbs, R. H. *J. Am. Chem. Soc.* **2005**, *127*, 2842-2843.

(47)   Duhaime, R. M.; Lombardo, D. A.; Skinner, I. A.; Weedon, A. C. *J. Org. Chem.* **1985**, *50*, 873-879.

(48)   Onaran, M. B.; Seto, C. T. *J. Org. Chem.* **2003**, *68*, 8136-8141.

(49)   Suffert, J.; Toussaint, D. *J. Org. Chem.* **1995**, *60*, 3550-3553.

(50)   Trahanovsky, W. S.; Fox, N. S. *J. Am. Chem. Soc.* **1974**, *96*, 7968-7974.

(51)   Chang, C.-L.; Kumar, M. P.; Liu, R.-S. *J. Org. Chem.* **2004**, *69*, 2793-2796.

(52)   Wu, Z.; Minhas, G. S.; Wen, D.; Jiang, H.; Chen, K. et al. *J. Med. Chem.* **2004**, *47*, 3282-3294.

CONJUGATED METHYL LINOLEATE PEROXYL RADICAL β-FRAGMENTATION TO CLOCK k_p'S OF HYDROCARBONS, AND k_{inh}'S OF PHENOLS

Introduction

Lipid peroxidation is a complex process in which molecular oxygen and a lipid react by a free-radical chain sequence. This process, known as autoxidation, leads to the degradation of naturally occurring fats and oils, and has been of interest to the chemical and biological community ever since lipids were first purified and shown to be reactive with oxygen.[1]

Toxicity by oxygen radicals has been suggested to be involved in a variety of biological events such as aging, heart disease and cancer.[2,3] Lipid peroxidation has been proposed to play a considerable role in these events, and because of this, the mechanism of lipid peroxidation has attracted considerable interest.[4] A better understanding of the mechanism of lipid peroxidation can come from careful examination of hydroperoxide products formed in the autoxidation of polyunsaturated fatty acids.

Although hydrocarbon autoxidation has been studied for some time, and many of the mechanistic details have been well determined for two generations, the significance of lipid peroxidation in human health has only become evident over the last two decades. Over this time period, there has been an explosion of research in the area of radical-mediated damage to biomolecules, and attempts

have been made to connect these events to the onset or development of various pathophysiological conditions. The extent of lipid peroxidation is now considered a biological marker of cellular oxidative stress.[5,6] Cellular oxidative stress is recognized to contribute to oxidative damage resulting from the metabolism of xenobiotic compounds, as well as from inflammatory processes, such as ischemia and reperfusion injury.[7,8]

Lipid peroxidation has the potential to affect humans on many levels. The peroxidation of membrane lipids can alter the structural dynamics of cell, organelle, and nuclear membranes, which affects cellular homeostasis and leads to apoptosis.[9] The peroxidation of lipids in LDL particles has been implicated in the oxidative modification of LDL, as well as the initiating events of cardiovascular disease; LDL uptake by macrophages.[10] While the direct consequences of lipid peroxidation are of significance, the accumulation and fate of the secondary products of lipid peroxidation have the potential to be the most significant to human health.

Lipid hydroperoxides are the initial products of lipid peroxidation, but they are relatively short-lived species. They can either be reduced by glutathione peroxidases to unreactive lipid alcohols or they can undergo metal-catalyzed decomposition reactions to give way to a variety of products that are generally more reactive than the parent lipid hydroperoxide. Most common among these are the electrophilic aldehydes acrolein, malondialdehyde, and 4-hydroxynonenal (Figure IV-1).[11,12]
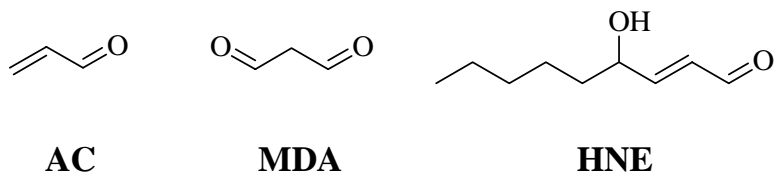
Figure IV-1: Electrophilic aldehydes formed from lipid peroxidation.

To help understand the magnitude of oxidation products that can potentially form in our bodies, remember that most phospholipids contained in every cellular membrane are known to possess an unsaturated fatty acid residue esterified to the 2-position of the glycerol backbone. Many of these acids are polyunsaturated, and the presence of a methylene-interrupted diene such as in linoleic and arachidonic acid allows them to be easily oxidized. The high local concentration of these PUFAs in phospholipids makes the lipid bilayer a prime target for reaction with oxidizing agents and also provides the opportunity for these PUFAs to participate in lengthy free radical chain reactions. The susceptibility of the PUFAs in our cellular membranes to oxidation has prompted the evolution of an extensive framework of small molecule antioxidants and enzymes whose sole functions are to prevent radical chain oxidation of membrane lipids and to minimize damage caused by oxidation.

Even though lipid peroxidation has been the focus of much recent research, details of the chemical mechanisms involved in the process have been limited until recent years. Most biological studies of peroxidation have utilized calorimetric assays such as the formation of conjugated dienes[13] or the reaction of a lipid oxidation product with thiobarbituric acid to give a colored adduct[14,15] as

a measure of autoxidation. Titrimetric methods have also been used to measure peroxide formation in the oxidations.[16] The assays mentioned above only give a crude indication of the oxidation process, and the nature of the chemical events involved in the autoxidation of fatty acids and unsaturated phospholipids have remained unclear.

Product mixtures obtained in polyunsaturated fatty acid random autoxidation are complex. However, the primary processes leading to products have been firmly established.[17-21] The four major products formed from methyl linoleate (**1**) autoxidation are conjugated diene hydroperoxides (Figure IV-2).[22] Two products (**2** and **3**) have *trans*, *cis*-stereochemistry, while the other two (**4** and **5**) have *trans*, *trans*-stereochemistry. Together, these four products account for over 97% of the oxygen consumed during the autoxidation. Other minor products that are formed in the autoxidation of linoleate include nonconjugated diene hydroperoxides formed by abstraction of allylic hydrogens at the C8 and C14 positions of the linoleate precursor.[23]

The distribution of the primary products of methyl linoleate autoxidation depends upon the conditions used for the autoxidation.[24,25] The following observations concerning the products formed are relevant to a consideration of the mechanism of the autoxidation:

1. The sum total of products formed from oxygen addition at C9 (**3** and **4**) is the same as the products formed from oxygen addition at C13 (**2** and **5**).

2. Higher autoxidation temperatures give rise to more *trans, trans* products.

3. Higher concentrations of linoleate give rise to more *trans, cis* products.

4. Product distributions are independent of oxygen pressure between 10 and 100 mm O_2.

The hydroperoxide **2** rearranges to a mixture of the four hydroperoxides by a free-radical mechanism and during this rearrangement, atmospheric oxygen and the hydroperoxide oxygen exchanges.[26]
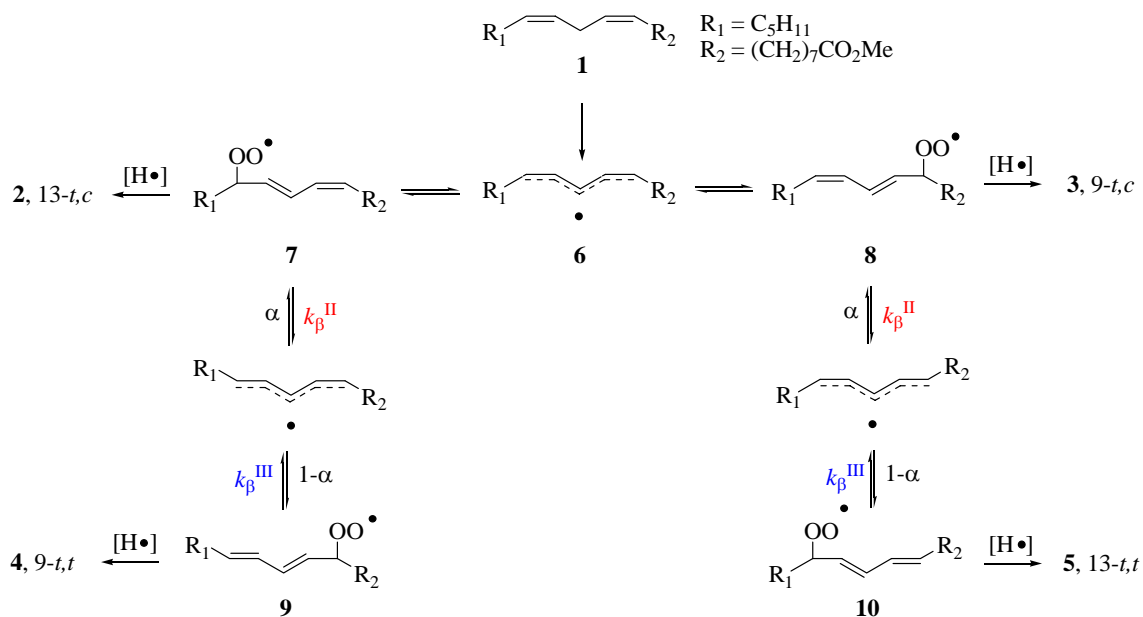
Figure IV-2: Mechanism of methyl linoleate autoxidation.

In a previously proposed kinetic scheme,[19,24] hydrogen atom abstraction occurs at the bis-allylic carbon of the diene system to generate the pentadienyl radical **6**. Oxygen addition at either end of the delocalized radical system occurs

at the diffusion-controlled rate (10^9 s^{-1}) in the absence of a sufficient hydrogen atom donor, leading to peroxyl radicals **7** and **8**, which are immediate precursors to hydroperoxides **2** and **3**, respectively. Hydroperoxides **4** and **5** most likely occur from loss of oxygen from peroxyl radicals **7** and **8** to give isomerized carbon radicals. Oxygen adds to the ends of these new pentadienyl radicals to give the corresponding peroxyl radicals **9** and **10**, which are, again, immediate precursors to hydroperoxides **4** and **5** (Figure IV-2).

The data concerning linoleate autoxidation is consistent with this mechanism. Products are formed from oxygen addition at either end of the intermediate pentadienyl radicals and consequently the pseudosymmetry of the system leads to equal amounts of 9- and 13-substituted hydroperoxides. At higher temperatures, β-fragmentation pathways become competitive with hydrogen atom transfer reactions and more thermodynamic (*trans, trans*) products are formed. Higher concentrations of linoleate lead to more kinetic (*trans, cis*) products because increasing the concentration of the hydrogen atom donor [H•] favors hydrogen atom addition to peroxyl radical **8**, giving hydroperoxide **3**. Product distributions of hydroperoxide products are independent of oxygen concentration at pressures above 10 mm O_2 because all carbon centered radicals are trapped at these concentrations of oxygen and the important stereochemical branch point in the sequence involves the peroxyl radicals **7**-**10** and not the pentadienyl radical **6**. Lastly, the kinetic hydroperoxides (**2** and **3**) rearrange to give a mixture of all four hydroperoxide products. During this rearrangement, atmospheric oxygen is exchanged with the

hydroperoxide oxygen via a β-fragmentation process seen in Figure IV-2 and IV-3.
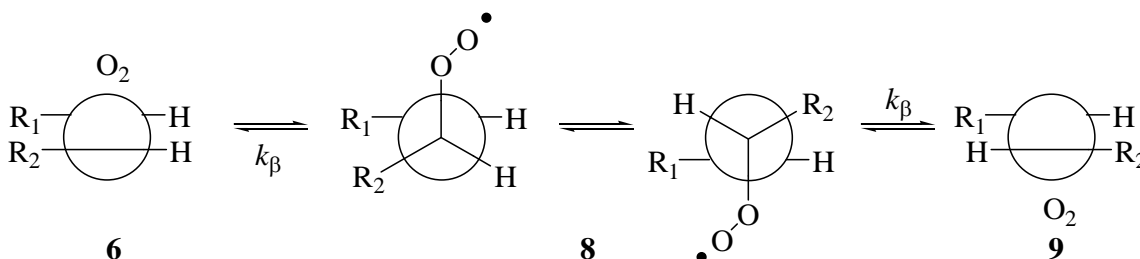
Figure IV-3: Newman projection of oxygen addition to the pentadienyl radical **6**.

Previous studies have suggested that the distribution of products in fatty acid or ester autoxidation may be understood by a reversible oxygen addition to intermediate pentadienyl radicals. This reversible addition results in the isomerization of the pentadienyl radical. Figure IV-3 shows a Newman projection of oxygen addition to radical **6**. Oxygen addition occurs via an approach perpendicular to the plane of the π radical to give peroxyl radical **8**, which is now free to undergo conformational equilibrium. A new, isomerized carbon radical is formed from loss of oxygen from the opposite side of the π system from which oxygen entered. Similar arguments apply for the isomerization of **6** to **10**.

The allylbenzene derived peroxyl radical clocks described in Chapter III are useful over a range of k_{inh}'s from 10^4 to 10^6 M^{-1} s^{-1}. These clocks, coupled with the non-conjugated methyl linoleate β-fragmentation, will allow hydrogen atom transfer processes to be clocked over a range of four orders of magnitude (10^4-10^7 M^{-1} s^{-1}). A peroxyl radical clock has been developed in the Porter lab based on the conjugated linoleate β-fragmentation described in Figure IV-2.

Because this fragmentation occurs much slower[21] than the non-conjugated linoleate fragmentation and the allylbenzene derived fragmentation, it has proven to be useful in clocking hydrogen atom transfer processes from 10^0-10^4 M^{-1} s^{-1}. For our purposes, the hydroperoxides **2** through **5** were reduced with triphenylphosphine (PPh$_3$) to give the alcohols **11** through **14** (Figure IV-4). Analysis of the alcohols provided better chromatography, as well as easier manipulation of the oxidation mixture. Reduction to the alcohols has no effect on the product distribution or kinetics of the following experiments.
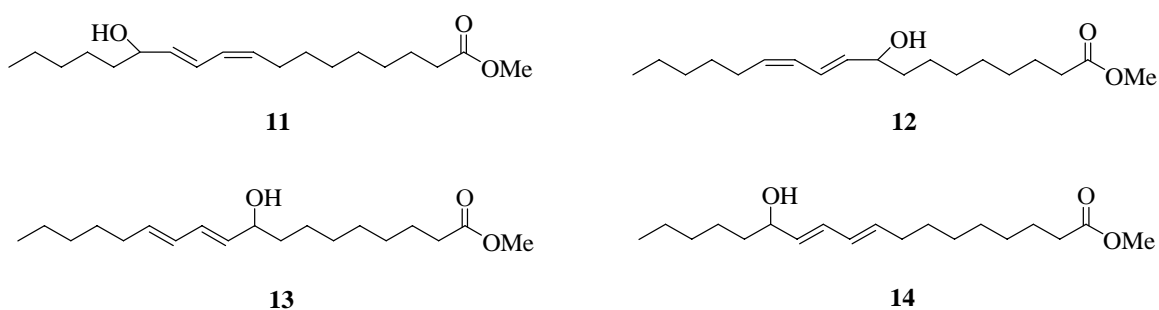
Figure IV-4: Alcohol autoxidation products of methyl linoleate.

The Use of *N*-MBHA to Calibrate the Slow Methyl Linoleate Peroxyl Radical Clock

It became evident for the selective synthesis of *trans, cis* hydroperoxides from catalytic autoxidation, a catalyst that was a better H-atom donor than *N*-hydroxyphthallimide (*N*HPI) would be required. 2,2,6,6-tetramethyl-*N*-piperidine, which leads to the persistent N-oxyl radical TEMPO, was the first such compound looked at by the Porter group due to its low O-H BDE, approximately 70 kcal/mol.[27] Coseri and Ingold have demonstrated that TEMPO-like radicals react with cyclohexene primarily through initial abstraction

of an allylic hydrogen atom under mild conditions (70°C) rather than by addition to the olefinic bond.[28] Unfortunately, the persistent nitroxyl radicals then couple with the newly formed carbon-centered radicals at close to the diffusion-controlled limit. TEMPO can therefore serve as a strong inhibitor of autoxidation, a fact that diminishes its use for the synthesis of regiochemically specific hydroperoxides of methyl linoleate.

N-methyl-benzohydroxamic acid (*N*MBHA) has an O-H BDE value of 79.2 kcal/mol,[29] which is intermediate between *N*-hydroxypiperidine (~70 kcal/mol) and NHPI (88.1 kcal/mol).[27] The rate of hydrogen abstraction from the O-H bond in *N*MBHA by peroxyl radicals has been determined to be $3.1 \times 10^5 \, M^{-1}s^{-1}$, by the peroxyl radical clock method described in Chapter III. *N*MBHA thus appears to be a viable candidate for use as an autoxidation catalyst based on its O-H BDE and its predisposition for being an excellent H-atom donor. *N*MBHA can be easily synthesized in one step by the addition of benzoyl chloride to a mixture of *N*-methylhydroxylamine and potassium carbonate in benzene at 0°C, as seen in Figure IV-5.
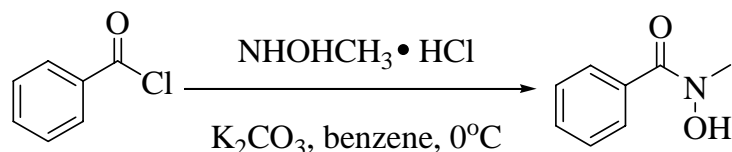
Figure IV-5: Synthesis of *N*MBHA.

Results from the Porter group indicate that *N*MBHA is an effective catalytic system for the synthesis of hydroperoxides.[30] As shown in Figure IV-

6, the nitroxyl radical derived from *N*MBHA catalyses the hydrogen abstraction from the bisallylic position of the lipid since the BDE of the *N*MBHA O-H bond is approximately 6 kcal/mol higher than that of the C-H bond.[31] Because *N*MBHA is a good hydrogen atom donor, the slower β-fragmentation or cyclization (~10^2 to 10^3 M^{-1}s^{-1}) of the intermediate peroxyl radicals is minimized, conferring a higher selectivity to the system and generating the free radical chain while forming the kinetically favored hydroperoxide.
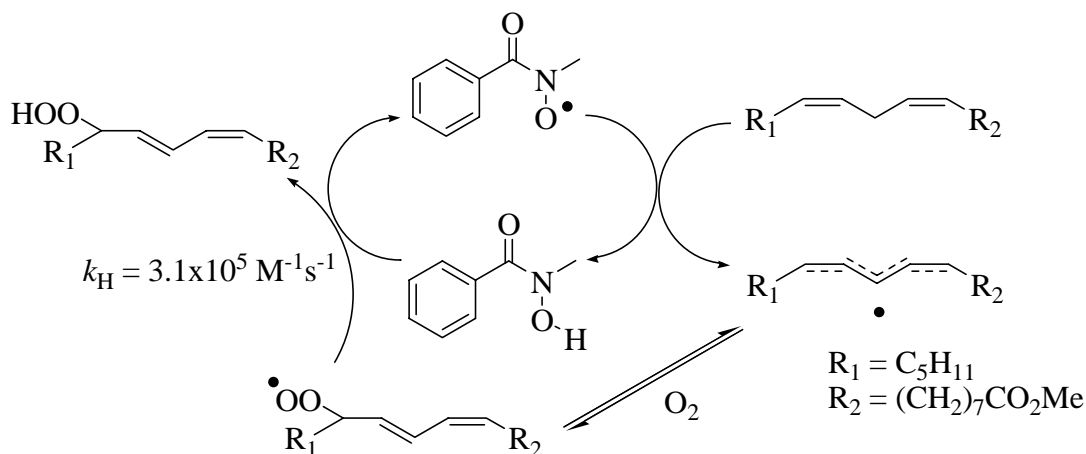
Figure IV-6:   Peroxidation of fatty acid methyl esters in the presence of *N*MBHA.

The rates of β-fragmentation (k_β^{II} and k_β^{III}) in Figure IV-2 had to be calibrated. Values for k_β^{II} and k_β^{III} have been reported previously by Wujek and Porter[21], however there is some uncertainty as to the accuracy of these values. It was decided that *N*MBHA would be used as the hydrogen atom donor/pro-oxidant due to *N*MBHA's ability to effectively oxidize methyl linoleate to give all four oxidation products (**2** through **5**).

Equation 1 was used to determine both k_β^{II} and k_β^{III} by keeping the concentration of methyl linoleate ([ML] constant and varying the concentration of NMBHA ([RH]). The k_p of methyl linoleate used in the calibration was 62 $M^{-1}s^{-1}$, first determined by Howard.[32] k_β^{II} can be derived from the slope of the plot in Figure IV-7, and k_β^{III} can be derived from the y-intercept. From figure IV-7, k_β^{II} and k_β^{III} were determined to be 625 and 69 $M^{-1}s^{-1}$, respectively.

$$\frac{11 + 12}{13 + 14} = \frac{k_p[RH] + k_p[ML]}{k_\beta^{II}(1-\alpha)} + \frac{\alpha k_\beta^{III}}{k_\beta^{II}(1-\alpha)} \tag{1}$$
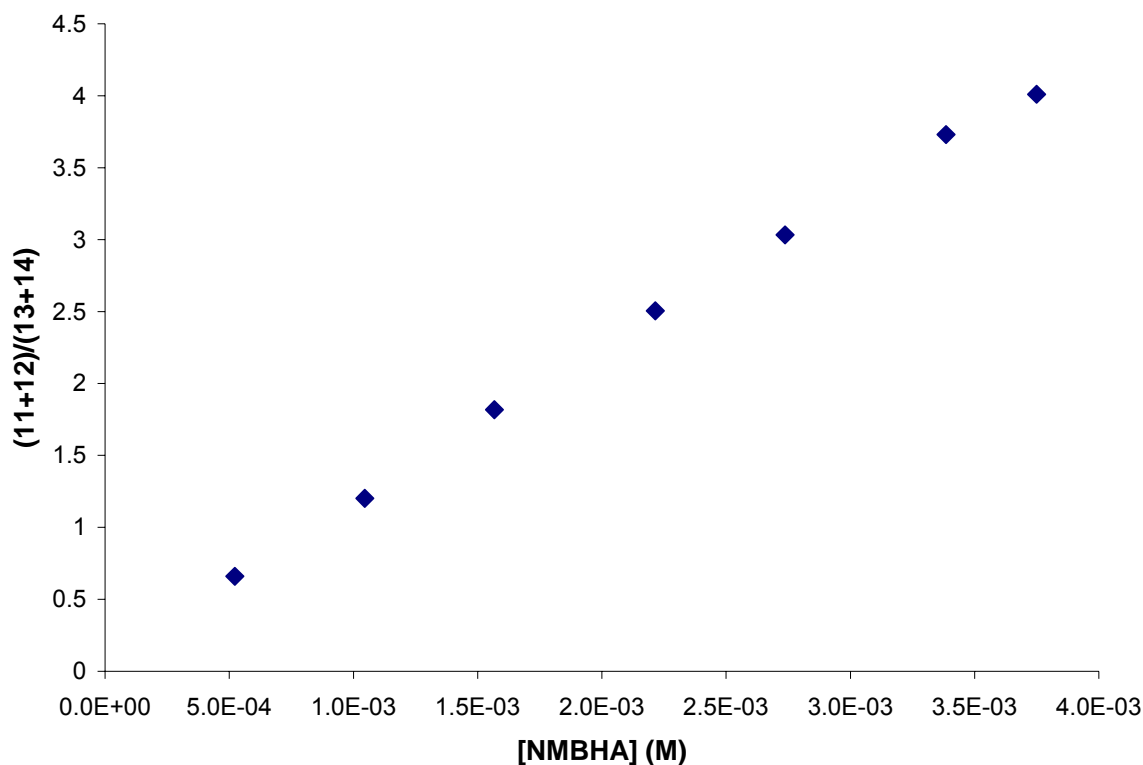
Figure IV-7: Calibration of the conjugated methyl linoleate clock using NMBHA. [methyl linoleate] = 0.2 M; [MeOAMVN] = 0.01 M; [NMHBA] = 0.5-4 mM; T = 37°C; t = 1 h.

The consumption of NMBHA was initially thought to not be an issue due to the fact that NMBHA was believed to act as a catalytic pro-oxidant, and therefore it would be continuously regenerated throughout the course of the oxidations (Figure IV-6). As can be seen in Figure IV-8 this was not the case, as a great majority of *N*MBHA was being consumed (60-95%) over the relatively short time course of the reaction.
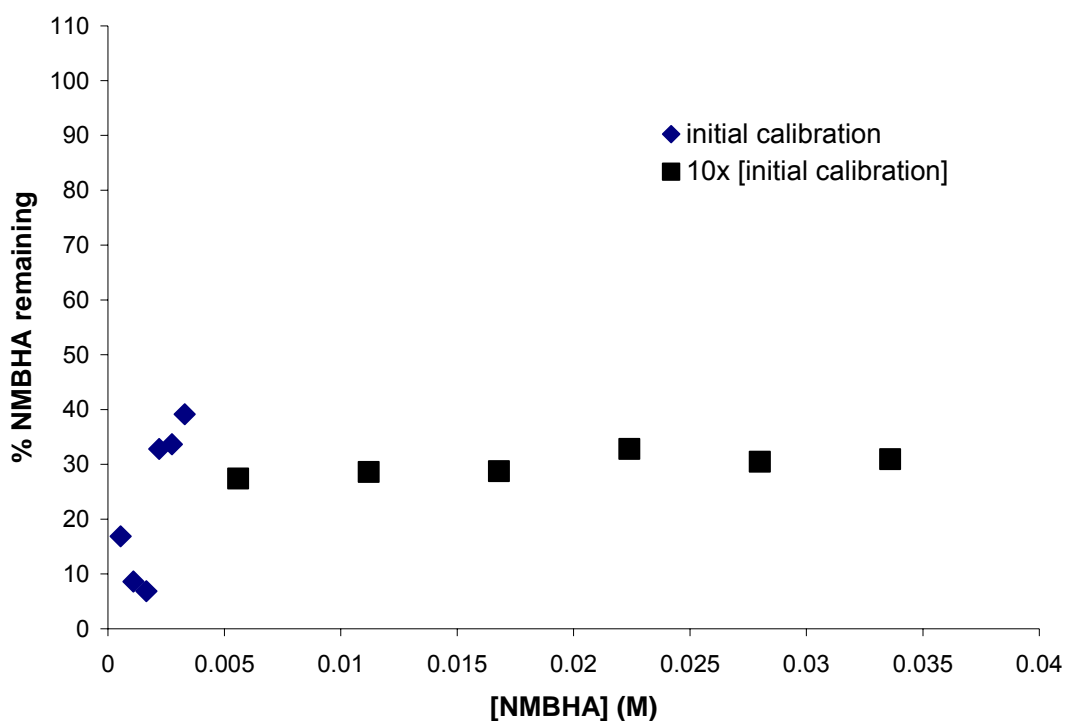
Figure IV-8: Consumption of *N*MBHA during the calibration of the conjugated methyl linoleate peroxyl radical clock. [methyl linoleate] = 0.2 M; [MeOAMVN] = 0.01 M; [NMHBA] = 0.5-4 mM; T = 37°C; t = 1 h.

Even at concentrations 10x the initial calibration concentrations, more than 70% of the hydrogen atom donor was being consumed. A 10-fold increase in the concentration of *N*MBHA not only continues to yield a large

amount of consumed hydrogen atom donor, but also prevents *N*MBHA from being a catalytic pro-oxidant. That is, only the kinetic products **2** and **3** could be identified. Hydroperoxides **4** and **5** were never obtained unless a very small amount of *N*MBHA was used. It would seem that at these concentrations (0.005 to 0.035 M), *N*MBHA is acting solely as an antioxidant.

Again, because *N*MBHA was being consumed so readily during the calibration experiments, it became necessary to determine k_β^{II} and k_β^{III} with another hydrogen atom donor in order to use the conjugated methyl linoleate peroxyl radical clock to determine k_p's of hydrocarbons and slower phenols. It was decided that methyl linoleate (ML) could be used to calibrate the conjugated methyl linoleate clock because the k_p of ML is known to be 59.9 M^{-1} s^{-1} at 37°C.[33] It is possible to use ML for this calibration because ML is a hydrogen atom donor, and by substituting the k_p of ML into equation 1, the only remaining variables are k_β^{II} and k_β^{III}, which are easily solved for from the slope and y-intercept of the line in Figure IV-9.

The values for k_β^{II} and k_β^{III} were derived from controlled autoxidations of methyl linoleate. The oxygen partition coefficient, α, has already been established at 0.686.[20] α-tocopherol would have been the most desirable hydrogen atom donor for the calibration of the conjugated methyl linoleate clock because its bimolecular rate constant is so well established. However, the rate constant for α-tocopherol is too high to reliably determine product ratios for the conjugated methyl linoleate clock.
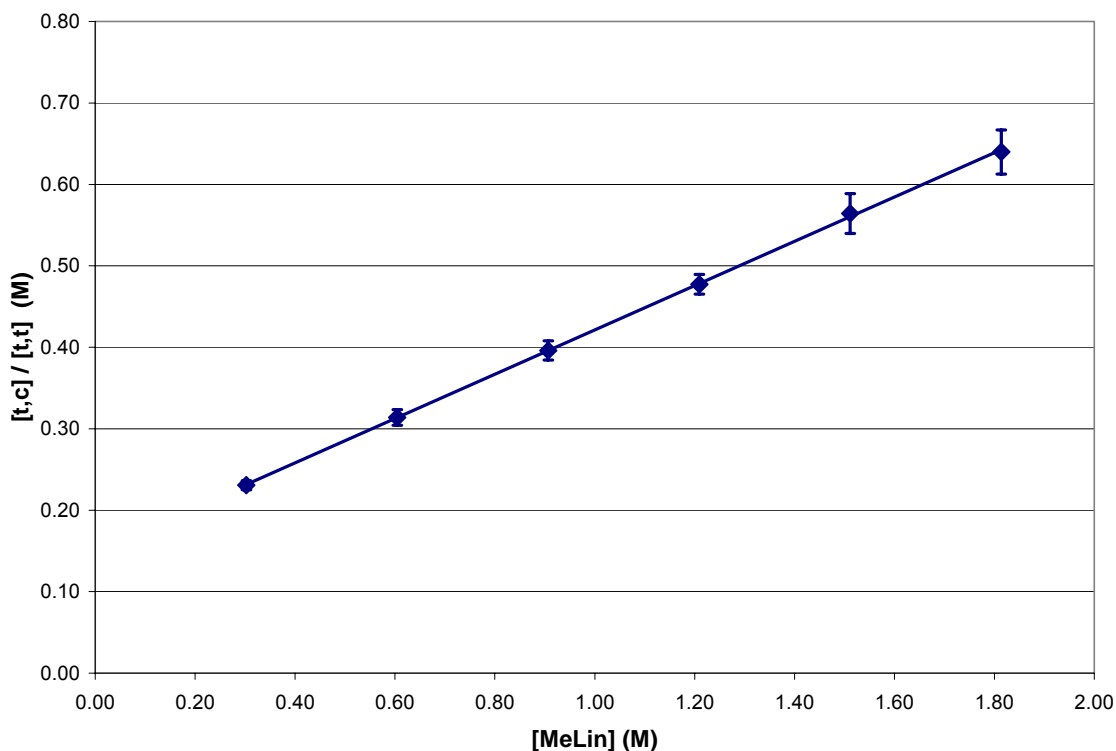
Figure IV-9: Calibration of the conjugated methyl linoleate peroxyl radical clock by controlled autoxidations of methyl linoleate. [ML] = 0.3-1.8 M; [MeOAMVN] = 0.01 M; T = 37°C; t = 1 h.

Calibrations were conducted in the same way as with *N*MBHA, however because k_H for ML and *N*MBHA are more than four orders (10^1 and 10^5 respectively) of magnitude different the concentrations of ML had to be adjusted accordingly. Consumption was monitored over the range of ML concentrations, as well as over varying reaction times in order to find the most suitable conditions that would ensure pseudo-first order kinetics. Because consumption was not an issue (Figure IV-10), autoxidations of ML could be used to calibrate the conjugated methyl linoleate peroxyl radical clock.
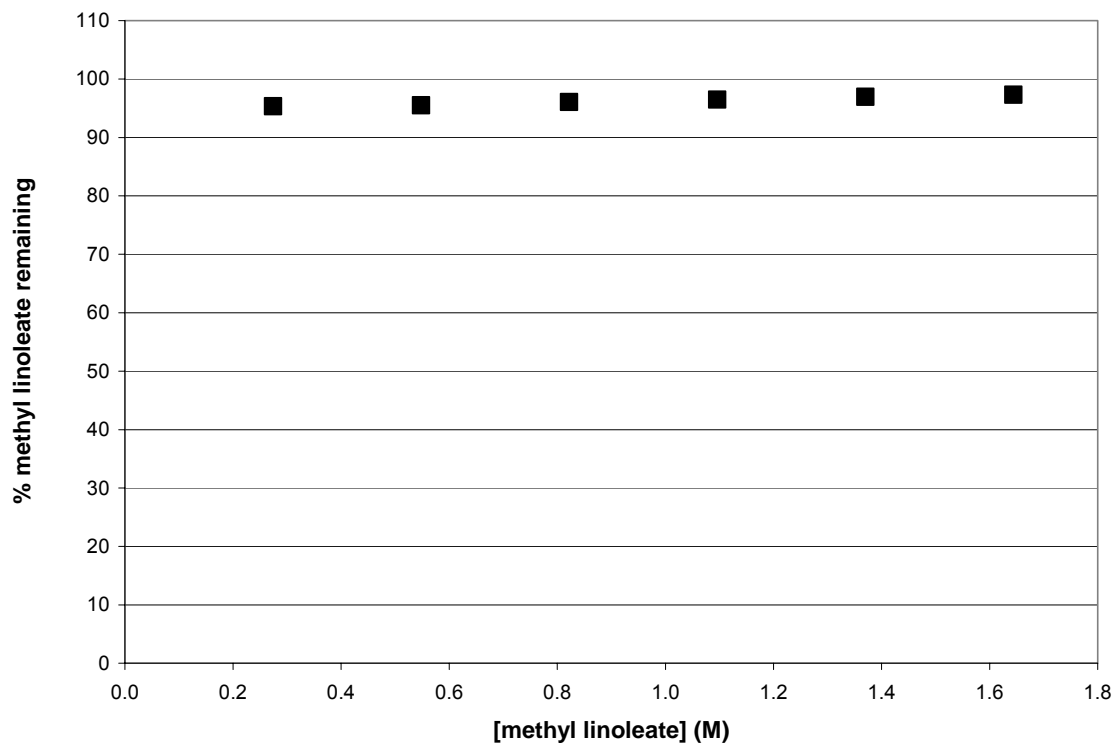
Figure IV-10: Consumption of ML during conjugated methyl linoleate peroxyl radical clock calibration. [ML] = 0.3-1.7 M; [MeOAMVN] = 0.01 M; T = 37°C; t = 1 h.

Autoxidations with varying concentrations of methyl linoleate, initiated by 2,2'-azobis-(4-methoxy-2,4-dimethylvaleronitrile) (MeOAMVN), were carried out in chlorobenzene at 37 °C. Conditions were chosen such that a negligible amount of hydrogen atom donor was consumed since the kinetic analysis assumes a constant concentration of hydrogen atom donor. The products of methyl linoleate oxidation were measured by HPLC analysis (Figure IV-11) described in the experimental section at the end of this chapter. Reduction of hydroperoxides **2** through **5** with triphenlyphosphine to the alcohols **11** through **14** was necessary in order to obtain optimal separation of the *trans, cis* and *trans, trans* oxidation products.
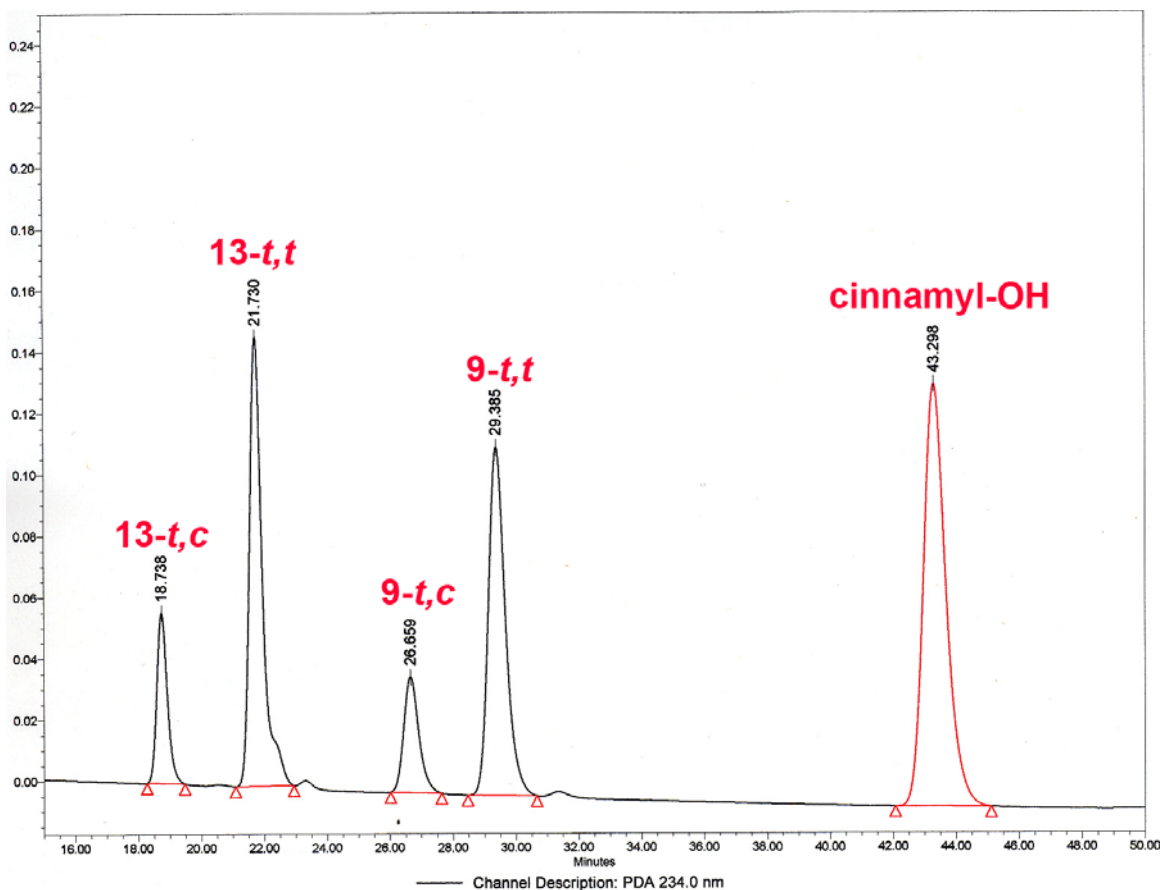
Figure IV-11: Representative HPLC of methyl linoleate autoxidations monitored at 234 nm. Cinnamyl alcohol (5 mM) was used as the internal standard. [ML] = 0.2 M; [MeOAMVN] = 0.01 M; T = 37°C; t = 1 h.

As can be seen from Figure IV-9, the calibration of the conjugated methyl linoleate clock with ML was very reproducible. Table IV-1 shows values for k_β^{II} and k_β^{III} derived from the slope and y-intercept of the line in Figure IV-9 using equation 1, as well as the α value determined by Tallman *et al*[20] used in the conjugated methyl linoleate clocking experiments. The α, k_β^{II}, and k_β^{III} originally reported by Porter and Wujek[21] are included in Table IV-1 for comparison. It can be seen that the experimental values of α, k_β^{II}, and k_β^{III} from

the calibration of the conjugated methyl linoleate peroxyl radical clock are in good agreement with the accepted values of the past twenty years.

Table IV-1: α, k_β^{II}, and k_β^{III} of the conjugated methyl linoleate peroxyl radical clock.

Variable	Porter and Wujek[21]	Peroxyl Radical Clock
α	0.67	0.686 [20]
k_β^{II}	430 s^{-1}	660($\pm$172) s^{-1}
k_β^{III}	27 s^{-1}	42($\pm$11) s^{-1}

Clocking Experiments with the Conjugated Methyl Linoleate Clock

In order to demonstrate the utility of the peroxyl radical clocks, a series of compounds were studied (Figure IV-12) to determine their rate constants by the radical clock method using the conjugated methyl linoleate clock. The compounds that have been clocked in this section have known rate constants reported elsewhere.[24,32,34,35] This provides an opportunity to validate the radical clock method. These specific hydrogen atom donors were chosen to study the hydrogen atom transfer processes through different structures (phenols, hydrocarbons) and spanning a wide range of rate constants ($10^0 - 10^4$ M^{-1}s^{-1}). This provides the opportunity to explore the general application of the radical clock method. The phenols that were studied fall into the antioxidant class given their ability to inhibit autoxidation processes (k_{inh}), whereas the hydrocarbons are known to propagate radical chemistry (k_p). Regardless of the different compounds classification as an antioxidant or hydrocarbon (k_{inh} or k_p,

153

respectively), the fundamental reaction is still a hydrogen atom transfer and the overall kinetics remain unchanged.
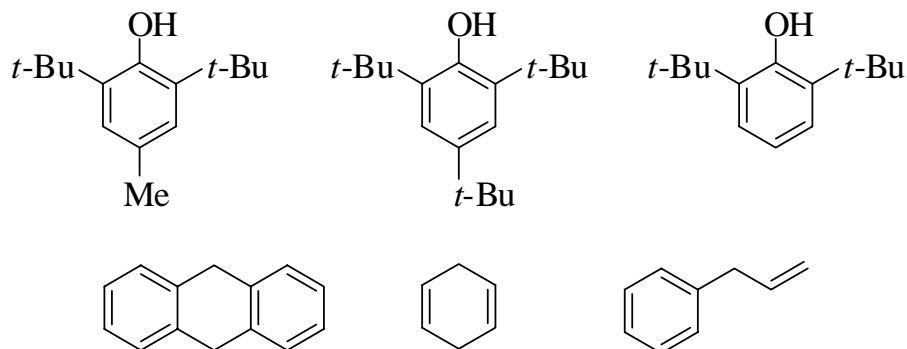
Figure IV-12: Phenols and hydrocarbons clocked with the conjugated methyl linoleate peroxyl radical clock.

The conjugated methyl linoleate peroxyl radical clock experiments were carried out in a similar manner to the calibration experiments described above. The hydrogen atom donor of interest was first monitored for consumption using reverse phase HPLC (Figure IV-13, described in the experimental section). The clocking experiments were conducted once suitable conditions (concentration of donor, time of oxidation, etc.) were established based upon the results of the consumption experiments. Again, by ensuring that a negligible amount of the hydrogen atom donor is being consumed, we can ensure pseudo-first order kinetics, and the steady-state approximation that gave equation 1 will hold true.
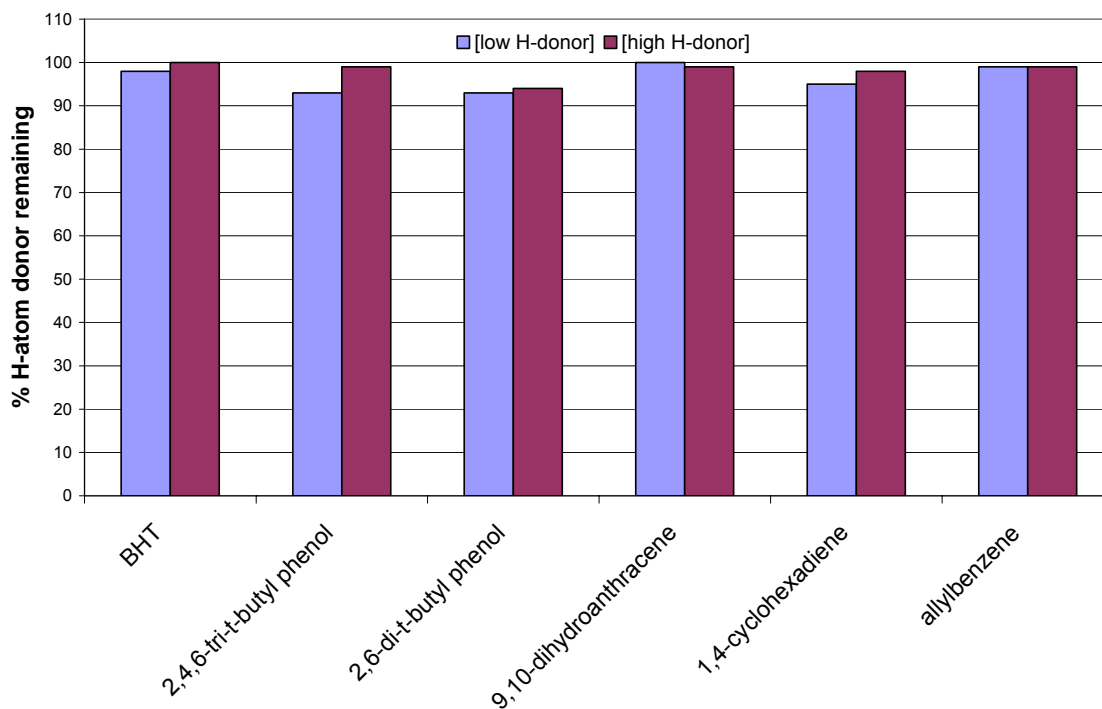
Figure IV-13: Consumption of H-atom donors during clocking experiments with the conjugated methyl linoleate peroxyl radical clock. 5 mM internal standard (different for each hydrogen atom donor) was used. [MeOAMVN] = 0.012 M; [methyl linoleate] = 0.2 M; T = 37°C; t = 1 – 4 h. [BHT] = 0.02, 0.05 M; [2,4,6-tri-*t*-butylphenol] = 0.02, 0.05 M; [2,6-di-*t*-butylphenol] = 0.03, 0.05 M; [9,10-DHA] = 0.25, 0.45 M; [1,4-CHD] = 0.41, 0.84 M; [allylbenzene] = 2.26, 6.04 M.

The values obtained by the peroxyl radical clock method are in good agreement with previously reported values for the inhibition and propagation rate constants that are available in the literature, as seen in Table IV-2, taking into account the temperature differences. While literature values have been measured in experiments that vary widely in solvent, temperature, and method, the values reported here were derived from experiments carried out in benzene or chlorobenzene at 37°C by a single method. As a result, comparison of the trends in k_H is straightforward and reliable. Furthermore, little is required to

determine a rate constant in terms of quantity of antioxidant, equipment, and time investment. Therefore, the conjugated methyl linoleate peroxyl radical clock method developed here offers several advantages over the traditional methods.

Table IV-2: k_{inh}'s of phenols and k_p's of hydrocarbons determined by the conjugated methyl linoleate peroxyl radical clock compared to literature and theoretical k_H's.

H-atom donor	Exp. k_H (clock) $(M^{-1}s^{-1})$	Lit. k_H $(M^{-1}s^{-1})$	Theor. k_H[31] $(M^{-1}s^{-1})$
BHT	$1.9(\pm0.9) \times 10^4$	$1.4(\pm0.2) \times 10^4$ [35]	N/A
2,4,6-tri-*tert*-butylphenol	$1.7(\pm0.6) \times 10^4$	$1.6(\pm0.2) \times 10^4$ [34]	N/A
2,6-di-*tert*-butylphenol	$3.2(\pm0.3) \times 10^3$	$3.1(\pm0.3) \times 10^3$ [35]	N/A
9,10-dihydroanthracene	$384(\pm46)$	397 [24]	85
1,4-cyclohexadiene	$265(\pm33)$	$362(\pm17)$ [24]	314
allylbenzene	$5.5(\pm0.6)$	10 [32]	109

The theoretical k_H's in Table IV-2 were predicted using Equation 2 published by Pratt, *et al.*[31]:

$$\text{Log } k_p = -0.0219(\text{C-H BDE}) + 18.9 \qquad (2)$$

Knowing the C-H BDE (kcal/mol) of a specific hydrocarbon, an approximate k_p can be determined. It can be seen from Table IV-2 that the theoretical k_H's vary quite dramatically from the literature and experimental data for 9,10-dihydroanthracene and allylbenzene. This is not a concern because Equation 2 was derived from the line of best fit from C-H BDE (kcal/mol) data obtained

from theoretical investigations[31] and from k_p's that contain significant associated error.[32] The theoretical investigations also did not take into account the effect of aromatization on the energetics of 9,10-dihydroanthracene (which was dramatically under predicted), nor did the calculations take into account initially breaking the aromatization of allylbenzene (which was dramatically over predicted). Therefore, the line of best fit of all this data may not be as reliable as desired, but it does provide a good starting point for the theoretical determination of k_p's of hydrocarbons that are unknown. The literature values were typically collected using the rotating sector method.[32] This method requires that rates of initiation and termination be determined as well as the rate of substrate and/or oxygen consumption. The experimental values using the peroxyl radical clock method, are more uniform in nature, but have yet to be validated. It should be understood that there is error associated with the calculations, as well as experimental error, that must be propagated in these predictions.[31,36]

As the rate constant for hydrogen atom donation (k_H) increases, it can be seen in Table IV-2, that the relative error associated with that compound increases. This presents somewhat of a limitation of the conjugated methyl linoleate peroxyl radical clock. That is, the conjugated methyl linoleate clock has a "window" of rate constants that it is capable of clocking. This window is approximately one order of magnitude greater and lower than the rate of β-fragmentation (k_β^{II} and k_β^{III}, for this example) associated with a particular clock. Therefore, while the allylbenzene peroxyl radical clock (Chapter III) was capable

of determining rate constants from 10^6 to 10^4 $M^{-1}s^{-1}$ (k_β = 2.6x10^5 s^{-1}), the conjugated methyl linoleate peroxyl radical clock is capable of determining rate constants of hydrogen atom donation reactions in the 10^0 to low 10^4 range (k_β^{II} = 6.6x10^2 s^{-1} and k_β^{III} = 4.2x10^1 s^{-1}). This observation will help in future experiments when trying to determine the appropriate clock for a specific hydrogen atom transfer reaction that is unknown.

Another requirement of the peroxyl radical clock system is that the substrate must propagate the free radical chain. This is not typically a problem for hydrocarbons such as 9,10-dihydroanthracene or 1,4-cyclohexadiene, or phenols such as α-tocopherol or 2,4,6-tri-methylphenol. However, with bulky ortho substituents like the *tert*-butyl groups in BHT, 2,4,6-tri-*t*-butylphenol, or 2,6-di-*t*-butylphenol, propagation does not occur as easily. Therefore these phenols are slightly more difficult to clock with reproducible results, and have more associated error than the easily propagating compounds. (Table IV-2, Table III-3).

Conclusions

Clock selection should be paired to the substrate being investigated. The peroxyl radical clock approach involves a competition leading to two different products, and the essential part of the experiments is the determination of the relative amounts of these two products formed at a known concentration of hydrogen atom donor. As a general guide, a unimolecular clock reaction should

be selected to time H-atom transfer reactions having bimolecular rate constants that are 0.05 to 20 times the rate of the clock reaction.

Conditions should be selected such that the concentration of the hydrogen atom donor is known and the ratio of products can be reliably determined. If the oxidation reactions are carried out to low conversions of hydrogen atom donor one can, within the errors of the method, assume a constant concentration of the donor in the experiment. Typically, oxidations should be carried out to 0.5 – 2% oxidation, depending on the concentration of the clock used in the experiment, to meet both of these requirements. The oxidation conditions should never result in the consumption of a significant amount of the hydrogen atom donor. This is typically not a problem with the peroxyl radical clock method because the oxidation relies on propagation by the ArO•. As a result, the hydrogen atom donor is regenerated during the course of an oxidation.

A final *caveat* concerns the fact that the clocks are themselves oxidizable compounds, which is a requirement of the approach. This can give rise to problems in the analysis if sufficient care is not taken to ensure the appropriate purity of the clock. Commercial methyl linoleate may have substantial amounts (1-2%) of oxidation products as received and blank analyses should always be performed to assure that clock substrates are uncontaminated by the very products that are formed in the clock experiment.

Experimental Methods

Materials

The initiator, 2,2'-azobis-(4-methoxy-2, 4-dimethylvaleronitrile) (MeOAMVN), was obtained from Wako and dried under high vacuum for 2 h. Benzene and chlorobenzene were passed through a column of neutral alumina and stored over 4Å molecular sieves. Hexanes used in HPLC analysis and column chromatography was HPLC grade from Burdick & Jackson. Methyl linoleate was purchased from NuChek Prep and chromatographed on silica (10% EtOAc/hexanes) prior to use. *N*MBHA was synthesized as described below following a literature procedure.[37] All other hydrogen atom donors used in conjugated methyl linoleate clocking experiments were purchased from Aldrich and were used as received except for 9, 10-dihydroanthracene which was recrystallized twice from ethanol. The oxidation products of methyl linoleate have been characterized in previous publications.[18,19,21,30]

Procedure for the conjugated methyl linoleate peroxyl radical clock calibration

The oxidations were carried out using methyl linoleate (0.1 M) MeOAMVN (0.01 M) in chlorobenzene for 2 h @ 37°C. The oxidations were stopped by the addition of excess BHT, reduced with PPh$_3$, and followed by the addition of the internal standard (5mM cinnamyl alcohol). HPLC analyses were carried out with a Waters 600 liquid chromatograph interfaced to a Waters 996 PDA detector at 234 nm. Oxidation products were separated on a Beckman Ultrasphere silica

column (0.46 x 25 cm), using 0.5% *iso*-propanol in hexanes as the mobile phase at 1.0 mL/min. The values for k_β^{II} and k_β^{III} were determined from the slope and the y-intercept respectively, using equation 1.

Procedure for clocking experiments using the conjugated methyl linoleate clock

The samples were prepared as described above for each clock in chlorobenzene with varying concentrations of hydrogen atom donor concentration (0.02-6.04 depending on the substrate). The samples were incubated at 37 °C for 0.5-2 h. Following the oxidation, BHT (50 mM) and internal standard (5 mM cinnamyl alcohol, except for allylbenzene, 5 mM benzyl alcohol) were added to each sample. Methyl linoleate oxidation mixtures were reduced with PPh$_3$ and analyzed by HPLC (0.5 % *i*-PrOH/hexanes, 1 mL/min, and detection at 234 nm).

General procedure for hydrogen atom donor consumption experiments

The oxidations were conducted with methyl linoleate (0.1-0.2 M), MeOAMVN (0.01 M), and hydrogen atom donor (0.02–6.04 M, depending on compound) in chlorobenzene. The samples were incubated at 37 °C for 0.5-2 h. The oxidation was stopped by the addition of excess 2,4,6- tri-*t*-butylphenol (except for the tri-*t*-butyl phenol experiments when 2,4,6-tri-methylphenol was added), followed by the addition of the internal standard (10 mM of BHT). In the BHT experiments, 10 mM 2,4,6-tri-methylphenol was added. The hydroperoxides were reduced to their corresponding alcohols with excess

trimethylphosphite and the samples were diluted with methanol (1.8 mL).

HPLC analyses were carried out with a Waters 600 liquid chromatograph

interfaced to a Waters 996 PDA detector with a SUPELCO Discovery C-18

(25cm x 4.6mm, 5 μm) RP-HPLC column. Methanol and water were used as

the mobile phase and the gradient was: (Methanol:water) 90:10 for 5 min, ramp

to 75:25 in 10 min, ramp to 20:80 in 15 min, ramp to 90:10 in 10 min.

Consumption was monitored at a wavelength >250 nm to ensure no peak

contamination from the oxidation products (Figure IV-14). When consumption

of *N*MBHA was monitored, acetonitrile was used instead of methanol due to

solubility issues.
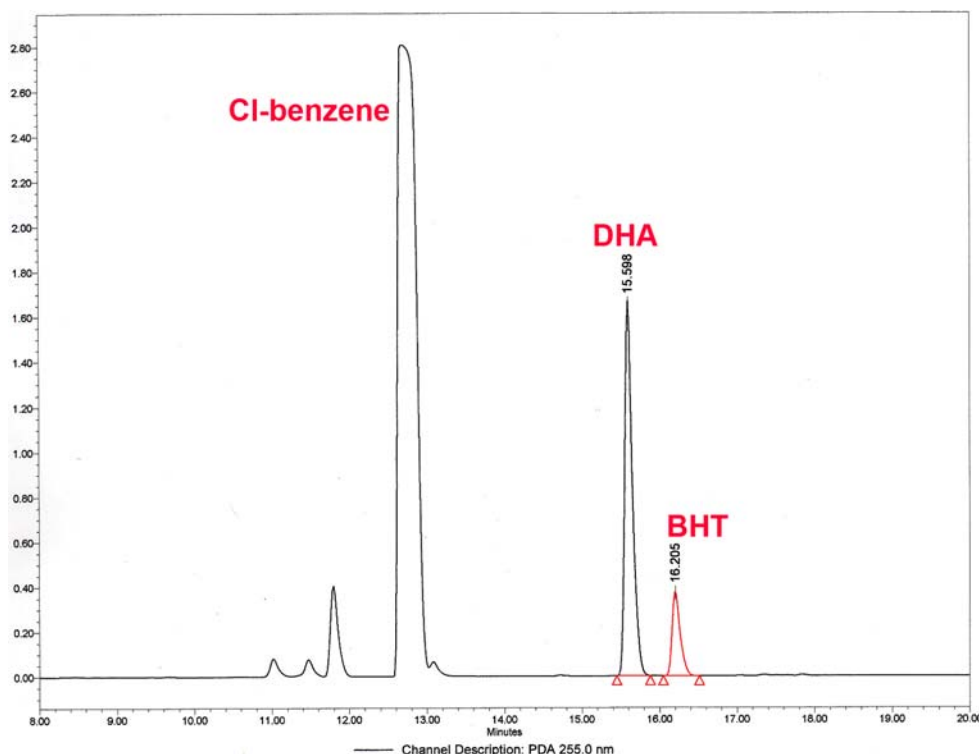
Figure IV-14: Representative HPLC chromatogram of the consumption of DHA monitored at 255 nm. [methyl linoleate] = 0.1 M; [DHA] = 0.25 M; [MeOAMVN] = 0.01 M; [BHT] = 0.01 M; T = 37°C; t = 0.5 h.

Error analysis

All errors reported are 95% confidence limits of the rate constant as determined by t tests, i.e. best fit ± (standard error)(t*). The standard error was determined from SigmaPlot or Origin and multiplied by t*. The value for t* was calculated in Excel using the equation TINV (0.05, df), where df is the degrees of freedom. The degrees of freedom were calculated by subtracting the number of parameters (2) from the total number of data points. The error in literature values for α-TOH (±10%) was also propagated into the error.

*Synthesis of N-Methylbenzohydroxamic Acid (N*MBHA)[37]
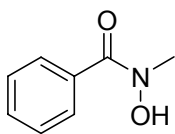
3.9 mL (33 mmol) of benzoyl chloride was added slowly, over one hour, to a slurry solution of *N*-methyl Hydroxylamine (3.17 g, 38 mmol) and potassium carbonate (18 g, 120 mmol) in 80 mL of benzene at 0°C. The reaction was allowed to warm to room temperature over two hours. Upon completion, the solvent was removed under vacuum, without warming, in order to avoid thermal decomposition. 100 mL of water was added to the remaining oil, and the pH was corrected to 6.0 with 37% aqueous hydrochloric acid. The acidic solution was extracted three times with 100 mL of diethyl ether, and the solvent was evaporated under vacuum, again without warming. The product was purified by Silica gel flash column chromatography using a 9 to 1 mixture of methylene chloride and diethyl ether mobile phase. The concentration of diethyl ether was rapidly increase to 100% diethyl ether, and 3.7 g (74%) of the desired product was eluted shortly thereafter as an orange oil, that

slowly solidified when stored at -78°C. ^{1}H NMR (300 MHz, CDCl$_3$): δ 7.42-7.48 (m, 5H, *Ph*); δ 3.36 (s, 3H, C*H$_3$*). ^{13}C NMR (300MHz; CDCl$_3$): δ 166.9, 132.4, 130.8, 128.4 (2C), 127.9 (2C), 38.3.

References

(1)   Bolland, J. L. *Quart. Reviews (London)* **1949***, 3*, 1.

(2)   *Free Radicals, Lipid Peroxidation, and Cancer*; Academic Press: London, 1982.

(3)   *Advances in PG Research*; Raven Press: New York, 1980.

(4)   *Free Radicals in Biology*; Academic Press: New York, 1980.

(5)   Awad, J. A.; Morrow, J. D.; Takahashi, K.; Roberts, L. J. *J. Biol. Chem.* **1993***, 268*, 4161-4169.

(6)   Morrow, J. D.; Roberts, L. J. *Biochem. Pharmacol.* **1996***, 51*, 1-9.

(7)   Ames, B. N. *Mutat. Res.* **1989**, 41-46.

(8)   Dargel, R. *Exp. Toxicol. Pathol.* **1992***, 44*, 169-181.

(9)   Sevanian, A.; Ursini, F. *Free Rad. Biol. Med.* **2000***, 29*, 306-311.

(10)   Chisolm, G.; Steinberg, D. *Free Rad. Biol. Med.* **2000***, 28*, 1815-1826.

(11)   Esterbauer, H.; Schaur, R. J.; Zollner, H. *Free Rad. Biol. Med.* **1991***, 11*, 81-128.

(12)   Schauenstein, E.; Esterbauer, H. *Submol. Biol. Cancer Ciba Fnd.* **1978***, 67*, 225-241.

(13)   Recknagel, R. O.; Choshal, A. K. *Exp. Mol. Pathol.* **1966***, 5*, 413.

(14)   Slater, T. *Methods in Enzymology*; Academic: Orlando, FL, 1984; 283.

(15)   Nair, V.; Turner, G. A. *Lipids* **1984***, 19*, 804.

(16)   Tagaki, T.; Mitsuno, Y.; Masumura, M. *Lipids* **1978***, 13*, 147.

(17)   Porter, N. A.; Caldwell, S. E.; Mills, K. A. *Lipids* **1995***, 30*, 277-290.

(18)   Brash, A. R. *Lipids* **2000***, 35*, 047-952.

(19)   Tallman, K. A.; Pratt, D. A.; Porter, N. A. *J. Am. Chem. Soc.* **2001***, 123*, 11827-11828.

(20)   Tallman, K. A.; Roschek, Jr., B; Porter, N. A. *J. Am. Chem. Soc.* **2004***, 126*, 9240-9247.

(21)   Porter, N. A.; Wujek, D. G. *J. Am. Chem. Soc.* **1984***, 106*, 2626-2629.

(22)   Chan, H. W.-S.; Levett, G. *Lipids* **1977***, 12*, 99.

(23)   Maillard, B.; Ingold, K. U.; Sciano, J. C. *J. Am. Chem. Soc.* **1983***, 105*, 5095.

(24)   Porter, N. A.; Lehman, L. S.; Weber, B. A.; Smith, K. J. *J. Am. Chem. Soc.* **1981***, 103*, 6447-6455.

(25)   Haslbeck, F.; Grosch, W.; Firl, J. *Biochim. Biophys. Acta* **1983***, 750*, 185.

(26)   Chan, H. W.; Levett, G.; Matthew, J. A. *Chem. Phys. Lipids* **1979***, 24*, 245.

(27)   Mahoney, L. R.; Mendenhall, G. D.; Ingold, K. U. *J. Am. Chem. Soc.* **1973***, 95*, 8610.

(28)   Coseri, S.; Ingold, K. U. *Org. Lett.* **2004***, 6*, 1641-1643.

(29)   Amorati, R.; Lucarini, M.; Mugnaini, V.; Pedulli, G.-F.; Minisci, F. et al. *J. Org. Chem.* **2003***, 68*, 1747-1754.

(30)   Punta, C.; Rector, C. L.; Porter, N. A. *Chem. Res. Toxicol.* **2005***, 18*, 349-356.

(31)   Pratt, D. A.; Mills, J. A.; Porter, N. A. *J. Am. Chem. Soc.* **2003***, 125*, 5801-5810.

(32)   Howard, J. A. *Adv. Free Rad. Chem.* **1972***, 4*, 49-173.

(33)   Cosgrove, J. P.; Church, D. F.; Pryor, W. A. *Lipids* **1987**, 299.

(34)   Howard, J. A.; Ingold, K. U. *Can. J. Chem.* **1965**, 2724-2729.

(35)   Burton, G. W.; Doba, T.; Gabe, E. J.; Hughes, L.; Lee, F. L. et al. *J. Am. Chem. Soc.* **1985***, 107*, 7053-7065.

(36)   Pratt, D. A.; Porter, N. A. *Org. Lett.* **2003***, 5*, 387-390.

(37)   Coates, R. M.; Firsan, S. J. *J. Org. Chem.* **1986***, 44*, 3177-3181.

CONCLUDING REMARKS

Olefin Geometry

The autoxidations of *cis*, *cis*; *cis*, *trans*; and *trans*, *trans* non-conjugated dienes and their corresponding octadecadienoates give rise to kinetically controlled hydroperoxides. Formation of the bis-allylic peroxyl radical and its subsequent β-fragmentation depends on the geometry of the alkene precursor and as a result the pentadienyl radical intermediate. Significant unpaired electron spin density is present at the central carbon of the pentadienyl radicals and the bis-allylic hydroperoxide product that arises from addition at this position is the major kinetic product for each of the systems studied, provided a sufficient hydrogen atom donor is present.[1]

However, unpaired spin density is not the only factor that determines the position of oxygen addition to a delocalized radical. We speculate that radical-triplet dioxygen complexes may be intermediates in the formation and rearrangement of delocalized radicals. Rearrangement of the bis-allylic peroxyl radicals to the conjugated peroxyl radicals occurs with rate constants between 2.2 and 2.8 x 10^6 s^{-1}. This rearrangement can be used as a peroxyl radical clock regardless of the mechanism by which this rearrangement occurs.[2,3]

The octadecadienoates studied in Chapter II are present in biological samples. Particularly methyl linoleate which is a very common lipid found in LDL. An understanding of the oxidation mechanism of methyl linoleate (and methyl linoelaidate) will give rise to a better understanding this oxidation process *in vivo*.

As discussed in Chapter I, oxidation of lipids in the body can have potentially harmful effects on the body. A better understanding of the mechanism of oxidation, and in turn, the breakdown products after lipid oxidation will give a better understanding to the pathogenesis of certain age-related diseases.

<center>Allylperoxyl Radical Rearrangement</center>

Many studies have been conducted trying to determine the nature of the allylperoxyl radical rearrangement (Chapter III). Many different mechanisms and theories have been proposed regarding the allylperoxyl radical rearrangement. Studies conducted in the Porter group for the last twenty years, as well as independent theoretical studies all seem to indicate that the most plausible mechanism for the allylperoxyl radical rearrangement is a β-fragmentation of the initial C-O bond of the peroxyl radical leading to a "caged pair" intermediate, followed by rearrangement to the isomerized peroxyl radical.

Using 1-phenyl-2-butene isomers it was very easy to see that in the presence of α-tocopherol, isomerization and racemization occurred very slowly if at all. However, when no antioxidant was present, isomerization and racemization occurred quite rapidly. From these studies, two major conclusions can be drawn regarding the mechanism of the allylperoxyl radical rearrangement:

1. The temperature of the reaction plays a vital role in the control of the rearrangement. That is, the higher the temperature, the more likely the rearrangement will occur at a faster rate and to a greater extent.

<center>167</center>

2. Antioxidants such as α-tocopherol not only impede the extent of oxidation, but also inhibit the peroxyl radical rearrangement. Perhaps due to the rapid hydrogen atom transfer, trapping the kinetic products.

The results presented in this work closely parallel theoretical investigations[4] as well as the experimental work by Porter[5,6] using symmetrically and unsymmetrically ^{18}O labeled hydroperoxides. The results of each of these studies strongly suggest the β-fragmentation of the peroxyl radical, leading to a caged pair of molecular oxygen and an allyl radical as the most plausible mechanism for allylperoxyl radical rearrangement.

Peroxyl Radical Clocks

Oxidation of allylbenzene was shown to be useful in determine rates of hydrogen atom transfer (k_H) for processes occurring from 10^6 $M^{-1}s^{-1}$ to 10^4 $M^{-1}s^{-1}$. Many commercially useful antioxidants, such as 2,6-di-t-butyl-4-methylphenol (BHT) and α-tocopherol (αTOH), donate a hydrogen atom in this range. Oxidation of allylbenzene proceeds *via* a mechanism similar to methyl linoleate; however the hydroperoxide oxidation products, once reduced to their corresponding hydroxy products, are easier to analyze by normal phase HPLC.[3]

When using allylbenzene as a peroxyl radical clock, one must take into the account the possibility of allylbenzene, as well as the hydrogen atom donor of interested, being consumed. Conditions should be selected such that the concentration of the hydrogen atom donor remains relatively constant, and the

clocking substrate (allylbenzene) is not competing with the hydrogen atom transfer process of interest. If the oxidation reactions are carried out to low conversions of hydrogen atom donor and the concentration of the oxidation products can be reliably determined; one can, within the errors of the peroxyl radical clock method, assume a constant concentration of the donor in the experiment, and therefore accurately determine the k_H for the hydrogen atom donor of interest.

The oxidation conditions should never result in the consumption of a significant amount of the hydrogen atom donor. This is typically not a problem with the peroxyl radical clock method because the oxidation relies on propagation by the ArO•. As a result, the hydrogen atom donor is regenerated during the course of an oxidation. When using allylbenzene, oxidations should be carried out to 0.5% conversion of allylbenzene to oxidation products, and hydrogen atom consumption should remain less than 5%. This will assure pseudo-1st order kinetics in the oxidation system.

Clock selection should be paired to the substrate being investigated. The peroxyl radical clock approach involves a competition leading to two different products, and the essential part of the experiments is the determination of the relative amounts of these two products formed at a known concentration of hydrogen atom donor. As a general guide, a unimolecular clock reaction should be selected to time H-atom transfer reactions having bimolecular rate constants that are 0.05 to 20 times the rate of the clock reaction.

While the allylbenzene clock works well for hydrogen atom transfer processes in the 10^6 - 10^4 $M^{-1}s^{-1}$ range, another useful clock is the "slow" methyl linoleate clock. This clock is based upon the isomerization of the parent pentadienyl radical affording the four thermodynamic products of methyl linoleate oxidation discussed in Chapter IV.

This "slow" methyl linoleate clock has proven useful in determining rates of hydrogen atom donation for processes that occur in the 10^4 – 10^0 $M^{-1}s^{-1}$ range. This allows the "slow" methyl linoleate clock to be useful for both commercially common antioxidants, as well as rates of propagation (k_p) for hydrocarbons such as 1,4-cyclohexadiene.[3]

Conditions should be selected such that the concentration of the hydrogen atom donor is known and the ratio of products can be reliably determined. If the oxidation reactions are carried out to low conversions of hydrogen atom donor one can, within the errors of the method, assume a constant concentration of the donor in the experiment. Typically, oxidations should be carried out to 2-4% conversion of methyl linoleate in order to reliably determine the concentration of oxidation products. Again, the oxidation conditions should never result in the consumption of a significant amount of the hydrogen atom donor.

A final *caveat* concerns the fact that the clocks are themselves oxidizable compounds, which is a requirement of the approach. This can give rise to problems in the analysis if sufficient care is not taken to ensure the appropriate purity of the clock. Commercial methyl linoleate may have substantial amounts (1-2%) of oxidation products as received and blank analyses should always be

performed to assure that clock substrates are uncontaminated by the very products that are formed in the clock experiment.

Ultimately the peroxyl radical clock method has proven to be a very efficient technique for the rapid determination of hydrogen atom processes over a broad range (10^6 – 10^0 M^{-1}s^{-1}). The methodology is straight forward and unified, and allows any organic or analytical lab reliably determine rate constants for reactions that have typically only been studies in a physical chemistry lab with specialized equipment.

References

(1)   Tallman, K. A.; Roschek Jr., B; Porter, N. A. *J. Am. Chem. Soc.* **2004**, *126*, 9240-9247.

(2)   Tallman, K. A.; Pratt, D. A.; Porter, N. A. *J. Am. Chem. Soc.* **2001**, *123*, 11827-11828.

(3)   Roschek Jr., B.; Tallman, K. A.; Rector, C. L.; Gillmore, J. G.; Pratt, D. A. et al. *J. Org. Chem.* **2006**, *in press*.

(4)   Olivella, S.; Sole, A. *J. Am. Chem. Soc.* **2003**, *125*, 10641-10650.

(5)   Porter, N. A.; Mills, K. A.; Caldwell, S. E.; Dubay, G. R. *J. Am. Chem. Soc.* **1994**, *116*, 6697-6705.

(6)   Lowe, J. R.; Porter, N. A. *J. Am. Chem. Soc.* **1997**, *119*, 11534.